Chapter 9: Stable Isotope Geochemistry

9.1 Introduction

Stable isotope geochemistry is concerned with variations of the isotopic compositions of elements arising from physicochemical processes rather than nuclear processes. Fractionation* of the isotopes of an element might at first seem to be an oxymoron. After all, in the last chapter we saw that the value of radiogenic isotopes was that the various isotopes of an element had identical chemical properties and therefore that isotope ratios such as $^{87}Sr/^{86}Sr$ are not changed measurably by chemical processes. In this chapter we will find that this is not quite true, and that the very small differences in the chemical behavior of different isotopes of an element can provide a very large amount of useful information about chemical (both geochemical and biochemical) processes.

The origins of stable isotope geochemistry are closely tied to the development of modern physics in the first half of the 20th century. The discovery of the neutron in 1932 by H. Urey and the demonstration of variations in the isotopic composition of light elements by A. Nier in the 1930's and 1940's were the precursors to the development of stable isotope geochemistry. The real history of stable isotope geochemistry begins in 1947 with the Harold Urey's publication of a paper entitled "*The Thermodynamic Properties of Isotopic Substances*". Urey not only showed why, on theoretical grounds, isotope fractionations could be expected, but also suggested that these fractionations could provide useful geological information. Urey then set up a laboratory to determine the isotopic compositions of natural substances and experimentally determine the temperature dependence of isotopic fractionations, in the process establishing the field of stable isotope geochemistry.

What has been learned in the fifty years since that paper was published would undoubtedly astonish even Urey. Stable isotope geochemistry, like radiogenic isotope geochemistry, has become an essential part of not only geochemistry, but the earth sciences as a whole. In this chapter, we will attempt to gain an understanding of the principles underlying stable isotope geochemistry and then briefly survey its many-fold applications in the earth sciences. In doing so, we add the final tool to our geochemical toolbox.

9.1.1 Scope of Stable Isotope Geochemistry

The principal elements of interest in stable isotope geochemistry are H, Li, B, C, N, O, Si, S, and Cl. Of these, O, H, C and S are of the greatest interest. Most of these elements have several common characteristics:

(1) They have low atomic mass.

(2) The relative mass difference between their isotopes is large.

(3) They form bonds with a high degree of covalent character.

(4) The elements exist in more than one oxidation state (C, N, and S), form a wide variety of compounds (O), or are important constituents of naturally occurring solids and fluids.

(5) The abundance of the rare isotope is sufficiently high (generally at least tenths of a percent) to facilitate analysis.

It was once thought that elements not meeting these criteria would not show measurable variation in isotopic composition. However, as new techniques offering greater sensitivity and higher precision have become available (particularly use of the MC-ICP-MS), geochemists have begun to explore isotopic variations of metals such as Mg, Ca, Ti, Cr, Fe, Zn, Cu, Ge, Se, Mo, and Tl. The isotopic variations observed in these metals have generally been quite small. Nevertheless, some geologically useful information has been obtained from isotopic study of these metals and exploration of their isotope geochemistry continues. We do not have space to consider them here, but their application is reviewed in a recent book (Johnson et al., 2004).

The elements of interest in radiogenic isotope geochemistry are heavy (Sr, Nd, Hf, Os, Pb), most form dominantly ionic bonds, generally exist in only one oxidation state, and there is only small rela-

*Fractionation refers to the change in an isotope ratio that arises as a result of some chemical or physical process.

TABLE 9.1. ISOTOPE RATIOS OF STABLE ISOTOPES

Element	Notation	Ratio	Standard	Absolute Ratio
Hydrogen	δD	D/H ($^2H/^1H$)	SMOW	1.557×10^{-4}
Lithium	δ^7Li	$^7Li/^6Li$	NIST 8545 (L-SVEC)	12.285
Boron	$\delta^{11}B$	$^{11}B/^{10}B$	NIST 951	4.044
Carbon	$\delta^{13}C$	$^{13}C/^{12}C$	PDB	1.122×10^{-2}
Nitrogen	$\delta^{15}N$	$^{15}N/^{14}N$	atmosphere	3.613×10^{-3}
Oxygen	$\delta^{18}O$	$^{18}O/^{16}O$	SMOW, PDB	2.0052×10^{-3}
	$\delta^{17}O$	$^{17}O/^{16}O$	SMOW	3.76×10^{-4}
Sulfur	$\delta^{34}S$	$^{34}S/^{32}S$	CDT	4.43×10^{-2}

tive mass differences between the isotopes of interest. Thus isotopic fractionation of these elements is quite small and can generally be ignored. Furthermore, any natural fractionation is corrected for in the process of correcting much larger fractionations that typically occur during analysis (with the exception of Pb). Thus is it that one group of isotope geochemists make their living by measuring isotope fractionations while the other group makes their living by ignoring them!

Stable isotope geochemistry has been be applied to a great variety of problems, and we will see a number of examples in this chapter. One of the most common is geothermometry. Another is process identification. For instance, plants that produce 'C_4' hydrocarbon chains (that is, hydrocarbon chains 4 carbons long) as their primary photosynthetic product fractionate carbon differently than to plants that produce 'C_3' chains. This fractionation is retained up the food chain. This allows us, for example, to draw some inferences about the diet of fossil mammals from the stable isotope ratios in their bones. Sometimes stable isotope ratios are used as 'tracers' much as radiogenic isotopes are. So, for example, we can use oxygen isotope ratios in igneous rocks to determine whether they have assimilated crustal material, as crust generally has different O isotope ratios than does the mantle.

9.1.2 SOME DEFINITIONS

9.1.2.1 THE δ NOTATION

As we shall see, variations in stable isotope ratios are typically in the parts per thousand to parts per hundred range and are most conveniently and commonly reported as *permil* deviations, δ, from some standard. For example, O isotope ratios are often reported as permil deviations from SMOW (standard mean ocean water) as:

$$\delta^{18}O = \left[\frac{(^{18}O / {}^{16}O)_{sam} - (^{18}O / {}^{16}O)_{SMOW}}{(^{18}O / {}^{16}O)_{SMOW}} \right] \times 10^3 \qquad 9.1$$

Unfortunately, a dual standard developed for reporting O isotopes. While O isotopes in most substances are reported relative to SMOW, the oxygen isotope composition of carbonates is reported relative to the Pee Dee Belemite (PDB) carbonate standard‡. This value is related to SMOW by:

$$\delta^{18}O_{PDB} = 1.03086\delta^{18}O_{SMOW} + 30.86 \qquad 9.2$$

A similar δ notation is used to report other stable isotope ratios. Hydrogen isotope ratios, δD, are also reported relative to SMOW, carbon isotope ratios relative to PDB, nitrogen isotope ratios relative to atmospheric nitrogen (denoted ATM), and sulfur isotope ratios relative to troilite in the Canyon Diablo iron meteorite (denoted CDT). Table 9.1 lists the isotopic composition of these standards.

9.1.2.2 THE FRACTIONATION FACTOR

The *fractionation factor*, α, is the ratio of isotope ratios in two phases:

$$\alpha_{A-B} \equiv \frac{R_A}{R_B} \qquad 9.3$$

‡ There is, however, a good historical reason for this: analytical difficulties in the measurement of carbonate oxygen prior to 1965 required it be measured against a carbonate standard.

The fractionation of isotopes between two phases is also often reported as $\Delta_{A\text{-}B} = \delta_A - \delta_B$. The relationship between Δ and α is:

$$\Delta \approx (\alpha - 1)10^3 \quad \text{or} \quad \Delta \approx 10^3 \ln \alpha \qquad 9.4^{\dagger}$$

As we will see, *at equilibrium*, α may be related to the equilibrium constant of thermodynamics by

$$\alpha_{A\text{-}B} = (K/K_\infty)^{1/n} \qquad 9.5$$

where *n* is the number of atoms exchanged, K_∞ is the equilibrium constant at infinite temperature, and K is the equilibrium constant written in the usual way (except that concentrations are used rather than activities because the ratios of the activity coefficients are equal to 1, i.e., there are no isotopic effects on the activity coefficient).

9.2 THEORETICAL CONSIDERATIONS

Isotope fractionation can originate from both *kinetic* effects and *equilibrium* effects. The former may be intuitively expected, but the latter may at first seem somewhat surprising. After all, we have been taught that the chemical properties of an element are dictated by its electronic structure, and that the nucleus plays no real role in chemical interactions. In the following sections, we will see that quantum mechanics predicts that the mass of an atom affect its vibrational motion therefore the strength of chemical bonds. It also affects rotational and translational motions. From an understanding of these effects of atomic mass, it is possible to predict the small differences in the chemical properties of isotopes quite accurately.

9.2.1 EQUILIBRIUM ISOTOPE FRACTIONATIONS

Most isotope fractionations arise from *equilibrium* effects. *Equilibrium fractionations arise from translational, rotational and vibrational motions of molecules in gases and liquids and atoms in crystals because the energies associated with these motions are mass dependent.* Systems tend to adjust themselves so as to minimize energy. Thus isotopes will be distributed so as to minimize the vibrational, rotational, and translational energy of a system. Of the three types of energies, vibrational energy makes by far the most important contribution to isotopic fractionation. Vibrational motion is the only mode of motion available to atoms in a solid. These effects are, as one might expect, small. For example, the equilibrium constant for the reaction

$$\tfrac{1}{2}C^{16}O_2 + H_2{}^{18}O \rightleftarrows \tfrac{1}{2}C^{18}O_2 + H_2{}^{16}O \qquad 9.6$$

is only about 1.04 at 25°C and the ΔG of the reaction, given by $-RT\ln K$, is only -100 J/mol (you'll recall most ΔG's for reactions are in typically in the kJ/mol range).

9.2.1.1 THE QUANTUM MECHANICAL ORIGIN OF ISOTOPIC FRACTIONATIONS

It is fairly easy to understand, at a qualitative level at least, how some isotope fractionations can arise from vibrational motion. Consider the two hydrogen atoms of a hydrogen molecule: they do not remain at a fixed distance from one and other, rather they continually oscillate toward and away from each other, even at absolute zero. The frequency of this oscillation is quantized, that is, only discrete

---

† To derive this, we rearrange equation 8.1 to obtain: $R_A = (\delta_A + 10^3)R_{STD}/\ 10^3$

Note that Δ is sometimes defined as $\Delta \equiv 10^3 \ln \alpha$, in which case $\Delta_{AB} \approx \delta_A - \delta_B$.

So that α may be expressed as: $\alpha = \dfrac{(\delta_A + 10^3)R_{STD}/10^3}{(\delta_B + 10^3)R_{STD}/10^3} \approx \dfrac{(\delta_A + 10^3)}{(\delta_B + 10^3)}$

Subtracting 1 from each side and rearranging, we obtain:

$$\alpha - 1 = \alpha - 1 = \frac{(\delta_A - \delta_B)}{(\delta_B + 10^3)} \approx \frac{(\delta_A - \delta_B)}{10^3} \approx \Delta \times 10^{-3}$$

since δ is small. The second equation in 9.4 results from the approximation that for $x \approx 1$, $\ln x \approx x\text{-}1$.

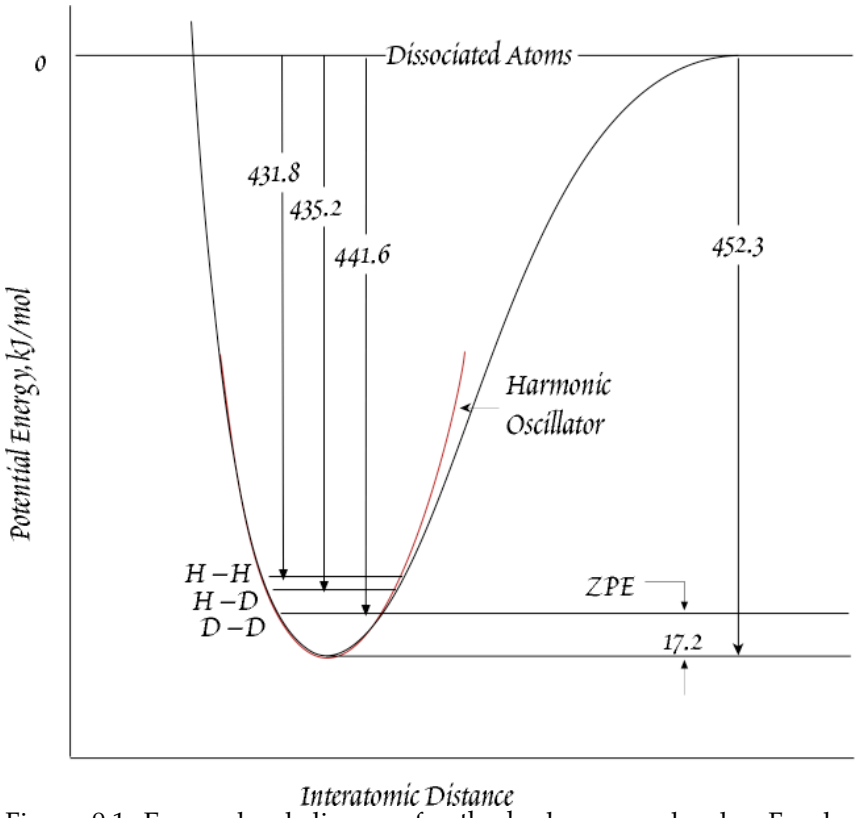

Figure 9.1. Energy-level diagram for the hydrogen molecule. Fundamental vibration frequencies are 4405 cm^{-1} for H_2, 3817 cm^{-1} for HD, and 3119 cm^{-1} for D_2. The zero-point energy of H_2 is greater than that of HD which is greater than that of D_2. Arrows show the energy, in kJ/mol, required to dissociate the 3 species. After O'Niel (1986).

frequency values are possible. Figure 9.1 is a schematic diagram of energy as a function of interatomic distance in the hydrogen molecule. As the atoms vibrate back and forth, their potential energy varies as shown by the curved line. The *zero point energy* (ZPE) is the energy level at which the molecule will vibrate in its ground state, which is the state in which the molecule will be in at low temperature. The zero point energy is always some finite amount above the minimum potential energy of an analogous harmonic oscillator.

The potential energy curves for various isotopic combinations of an element are identical, but as the figure shows, the zero point vibrational energies differ, as do vibration energies at higher quantum levels, being lower for the heavier isotopes. Vibration energies and frequencies are directly related to bond strength. Because of this, the energy required for the molecule to dissociate will differ for different isotopic combinations. For example, 440.6 kJ/mole is necessary to dissociate a D_2 ($^2H_2$) molecule, but only 431.8 kJ/mole is required to dissociate the $^1H_2$ molecule. Thus the bond formed by the two deuterium atoms is 9.8 kJ/mole stronger than the H–H bond. The differences in bond strength can also lead to kinetic fractionations, since molecules that dissociate easier will react faster. We will discuss kinetic fractionations a bit later.

9.2.1.2 Predicting Isotopic Fractionations from Statistical Mechanics

Now let's attempt to understand the origin of isotopic fractionations on a more quantitative level. We have already been introduced to several forms of the *Boltzmann distribution law* (e.g., equation 2.84), which describes the distribution of energy states. It states that the probability of a molecule having internal energy E_i is:

$$P_i = \frac{g_i e^{-E_i/kT}}{\sum_n g_n e^{-E_n/kT}} \qquad 9.7$$

where g is a statistical weight factor‡, k is Boltzmann's constant, and the sum in the denominator is taken over all possible states. The average energy (per molecule) is:

‡ This factor comes into play where more than one state corresponds to an energy level E_i (the states are said to be 'degenerate'). In that case g_i is equal to the number of states having energy level E_i.

$$\bar{E} = \sum_i E_i P_i = \frac{\sum_i g_i E_i e^{-E_i/kT}}{\sum_i g_i e^{-E_i/kT}} \qquad 9.8$$

As we saw in Chapter 2, the *partition function*, Q, is the denominator of this equation:

$$Q = \sum_n g_n e^{-E_n/kT} \qquad 9.9$$

The partition function is related to thermodynamic quantities U and S (equations 2.90 and 2.91). Since there is no volume change associated with isotope exchange reactions, we can use the relationship:

$$\Delta G = \Delta U - T\Delta S \qquad 9.10$$

and equations 2.119 and 2.123 to derive:

$$\Delta G_r = -RT \ln \prod_i Q_i^{\nu_i} \qquad 9.11$$

and comparing to equation 3.86, that the equilibrium constant is related to the partition function as:

$$K = \prod_i Q_i^{\nu_i} \qquad 9.12$$

for isotope exchange reactions. In the exchange reaction above (9.6) this is simply:

$$K = \frac{Q_{C^{18}O_2}^{0.5} Q_{H_2{}^{16}O}}{Q_{C^{16}O_2}^{0.5} Q_{H_2{}^{18}O}} \qquad 9.13$$

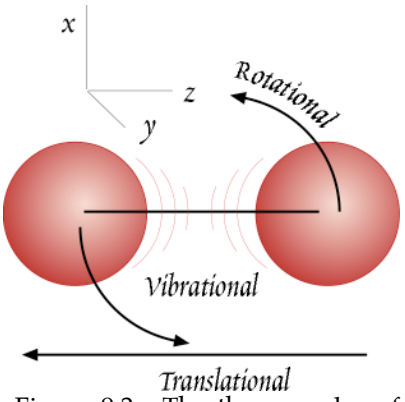

Figure 9.2. The three modes of motion, illustrated for a diatomic molecule. Rotations can occur about both the y and x axes; only the rotation about the y axis is illustrated. Since radial symmetry exists about the z axis, rotations about that axis are not possible according to quantum mechanics. Three modes of translational motion are possible: in the x, y, and z directions. Possible vibrational and rotational modes of motion of polyatomic molecules are more complex.

The usefulness of the partition function is that it can be calculated from quantum mechanics, and from it we can calculate equilibrium fractionations of isotopes.

There are three modes of motion available to gaseous molecules: vibrational, rotational, and translational (Figure 9.2). The partition function can be written as the product of the translational, rotational, vibrational, and electronic partition functions:

$$Q_{total} = Q_{vib} Q_{trans} Q_{rot} Q_{elec} \qquad 9.14$$

The electronic configurations and energies of atoms are unaffected by the isotopic differences, so the last term can be ignored in the present context.

The vibrational motion is the most important contributor to isotopic fractionations, and it is the only mode of motion available to atoms in solids. So we begin by calculating the vibrational partition function. We can approximate the vibration of atoms in a simple diatomic molecule such as CO or O_2 by that of a harmonic oscillator. The energy of a 'quantum' oscillator is:

$$E_{vib} = (n + 1/2)h\nu_0 \qquad 9.15$$

where ν_0 is the ground state vibrational frequency, h is Plank's constant and n is the vibrational quantum number. The partition function for vibrational motion of a diatomic molecule is given by:

$$Q_{vib} = \frac{e^{-h\nu/2kT}}{1 - e^{-h\nu/2kT}} \qquad 9.16^{\ddagger}$$

‡ Polyatomic molecules have many modes of vibrational motion available to them. The partition function is calculated by summing the energy over all available modes of motion; since energy occurs in the exponent, the result is a product:

Vibrations of atoms in molecules and crystals approximates that of harmonic oscillators. For an ideal harmonic oscillator, the relation between frequency and reduced mass is:

$$\nu = \frac{1}{2}\sqrt{\frac{k}{\mu}} \qquad 9.17$$

where k is the forcing constant, which depends on the electronic configuration of the molecule, but not the isotope involved, and μ is reduced mass:

$$\mu = \frac{1}{1/m_1 + 1/m_2} = \frac{m_1 m_2}{m_1 + m_2} \qquad 9.18$$

Hence we see that the vibrational frequency, and therefore also vibrational energy and partition function, depends on the mass of the atoms involved in the bond.

Rotational motion of molecules is also quantized. We can approximate a diatomic molecule as a dumbbell rotating about the center of mass. The rotational energy for a quantum rigid rotator is:

$$E_{rot} = \frac{j(j+1)h^2}{8\pi^2 I} \qquad 9.19$$

where j is the rotational quantum number and I is the moment of inertia, $I = \mu r^2$, where r is the interatomic distance. The statistical weight factor, g, in this case is equal to $(2j + 1)$ since there 2 axes about which rotations are possible. For example, if $j = 1$, then there are $j(j + 1) = 2$ quanta available to the molecule, and $(2j + 1)$ ways of distributing these two quanta: all to the x-axis, all to the y-axis or one to each. Thus:

$$Q_{rot} = \sum (2j+1) e^{-j(j+1)h^2/8\pi^2 IkT} \qquad 9.20$$

Because the rotational energy spacings are small, equation 9.20 can be integrated to yield:

$$Q_{rot} = \frac{8\pi^2 IkT}{\sigma h^2} \qquad 9.21^*$$

where σ is a symmetry factor whose value is 1 for heteronuclear molecules such as ^{16}O-^{18}O and 2 for homonuclear molecules such as ^{16}O-^{16}O. This arises because in homonuclear molecules, the quanta must be equally distributed between the rotational axes, i.e., the j's must be all even or all odd. This restriction does not apply to hetergeneous molecules, hence the symmetry factor.

Finally, translational energy associated with each of the three possible translational motions (x, y, and z) is given by the solution to the Schrödinger equation for a particle in a box:

$$E_{trans} = \frac{n^2 h^2}{8ma^2} \qquad 9.22$$

where n is the translational quantum number, m is mass, and a is the dimension of the box. This expression can be inserted into equation 9.8. Above about 2 K, spacings between translational energies levels are small, so equ. 9.8 can also be integrated. Recalling that there are 3 degrees of freedom, the result is:

$$Q_{vib} = \prod_i \frac{e^{-h\nu_i/2kT}}{1 - e^{-h\nu_i/2kT}} \qquad 9.16a$$

* Equation 9.21 also holds for linear polyatomic molecules such as CO_2. The symmetry factor is 1 if it has plane symmetry, and 2 if it does not. For non-linear polyatomic molecules, 9.21 is replaced by:

$$Q_{rot} = \frac{8\pi^2 (8\pi^3 ABC)^{1/2} (kT)^{3/2}}{\sigma h^3} \qquad 9.21a$$

where A, B, and C are the three principle moments of inertia.

$$Q_{trans} = \frac{(2\pi m\mathrm{k}T)^{3/2}}{h^3}V \qquad 9.23$$

where V is the volume of the box (a^3). Thus the full partition function is:

$$Q_{total} = Q_{vib}Q_{trans}Q_{rot} = \frac{e^{-h\nu/2\mathrm{k}T}}{1-e^{-h\nu/2\mathrm{k}T}}\frac{8\pi^2 I\mathrm{k}T}{\sigma h^2}\frac{(2\pi m\mathrm{k}T)^{3/2}}{h^3}V \qquad 9.24$$

It is the ratio of partition functions that occurs in the equilibrium constant expression, so that many of the terms in 9.24 eventually cancel. Thus the partition function ratio for 2 different isotopic species of the same diatomic molecule, A and B, reduces to:

$$\frac{Q_A}{Q_B} = \frac{\frac{e^{-h\nu_A/2\mathrm{k}T}}{1-e^{-h\nu_A/2\mathrm{k}T}}\frac{I_A}{\sigma_A}m_A^{3/2}}{\frac{e^{-h\nu_B/2\mathrm{k}T}}{1-e^{-h\nu_B/2\mathrm{k}T}}\frac{I_B}{\sigma_B}m_B^{3/2}} = \frac{e^{-h\nu_A/2\mathrm{k}T}(1-e^{-h\nu_B/2\mathrm{k}T})I_A\sigma_B m_A^{3/2}}{e^{-h\nu_B/2\mathrm{k}T}(1-e^{-h\nu_A/2\mathrm{k}T})I_B\sigma_A m_B^{3/2}} \qquad 9.25$$

Since bond lengths are essentially independent of the isotopic composition, this further reduces to:

$$\frac{Q_A}{Q_B} = \frac{e^{-h\nu_A/2\mathrm{k}T}(1-e^{-h\nu_B/2\mathrm{k}T})\mu_A\sigma_B m_A^{3/2}}{e^{-h\nu_B/2\mathrm{k}T}(1-e^{-h\nu_A/2\mathrm{k}T})\mu_B\sigma_A m_B^{3/2}} = \frac{e^{-h(\nu_A-\nu_B)/2\mathrm{k}T}(1-e^{-h\nu_B/2\mathrm{k}T})\mu_A\sigma_B m_A^{3/2}}{(1-e^{-h\nu_A/2\mathrm{k}T})\mu_B\sigma_A m_B^{3/2}} \qquad 9.26$$

Notice that all the temperature terms cancel except for those in the vibrational contribution. Thus vibrational motion alone is responsible for the temperature dependency of isotopic fractionations.

To calculate the fractionation factor α from the equilibrium constant, we need to calculate K_∞. For a reaction such as:

$$aA_1 + bB_2 \rightleftarrows aA_2 + bB_1$$

where A_1 and A_2 are two molecules of the same substance differing only in their isotopic composition, and a and b are the stoichiometric coefficients, the equilibrium constant is:

$$K_\infty = \frac{(\sigma_{A_2}/\sigma_{A_1})^a}{(\sigma_{B_1}/\sigma_{B_2})^b} \qquad 9.27$$

Thus for a reaction where only a single isotope is exchanged, K_∞ is simply the ratio of the symmetry factors.

9.2.1.3 Temperature Dependence of the Fractionation Factor

As we noted above, the temperature dependence of the fractionation factor depends only on the vibrational contribution. At temperatures where $T << h\nu/k$, the $1 - e^{-h\nu/kT}$ terms in 9.16 and 9.26 tend to 1 and can therefore be neglected, so the vibrational partition function becomes:

$$Q_{vib} \cong e^{-h\nu/2\mathrm{k}T} \qquad 9.28$$

In a further simplification, since Δν is small, we can use the approximation $e^x \approx 1 + x$ (valid for $x<<1$), so that the ratio of vibrational energy partition functions becomes

$$Q_{vib}^A / Q_{vib}^B \cong 1 - h\Delta\nu/2\mathrm{k}T$$

Since the translational and rotational contributions are temperature independent, we expect a relationship of the form:

$$\alpha \cong A + \frac{B}{T} \qquad 9.29$$

In other words, α should vary inversely with temperature at low temperature.

At higher temperature, the $1 - \exp(-h\nu/\mathrm{k}T)$ term differs significantly from 1. Furthermore, at higher vibrational frequencies, the harmonic oscillator approximation breaks down (as suggested in Figure

9.1), as do several of the other simplifying assumptions we have made, so that the relation between the fractionation factor and temperature approximates:

$$\ln\alpha \propto \frac{1}{T^2} \qquad 9.30$$

Since α is generally small, ln α ≈ 1 + α, so that α ∝ 1 + $1/T^2$. At infinite temperature, the fractionation is unity, since ln α = 0. This illustrated in Figure 9.3 for distribution of ^{18}O and ^{16}O between CO_2 and H_2O. The α ∝ 1/T relationship breaks down around 200°C; above that temperature the relationship follows α ∝ $1/T^2$.

It must be emphasized that the simple calculations performed in Example 9.1 are applicable only to a gas whose vibrations can be approximated by a simple harmonic oscillator. Real gases often show fractionations that are complex functions of temperature, with minima, maxima, inflections, and crossovers. Vibrational modes of silicates, on the other hand, are relatively well behaved.

9.2.1.4 Composition and Pressure Dependence

The nature of the chemical bonds in the phases involved is most important in determining isotopic fractionations. *A general rule of thumb is that the heavy isotope goes into the phase in which it is most strongly bound*. Bonds to ions with a high ionic potential and low atomic mass are associated with high vibrational frequencies and have a tendency to incorporate the heavy isotope preferentially. For example, quartz, SiO_2 is typically the most ^{18}O rich mineral and magnetite the least. Oxygen is dominantly covalently bonded in quartz, but dominantly ionically bonded in magnetite. The O is bound more strongly in quartz than in magnetite, so the former is typically enriched in ^{18}O.

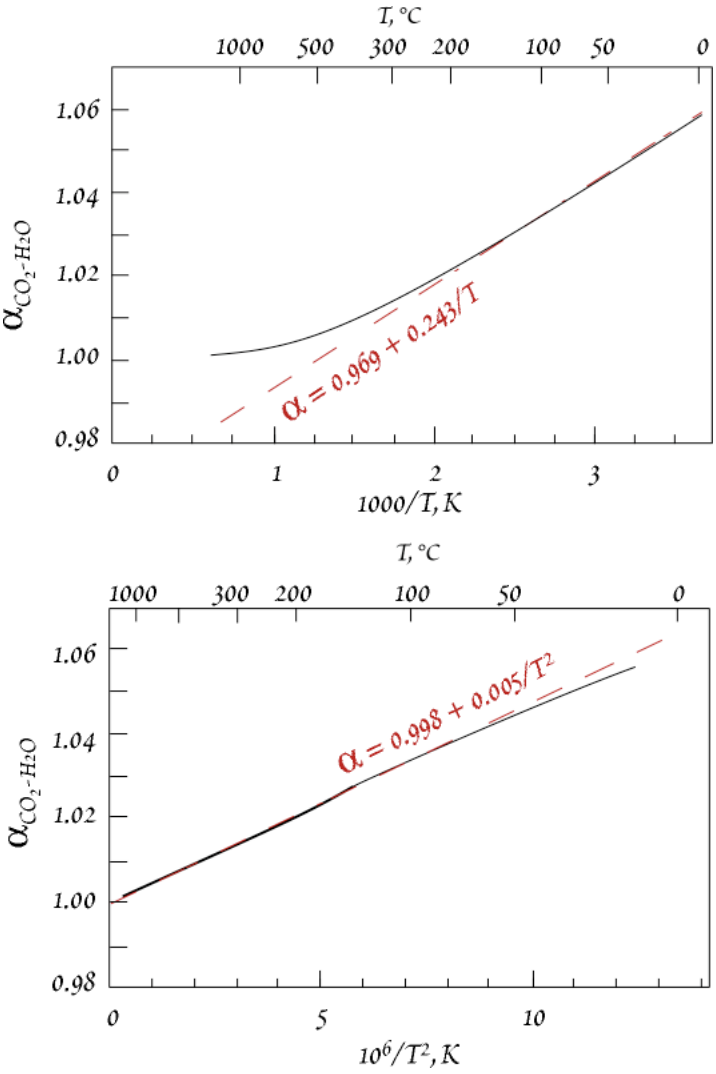

Figure 9.3. Calculated value of $\alpha^{18}O$ for CO_2–H_2O, shown vs. $1/T$ and $1/T^2$. Dashed lines show that up to ~200° C, α ≈ 0.969 + 0.0243/T. At higher temperatures, α ≈ 0.9983 + 0.0049/T^2. Calculated from the data of Richet et al. (1977).

Substitution of cations in a dominantly ionic site (typically the octahedral sites) in silicates has only a secondary effect on the O bonding, so that isotopic fractionations of O isotopes between similar silicates are generally small. Substitutions of cations in sites that have a strong covalent character (generally tetrahedral sites) result in greater O isotope fractionations. Thus, for example, we would expect the fractionation between the end-members of the alkali feldspar series and water to be similar, since only the substitution of K^+ for Na^+ is involved. We would expect the fractionation factors between end-members of the plagioclase series and water to be greater, since this series involves the substitution of Al for Si as well as Ca for Na, and the bonding of O to Si and Al in tetrahedral sites has a large covalent component.

EXAMPLE 9.1. PREDICTING ISOTOPIC FRACTIONATIONS

Consider the exchange of ^{18}O and ^{16}O between carbon monoxide and oxygen:

$$C^{16}O + {}^{16}O^{18}O \rightleftarrows C^{18}O + {}^{16}O_2$$

The frequency for the C-^{16}O vibration is 6.505×10^{13} sec^{-1}, and the fre quency of the $^{16}O_2$ vibration is 4.738×10^{13} sec^{-1}. How will the fractionation factor, $\alpha = (^{18}O/^{16}O)_{CO}/^{18}O/^{16}O)_{O2}$, vary as a function of temperature?

Answer: The equilibrium constant for this reaction is:

$$K = \frac{Q_{C^{18}O} Q_{^{16}O_2}}{Q_{C^{16}O} Q_{^{18}O^{16}O}} \qquad 9.31$$

The rotational and translational contributions are independent of temperature, so we calculate them first. The rotational contribution is:

$$K_{rot} = \left(\frac{Q_{C^{18}O} Q_{^{16}O_2}}{Q_{C^{16}O} Q_{^{18}O^{16}O}} \right)_{rot} = \frac{\mu_{C^{18}O} \sigma_{C^{16}O}}{\mu_{C^{16}O} \sigma_{C^{18}O}} \frac{\mu_{^{16}O_2} \sigma_{^{18}O^{16}O}}{\mu_{^{18}O^{16}O} \sigma_{^{16}O_2}} = \frac{1}{2} \frac{\mu_{C^{18}O} \mu_{^{16}O_2}}{\mu_{C^{16}O} \mu_{^{18}O^{16}O}} \qquad 9.32$$

(the symmetry factor, σ, is 2 for $^{16}O_2$ and 1 for the other molecules). Substituting values $\mu_{C^{16}O} = 6.857$, $\mu_{C^{18}O} = 7.20$, $\mu_{^{18}O^{16}O} = 8.471$, $\mu_{^{16}O_2} = 8$, we find: $K_{rot} = 0.9917/2$.

The translational contribution is:

$$K_{trans} = \frac{m_{C^{18}O}^{3/2}}{m_{C^{16}O}^{3/2}} \frac{m_{^{16}O_2}^{3/2}}{m_{^{18}O^{16}O}^{3/2}} \qquad 9.33$$

Substituting $m_{C^{16}O} = 28$, $m_{C^{18}O} = 30$, $m_{^{18}O^{16}O} = 34$, $m_{^{16}O_2} = 32$ into 9.33, we find $K_{trans} = 1.0126$.

The vibrational contribution to the equilibrium constant is:

$$K_{vib} = \frac{e^{-h(\nu_{C^{18}O} - \nu_{C^{16}O} + \nu_{^{16}O_2} - \nu_{^{18}O^{16}O})/2kT} (1 - e^{-h\nu_{C^{16}O}/kT})(1 - e^{-h\nu_{^{18}O^{16}O}/kT})}{(1 - e^{-h\nu_{C^{18}O}/kT})(1 - e^{-h\nu_{^{16}O_2}/kT})} \qquad 9.34$$

To obtain the vibrational contribution, we can a ssume the atoms vibrate as harmonic oscillators and, using experimentally determined vibrational frequencies for the ^{16}O molecules, solve equation 9.17 for the forcing constant, k, and calculate the vibrational frequencies for the ^{18}O-bearing molecules. These turn out to be 6.348×10^{13} sec^{-1} for C-^{18}O and 4.605×10^{13} sec^{-1} for $^{18}O^{16}O$, so that 8.33a becomes:

$$K_{vib} = \frac{e^{-5.580/T} (1 - e^{-3119/T})(1 - e^{-2208/T})}{(1 - e^{-3044/T})(1 - e^{-2272/T})}$$

If we carry the calculation out at T = 300 K, we find:

$$K = K_{rot} K_{trans} K_{vib} =$$

$$\frac{1}{2}\ 0.9917 \times 1.0126 \times 1.1087 = \frac{1.0229}{2}$$

To calculate the fractionation factor α from the equilibrium constant, we need to calculate K_∞

$$K_\infty = \frac{(1/1)^1}{(2/1)^1} = \frac{1}{2}$$

so that $\alpha = K / K_\infty = 2K$

At 300 K, $\alpha = 1.0233$. The variat ion of α with temperature is shown in Figure 9.4.

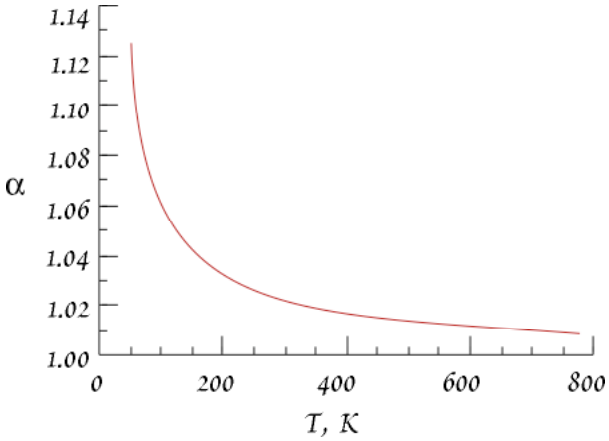

Figure 9.4. Fractionation factor, $\alpha = (^{18}O/^{16}O)_{CO}/(^{18}O/^{16}O)_{O2}$, calculated from partition functions as a function of temperature.

Carbonates tend to be very ^{18}O rich because O is bonded to a small, highly charged atom, C^{4+}. The fractionation, $\Delta^{18}O_{cal\text{-}water}$, between calcite and water is about 30 per mil at 25° C. The cation in the carbonate has a secondary role (due to the effect of the mass of the cation on vibrational frequency). The $\Delta^{18}O_{carb\text{-}H_2O}$ decreases to about 25 when Ba replaces Ca (Ba has about 3 times the mass of Ca).

Crystal structure plays a secondary role. The $\Delta^{18}O$ between aragonite and calcite is of the order of 0.5 permil. However, is there apparently a large fractionation (10 permil) of C between graphite and diamond.

Pressure effects on fractionation factors turn out to be small, no more than 0.1 permil over 0.2 GPa. We can understand the reason for this by recalling that $\partial\Delta G/\partial P = \Delta V$. The volume of an atom is entirely determined by its electronic structure, which does not depend on the mass of the nucleus. Thus the volume change of an isotope exchange reaction will be small, and hence there will be little pressure dependence. There will be a minor effect because vibrational frequency and bond length change as crystals are compressed. The compressibility of silicates is of the order of 1 part in 10^4, so we can expect effects on the order of 10^{-4} or less, which are generally insignificant.

9.2.2 Kinetic Isotope Fractionations

Kinetic isotope fractionations are normally associated with fast, incomplete, or unidirectional processes like evaporation, diffusion, dissociation reactions, and biologically mediated reactions. As an example, recall that temperature is related to the average kinetic energy. In an ideal gas, the average kinetic energy of all molecules is the same. The kinetic energy is given by:

$$E = \frac{1}{2}mv^2 \qquad 9.35$$

Consider two molecules of carbon dioxide, $^{12}C^{16}O_2$ and $^{13}C^{16}O_2$, in such a gas. If their energies are equal, the ratio of their velocities is $(45/44)^{1/2}$, or 1.011. Thus $^{12}C^{16}O_2$ can diffuse 1.1% further in a given amount of time than $^{13}C^{16}O_2$. This result, however, is largely limited to ideal gases, i.e., low pressures where collisions between molecules are infrequent and intermolecular forces negligible. For the case where molecular collisions are important, the ratio of their diffusion coefficients is the ratio of the square roots of the reduced masses of CO_2 and air (mean molecular weight 28.8):

$$\frac{D_{^{12}CO_2}}{D_{^{13}CO_2}} = \frac{\sqrt{\mu_{^{12}CO_2-air}}}{\sqrt{\mu_{^{13}CO_2-air}}} = \frac{17.561}{17.406} = 1.0044 \qquad 9.36$$

Hence we would predict that gaseous diffusion will lead to a 4.4‰ rather than 11‰ fractionation.

Molecules containing the heavy isotope are more stable and have higher dissociation energies than those containing the light isotope. This can be readily seen in Figure 9.1. The energy required to raise the D_2 molecule to the energy where the atoms dissociate is 441.6 kJ/mole, whereas the energy required to dissociate the H_2 molecule is 431.8 kJ/mole. Therefore it is easier to break the H-H than D-D bond. Where reactions attain equilibrium, isotopic fractionations will be governed by the considerations of equilibrium discussed above. *Where reactions do not achieve equilibrium the lighter isotope will usually be preferentially concentrated in the reaction products*, because of this effect of the bonds involving light isotopes in the reactants being more easily broken. Large kinetic effects are associated with biologically mediated reactions (e.g., photosynthesis, bacterial reduction), because such reactions generally do not achieve equilibrium and do not go to completion (e.g., plants don't convert all CO_2 to organic carbon). Thus ^{12}C is enriched in the products of photosynthesis in plants (hydrocarbons) relative to atmospheric CO_2, and ^{32}S is enriched in H_2S produced by bacterial reduction of sulfate.

We can express this in a more quantitative sense. In Chapter 5, we found the reaction rate constant could be expressed as:

$$k = Ae^{-E_b/kT} \qquad (5.24)$$

where k is the rate constant, A the frequency factor, and E_b is the barrier energy. For example, in a dissociation reaction, the barrier energy is the difference between the dissociation energy and the zero-point energy when the molecule is in the ground state, or some higher vibrational frequency when it is

not (Fig. 9.1). The frequency factor is independent of isotopic composition, thus the ratio of reaction rates between the HD molecule and the H_2 molecule is:

$$\frac{k_D}{k_H} = \frac{e^{-(\varepsilon - 1/2 h\nu_D)/kT}}{e^{-(\varepsilon - 1/2 h\nu_H)/kT}} \qquad 9.37$$

or

$$\frac{k_D}{k_H} = e^{(\nu_H - \nu_D)h/2kT} \qquad 9.38$$

Substituting for the various constants, and using the wavenumbers given in the caption to Figure 9.1 (remembering that $\omega = c\nu$, where c is the speed of light) the ratio is calculated as 0.24; in other words we expect the H_2 molecule to react four times faster than the HD molecule, a very large difference. For heavier elements, the rate differences are smaller. For example, the same ratio calculated for $^{16}O_2$ and $^{18}O^{16}O$ shows that the $^{16}O_2$ will react about 15% faster than the $^{18}O^{16}O$ molecule.

The greater translational velocities of lighter molecules also allow them to break through a liquid surface more readily and hence evaporate more quickly than a heavy molecule of the same composition. Thus water vapor above the ocean is typically around $\delta^{18}O = -13$ per mil, whereas at equilibrium the vapor should only be about 9 per mil lighter than the liquid.

Let's explore this a bit further. An interesting example of a kinetic effect is the fractionation of O isotopes between water and water vapor. This is an example of Rayleigh distillation (or condensation), and is similar to fractional crystallization. Let A be the amount of the species containing the major isotope, e.g., $H_2{}^{16}O$, and B be the amount of the species containing the minor isotope, e.g., $H_2{}^{18}O$. The rate at which these species evaporate is proportional to the amount present:

$$dA = k_A A \qquad 9.39a$$

and

$$dB = k_B B \qquad 9.39b$$

Since the isotopic composition affects the reaction, or evaporation, rate, $k_A \neq k_B$. Earlier we saw that for equilibrium fractionations, the fractionation factor is related to the equilibrium constant. For kinetic fractionations, the fractionation factor is simply the ratio of the rate constants, so that:

$$\frac{k_B}{k_A} = \alpha \qquad 9.40$$

and

$$\frac{dB}{dA} = \alpha \frac{B}{A} \qquad 9.41$$

Rearranging and integrating, we have:

$$\ln \frac{B}{B^\circ} = \alpha \ln \frac{A}{A^\circ}$$

or

$$\frac{B}{B^\circ} = \left(\frac{A}{A^\circ} \right)^\alpha \qquad 9.42$$

where A° and B° are the amount of A and B originally present. Dividing both sides by A/A°:

$$\frac{B/A}{B^\circ/A^\circ} = \left(\frac{A}{A^\circ} \right)^{\alpha - 1} \qquad 9.43$$

Since the amount of B makes up only a trace of the total amount of H_2O present, A is essentially equal to the total water present, and A/A° is essentially identical to f, the fraction of the origi-

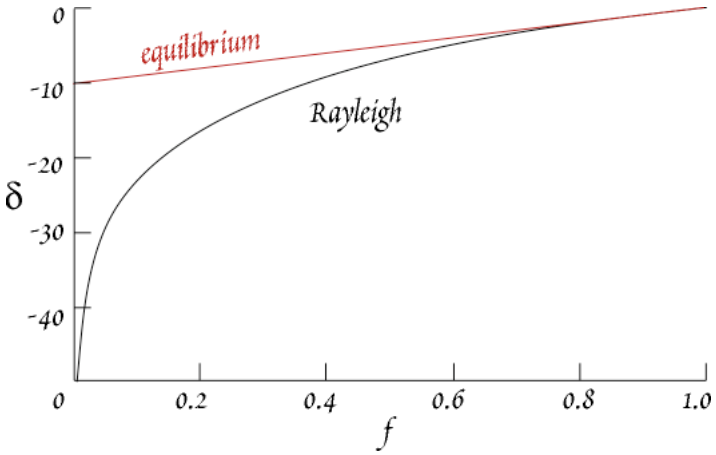

Figure 9.5. Fractionation of isotope ratios during Rayleigh and equilibrium condensation. δ is the per mil difference between the isotopic composition of original vapor and the isotopic composition when fraction f of the vapor remains.

nal water remaining. Hence:

$$\frac{B/A}{B^\circ/A^\circ} = f^{\alpha-1} \qquad 9.44$$

Subtracting 1 from both sides, we have:

$$\frac{B/A - B^\circ/A^\circ}{B^\circ/A^\circ} = f^{\alpha-1} - 1 \qquad 9.45$$

The left side of 9.45 is the relative deviation from the initial ratio. The permil relative deviation is simply:

$$\Delta = 1000(f^{\alpha-1} - 1) \qquad 9.46$$

Of course, the same principle applies when water condenses from vapor. Assuming a value of α of 1.01, δ will vary with f, the fraction of vapor remaining, as shown in Figure 9.5.

Even if the vapor and liquid remain in equilibrium through the condensation process, the isotopic composition of the remaining vapor will change continuously. The relevant equation is:

$$\Delta = \left(1 - \frac{1}{(1-f)/\alpha + f}\right) \times 1000 \qquad 9.47$$

The effect of equilibrium condensation is also shown in Figure 9.5.

9.2.3 Mass Dependent and Mass Independent Fractionations

Oxygen and sulfur have both have more than two isotopes, as do, of course, many other elements. How do we expect the fractionations between various isotope ratios to be related? For example, if a 4‰ fractionation of $\delta^{18}O$ is observed in a particular sample, what value of $\delta^{17}O$ do we predict? A first guess might be that we would expect the difference in the fractionation to be proportional to the mass difference. In other words, if $\delta^{18}O$ is increased by 4‰ in some process, we would expect $\delta^{17}O$ to be increased by about 2‰. If we think about this in a little more detail, we realize that fractionation factors are more complex functions of mass. Looking at equation 9.26, for example, we see that mass occurs in a variety of ways, as $m^{3/2}$, as reduced mass, and complexly in the exponential term. Consequently, the ratio of fractionation of $^{17}O/^{16}O$ to that of $^{18}O/^{16}O$ won't be exactly ½. In fact, in almost all cases the ratio is, on average, about 0.52. Thus the fractionation between isotopes does seem to be proportional to the difference in mass – this is referred to as *mass dependent fractionation*.

There are, however, some exceptions where the ratio of fractionation of $^{17}O/^{16}O$ to that of $^{18}O/^{16}O$ is close to 1. Since the extent of fractionation in these cases seems independent of the mass difference, this is called *mass independent fractionation*. Mass independent fractionation is rare. It was first observed oxygen isotope ratios in meteorites (see Chapter 10) and has subsequently been observed in oxygen isotope ratios of atmospheric gases, most dramatically in stratospheric ozone (Figure 9.6), and most recently in sulfur isotope ratios of Archean sediments and modern sulfur-bearing aerosols in ice. The causes of mass independent fractionation are poorly understood and it seems likely there may be more than one cause.

There is at least a partial theoretical explanation in the case of atmospheric ozone (Gao and Marcus, 2001). Their theory can be roughly explained as follows. Formation of ozone in the stratosphere typically involves the energetic collision of monatomic and molecular oxygen, i.e.:

$$O + O_2 \rightarrow O_3$$

The ozone molecule thus formed is in an vibrationally excited state and, consequently, subject to dissociation if it cannot loose this excess energy. The excess vibrational energy can be lost either by collisions with other molecules, or by partitioning to rotational energy. In the stratosphere, collisions infrequent compared hence repartitioning of vibrational energy represents an important pathway to stability. Because there are more possible energy transitions for asymmetric species such as $^{16}O^{16}O^{18}O$ and $^{16}O^{16}O^{17}O$ than symmetric ones such as $^{16}O^{16}O^{16}O$, the latter is repartition its excess energy and form a stable molecule. At higher pressures, such as prevail in the troposphere, the symmetric molecule can loose energy through far more frequent collisions, lessening the importance of the vibrational to rotational

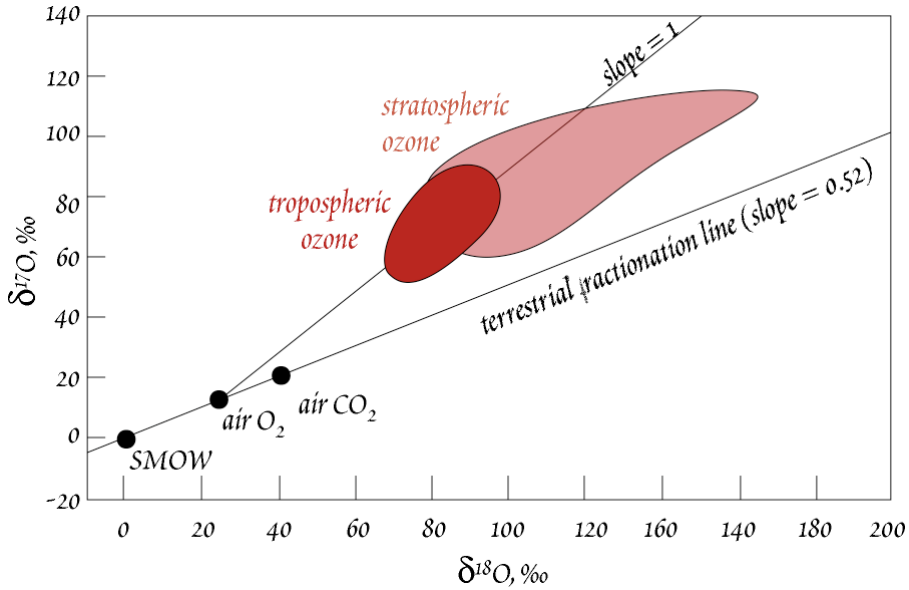

Figure 9.6. Oxygen isotopic composition in the stratosphere and troposphere show the effects of mass independent fractionation. A few other atmospheric trace gases show similar effects. Essentially all other material from the Earth and Moon plot on the *terrestrial fractionation line*.

energy conversion. Gao and Marcus (2001) were able to closely match observed experimental fractionations, but their approach was in part empirical because a fully quantum mechanical treatment is not yet possible.

Theoretical understanding of mass independent sulfur isotope fractionations is less advanced. Mass independent fractionations similar to those observed (discussed below) have been produced in the laboratory by photo dissociation (photolysis) of SO_2 and SO using deep ultraviolet radiation (wavelengths <220 nm). Photolysis at longer wavelengths does not produce mass independent fractionations. Current explanations therefore focus on ultraviolet photolysis. However, there as yet is no theoretical explanation of this effect and alternative explanations, including ones that involve the role in symmetry in a manner analogous to ozone, cannot be entirely ruled out.

9.3 Isotope Geothermometry

One of the principal uses of stable isotopes is geothermometry. Like "conventional" chemical geothermometers, stable isotope geothermometers are based on the temperature dependence of the equilibrium constant. As we have seen, this dependence may be expressed as:

$$\ln K = \ln \alpha = A + \frac{B}{T^2} \qquad 9.48$$

In actuality, the constants *A* and *B* are slowly varying functions of temperature, such that K tends to zero at absolute 0, corresponding to complete separation, and to 1 at infinite temperature, corresponding to no isotope separation. We can obtain a qualitative understanding of why this as so by recalling

Table 9.2. Coefficients for Oxygen Isotope Fractionation at Low Temperatures:
$\Delta_{Qz\text{-}\phi} = A + B \times 10^6/T^2$

ϕ	A	B
Feldspar	0	0.97 + 1.04b*
Pyroxene	0	2.75
Garnet	0	2.88
Olivine	0	3.91
Muscovite	–0.60	2.2
Amphibole	–0.30	3.15
Biotite	–0.60	3.69
Chlorite	–1.63	5.44
Ilmenite	0	5.29
Magnetite	0	5.27

* *b* is the mole fraction of anorthite in the feldspar. This term therefore accounts for the compositional dependence discussed above. From Javoy (1976).

that the entropy of a system increases with temperature. At infinite temperature, there is complete disorder, hence isotopes would be mixed randomly between phases (ignoring for the moment the slight problem that at infinite temperature there would be neither phases nor isotopes). At absolute 0, there is perfect order, hence no mixing of isotopes between phases. A and B are, however, sufficiently invariant over a limited range temperatures that they can be viewed as constants. We have also noted that at low temperatures, the form of equation 9.48 changes to $K \propto 1/T$.

TABLE 9.3 COEFFICIENTS FOR OXYGEN ISOTOPE FRACTIONATIONS AT ELEVATED TEMPERATURES (600° - 1300°C)

	Cc	Ab	An	Di	Fo	Mt
Qz	0.38	0.94	1.99	2.75	3.67	6.29
Cc		0.56	1.61	2.37	3.29	5.91
Ab			1.05	1.81	2.73	5.35
An				0.76	1.68	4.30
Di					0.92	3.54
Fo						2.62

Coefficients are for mineral pair fractionations expressed as $1000\alpha = B \times 10^6/T^2$ where B is given in the Table. Qz: quartz, Cc: calcite, Ab: albite, An: anorthite, Di: diopside, Fo: forsterite, Mt: magnetite. For example, the fractionation between albite and diopside is $1000\alpha_{An\text{-}Di} = 1.81 \times 10^6/T^2$ (T in kelvins). From Chiba et al. (1989).

In principal, a temperature may be calculated from the isotopic fractionation between any two phases provided the phases equilibrated and the temperature dependence of the fractionation factor is known. And indeed, there are too many isotope geothermometers for all of them to be mentioned here. Figure 9.7 shows some fractionation factors between quartz and other minerals as a function of temperature. Figure 9.8 shows sulfur isotope fractionation factors between various sulfur-bearing species and H_2S. Table 9.2 lists coefficients *A* and *B* for equation 9.48 for the oxygen isotope fractionation factor between quartz and other oxides and silicates.

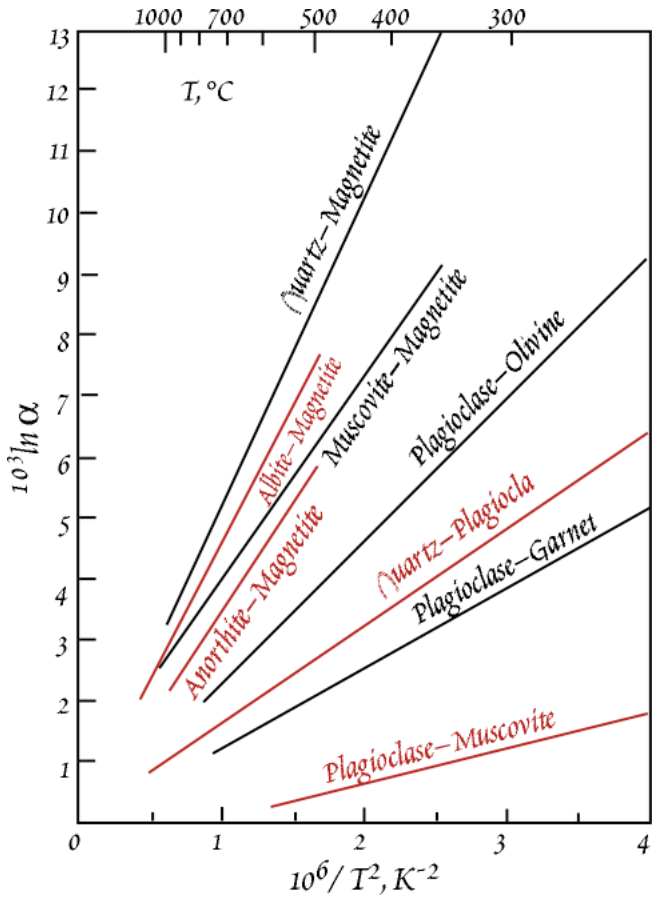

Figure 9.7. Oxygen isotope fractionation for several mineral pairs as a function of temperature.

Because of the dependence of the equilibrium constant on the inverse square of temperature, stable isotope geothermometry is employed primarily at low temperatures, that is, non-magmatic temperatures. At temperatures in excess of 800°C or so, the fractionations are generally small, making accurate temperatures difficult to determine from them. However, even at temperatures of the upper mantle (1000°C or more), fractionations, although small, remain significant. Experimentally determined fractionation factors for minerals in the temperature range of 600° to 1300°C, which agree well with theoretical calculations, are given in Table 9.3.

Table 9.4 lists similar coefficients for the sulfur fractionation between H_2S and sulfur-bearing compounds. Recall that if phases α and γ and α and β are in equilibrium with each other, then γ is also in equilibrium with β. Thus these tables may be used to obtain the fractionation between any two of the phases listed.

All geothermometers are based on the ap-

parently contradictory assumptions that complete equilibrium was achieved between phases during, or perhaps after, formation of the phases, but that the phases did not re-equilibrate when they subsequently cooled. The reason these assumptions can be made and geothermometry works at all is the exponential dependence of reaction rates on temperature that we discussed in Chapter 5. Isotope geothermometers have the same implicit assumptions about the achievement of equilibrium as other geothermometers.

The importance of the equilibrium basis of geothermometry must be emphasized. Because most stable isotope geothermometers (though not all) are applied to relatively low temperature situations, violation of the assumption that complete equilibrium was achieved is not uncommon. We have seen that isotopic fractionations may arise from kinetic as well as equilibrium effects. If reactions do not run to completion, the isotopic differences may reflect kinetic effects as much as equilibrium effects. There are other problems that can result in incorrect temperature as well; for example, the system may partially re-equilibration at some lower temperature during cooling. A further problem with isotope geothermometry is that free energies of the exchange reactions are relatively low; meaning there is little chemical energy available to drive the reaction. Indeed, isotopic equilibrium probably often depends on other reactions occurring that mobilize the element involved in the exchange. Solid-state exchange reactions will be particularly slow at temperatures well below the melting point. Equilibrium between solid phases will thus generally depend on reaction of these phases with a fluid. This latter point is true of 'conventional' geothermometers as well, and metamorphism, one of the important areas of application of isotope geothermometry, generally occurs in the presence of a fluid.

Isotope geothermometers do have several advantages over conventional chemical ones. First, as we have noted, there is no volume change associated with isotopic exchange reactions and hence no pressure dependence of the equilibrium constant. However, Rumble has suggested an indirect pressure dependence, wherein the fractionation factor depends on fluid composition, which in turn depends on pressure. Second, whereas conventional chemical geothermometers are generally based on solid solution, isotope geothermometers can make use of pure phases such as SiO_2, etc. Generally, any dependence on the composition of phases involved is of relatively second order

TABLE 9.4. COEFFICIENTS FOR SULFUR ISOTOPE FRACTIONATION:

$\Delta\ \phi\text{-}H_2S = A\times10^6/T^2 + B\times10^3/T$ (T in kelvins)

ϕ	B	A	T°C Range
$CaSO_4$	6.0±0.5	5.26	200-350
SO_2	–5±0.5	4.7	350-1050
FeS_2		0.4±0.08	200-700
ZnS		0.10±0.05	50-705
CuS		–0.4±0.1	
Cu_2S		–0.75±0.1	
SnS		–0.45±0.1	
MoS_2		0.45±0.1	
Ag_2S		–0.8±0.1	
PbS		–0.63±0.05	50-700

From Ohmoto and Rye (1979)

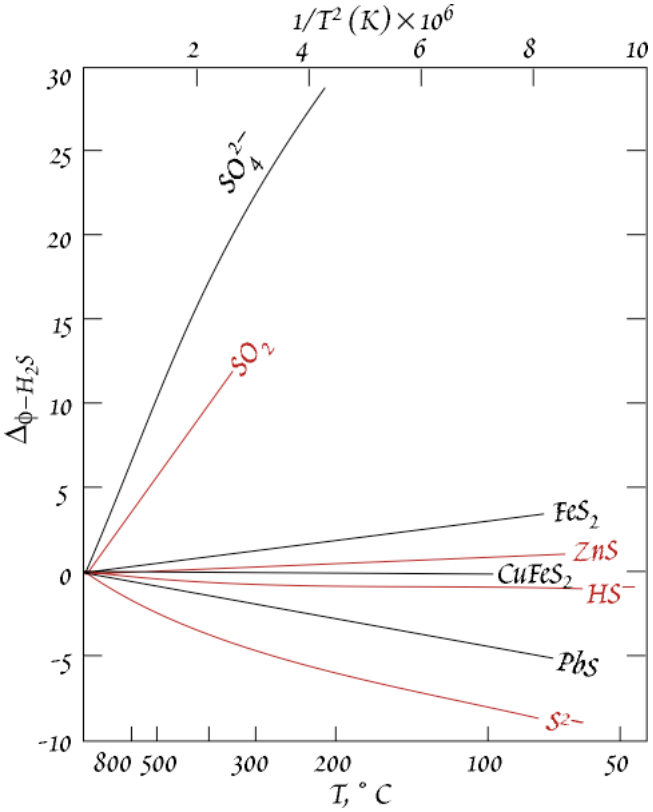

Figure 9.8. Relationship of S isotope fractionation between H_2S and other sulfur-bearing species and temperature.

EXAMPLE 9.2: OXYGEN ISOTOPE GEOTHERMOMETRY

A granite-gneiss contains coexisting quartz, muscovite and magnetite of with the following $\delta^{18}O$: quartz: 11.1, magnetite: 1.9. Find the temperature of equilibration.

Answer: According to Bottinga and Javoy (1973), the fraction factors for these minerals can be expressed as:

$$1000 \ln \alpha_{Qz-H_2O} = -3.70 + \frac{4.10 \times 10^6}{T^2} \qquad \text{and} \qquad 1000 \ln \alpha_{Mt-H_2O} = -3.10 + \frac{1.9 \times 10^6}{T^2}$$

The fractionation factor $\alpha_{Qz\text{-}Mt}$ can be found as: $\alpha_{Qz\text{-}H2O} / \alpha_{Mt\text{-}H2O}$, and

$$1000 \ln \alpha_{Qz-Mt} = 1000(\ln \alpha_{Qz-H_2O} - \ln \alpha_{Mt-H_2O})$$

$$= -3.70 + \frac{4.10}{T^2} + 3.10 - \frac{1.9 \times 10^6}{T^2} = 0.6 + \frac{2.20 \times 10^6}{T^2}$$

Substituting $\Delta_{Qz\text{-}Mag}$ for 1000 ln $\alpha_{Qz\text{-}Mag}$ and solving for T:

$$T = \sqrt{\frac{2.20 \times 10^6}{\Delta_{Qz-Mt} - 0.6}} \qquad 9.49$$

We calculate $\Delta_{Qz\text{-}Mag}$ as 9.2‰. Substituting this into 9.49, we find T = 505 K, = 232 ° C.

importance (there are, however, exceptions). For example, isotopic exchange between calcite and water is independent of the concentration of CO_2 in the water. Compositional effects can be expected only where it effects bonds formed by the element involved in the exchange. For example, we noted substitution of Al for Si in plagioclase affects O isotope fractionation factors because the nature of the bond with oxygen.

9.4 ISOTOPE FRACTIONATION IN THE HYDROLOGIC SYSTEM

As we noted above, isotopically light water has a higher vapor pressure, and hence lower boiling point, than isotopically heavy water. Let's consider this in a bit more detail. Raoult's Law (equ. 3.8) states that the partial pressure of a species above a solution is equal to its molar concentration in the solution times the partial pressure exerted by the pure solution. So for the two isotopic species of water (we will restrict ourselves to O isotopes for the moment), Raoult's Law is:

$$p_{H_2{}^{16}O} = p^o_{H_2{}^{16}O}[H_2{}^{16}O] \qquad 9.50a$$

and

$$p_{H_2{}^{18}O} = p^o_{H_2{}^{18}O}[H_2{}^{18}O] \qquad 9.49b$$

where p is the partial pressure and, as usual, the brackets indicate the aqueous concentration. Since the partial pressure of a species is proportional to the number of atoms of that species in a gas, we can define the fractionation factor, α, between liquid water and vapor as:

$$\alpha_{v/l} = \frac{p_{H_2{}^{18}O} / p_{H_2{}^{16}O}}{[H_2{}^{18}O] / [H_2{}^{16}O]} \qquad 9.51$$

Substituting 9.50a and 9.50b into 9.51, we arrive at the relationship:

$$\alpha_{v/l} = \frac{p^o_{H_2{}^{18}O}}{p^o_{H_2{}^{16}O}} \qquad 9.52$$

Thus interestingly enough, the fractionation factor for oxygen between water vapor and liquid turns out to be just the ratio of the standard state partial pressures. The next question is how the partial pressures vary with temperature. Thermodynamics provides the answer. The temperature dependence of the partial pressure of a species may be expressed as:

$$\frac{d\ln p}{dT} = \frac{\Delta H}{RT^2} \qquad 9.53$$

where T is temperature, ΔH is the enthalpy or latent heat of evaporation, and R is the gas constant. Over a sufficiently small range of temperature, we can assume that ΔH is independent of temperature. Rearranging and integrating, we obtain:

$$\ln p = \frac{\Delta H}{RT} + const \qquad 9.54$$

We can write two such equations, one for $[H_2^{16}O]$ and [one for $H_2^{18}O$]. Dividing one by the other we obtain:

$$\ln \frac{p^o_{H_2{}^{18}O}}{p^o_{H_2{}^{16}O}} = a - \frac{B}{RT} \qquad 9.55$$

where a and B are constants. This can be rewritten as:

$$\alpha = ae^{B/RT} \qquad 9.56$$

Over a larger range of temperature, ΔH is not constant. The log of the fractionation factor in that case depends on the inverse square of temperature, so that the temperature dependence of the fractionation factor can be represented as:

$$\ln\alpha = a - \frac{B}{T^2} \qquad 9.57$$

Given the fractionation between water and vapor, we might predict that there will be considerable variation in the isotopic composition of water in the hydrologic cycle, and indeed there is. Figure 9.9 shows the global variation in $\delta^{18}O$ in *precipitation*.

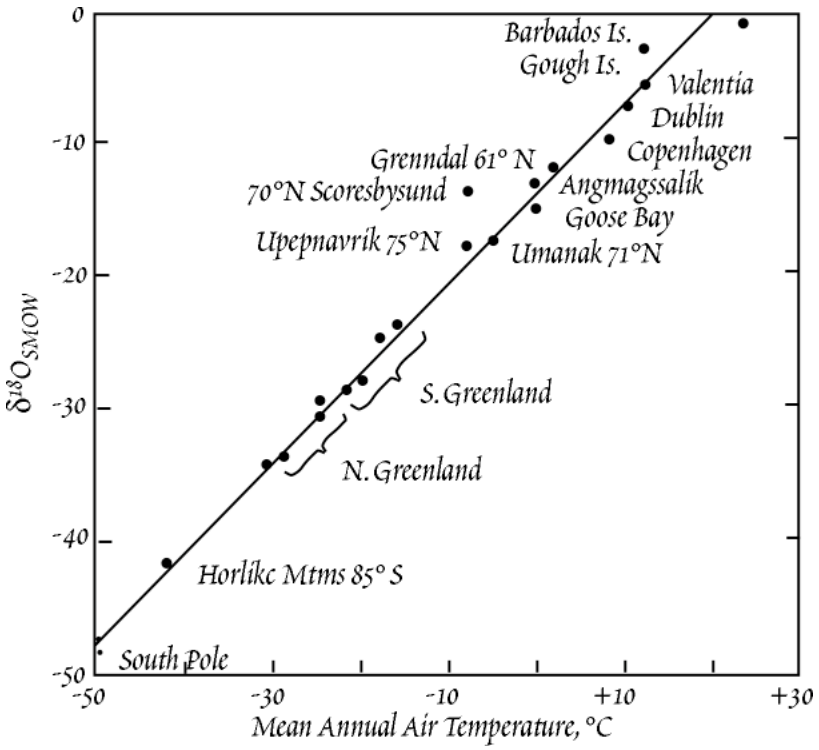

Figure 9.9. Variation of $\delta^{18}O$ in precipitation as a function of mean annual temperature.

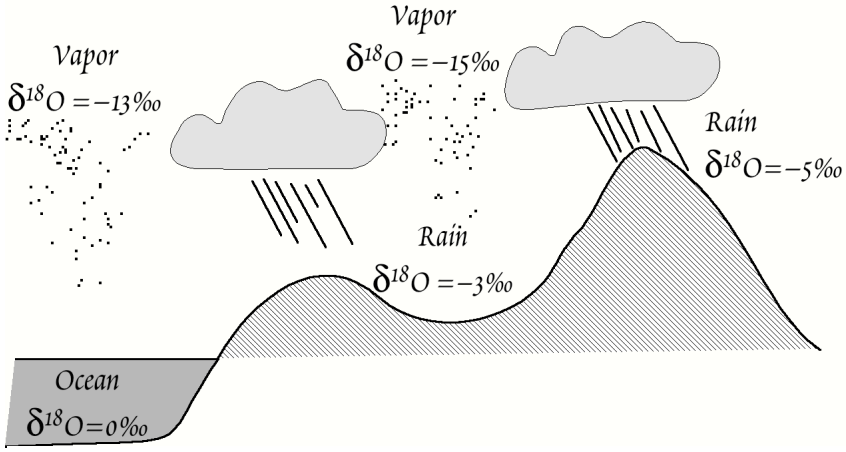

Figure 9.10. Cartoon illustrating the process of Rayleigh fractionation and the decreasing $\delta^{18}O$ in rain as it moves inland.

Precipitation of rain and snow from clouds is a good example of Rayleigh condensation. Isotopic fractionations will therefore follow equation 9.46. Thus in addition to the temperature dependence of α, the isotopic composition of precipitation will also depend on f, the fraction of water vapor remaining in the air. The further air moves from the site of evaporation, the more water is likely to have condensed and fallen as rain, and therefore, the smaller the value of f in equation 9.46. Thus fractionation will increase with distance from the region of evaporation (principally tropical and temperature oceans). Topography also plays a role as mountains force air up, causing it to cool and water vapor to

condense, hence decreasing f. Thus precipitation from air that has passed over a mountain range will be isotopically lighter than precipitation on the ocean side of a mountain range. These factors are illustrated in the cartoon in Figure 9.10.

Hydrogen as well as oxygen isotopes will be fractionated in the hydrologic cycle. Indeed, $\delta^{18}O$ and δD are reasonably well correlated in precipitation, as is shown in Figure 9.11. The fractionation of hydrogen isotopes, however, is greater because the mass difference is greater.

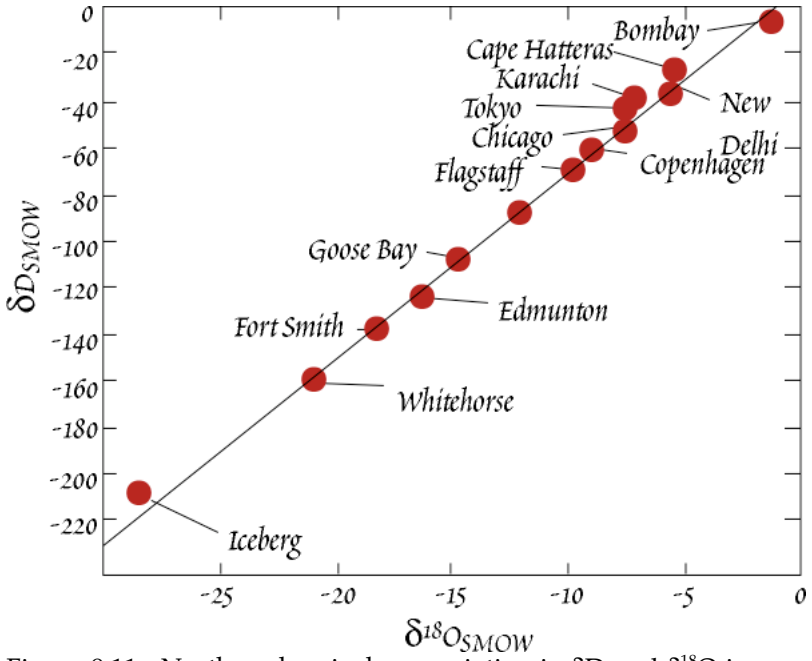

Figure 9.11. Northern hemisphere variation in δD and $\delta^{18}O$ in precipitation and meteoric waters. The relationship between δD and $\delta^{18}O$ is approximately $\delta D = 8 \times \delta^{18}O + 10$. After Dansgaard (1964).

9.5 Isotope Fractionation in Biological Systems

Biological processes often involve large isotopic fractionations. Indeed, for carbon, nitrogen, and sulfur, biological processes are the most important cause of isotope fractionations. For the most part, the largest fractionations occur during the initial production of organic matter by the so-called primary producers, or *autotrophs*. These include all plants and many kinds of bacteria. The most important means of production of organic matter is photosynthesis, but organic matter may also be produced by chemosynthesis, for example at mid-ocean ridge hydrothermal vents. Large fractionations of both carbon and nitrogen isotopes occur during primary production. Additional fractionations also occur in subsequent reactions and up through the food chain as *hetrotrophs* consume primary producers, but these are generally smaller.

9.5.1 Carbon Isotope Fractionation During Photosynthesis

Biological processes are the principal cause of variations in carbon isotope ratios. The most important of these processes is photosynthesis (a discussion of photosynthesis may be found in Chapter 14). As we earlier noted, photosynthetic fractionation of carbon isotopes is primarily kinetic. The early work of Park and Epstein (1960) suggested fractionation occurred in several steps. Subsequent work has elucidated the fractionations involved in these steps, which we will consider in slightly more detail.

For terrestrial plants (those utilizing atmospheric CO_2), the first step is diffusion of CO_2 into the boundary layer surrounding the leaf, through the stomata, and internally in the leaf. On theoretical grounds, a fractionation of –4.4‰ is expected, as we found in equation 9.36. Marine algae and aquatic plants can utilize either dissolved CO_2 or HCO_3^- for photosynthesis:

$$CO_{2(g)} \rightarrow CO_{2(aq)} + H_2O \rightarrow H_2CO_3 \rightarrow H^+ + HCO_3^-$$

An equilibrium fractionation of +0.9 per mil is associated with dissolution ($^{13}CO_2$ will dissolve more readily), and an equilibrium +7.0 to +8‰ fractionation occurs during hydration and dissociation of CO_2 (i.e., steps 2 and 3 in the reaction above).

At this point, there is a divergence in the chemical pathways. Most plants use an enzyme called *ribulose bisphosphate carboxylase oxygenase* (RUBISCO) to catalyze a reaction in which *ribulose bisphosphate carboxylase* reacts with one molecule of CO_2 to produce 3 molecules of 3-phosphoglyceric acid, a com-

pound containing 3 carbon atoms, in a process called *carboxylation* (Figure 9.12). The carbon is subsequently reduced, carbohydrate formed, and the ribulose bisphosphate regenerated. Such plants are called C_3 plants, and this process is called the Benson-Calvin Cycle, or simply the Calvin Cycle. C_3 plants constitute about 90% of all plants today and include algae and autotrophic bacteria and comprise the majority of cultivated plants, including wheat, rice, and nuts. There is a kinetic fractionation associated with carboxylation of ribulose bisphosphate that has been determined by several methods to be –29.4‰ in higher terrestrial plants. Bacterial carboxylation has different reaction mechanisms and a smaller fractionation of about -20‰. Thus for terrestrial plants a fractionation of about –34‰ is expected from the sum of the individual fractionations. The actual observed total fractionation is in the range of –20 to –30‰. The disparity between the observed total fractionation and that expected from the sum of the steps presented something of a conundrum. This solution appears to be a model that assumes the amount of carbon isotope fractionation expressed in the tissues of plants depends on the ratio of the concentration of CO_2 inside plants to that in the external environment: the more photosynthesis depletes the CO_2 in the plant interior, the less the fractionation that occurs.

The other photosynthetic pathway is the Hatch-Slack cycle, used by the C_4 plants that include hot-region grasses and related crops such as maize and sugarcane. These plants use *phosphenol pyruvate carboxylase* (PEP) to fix the carbon initially and form oxaloacetate, a compound that contains 4 carbons (Fig. 9.13). A much smaller fractionation, about -2.0 to -2.5‰, occurs during this step. In phosphophoenol pyruvate carboxylation, the CO_2 is fixed in outer mesophyll cells as oxaloacetate and carried as part of a C_4 acid, either malate or asparatate, to inner bundle sheath cells where it is decarboxylated and refixed by RuBP (Fig. 9.14). The environment in the bundle sheath cells is almost a closed system, so that virtually all the carbon carried there is refixed by RuBP, so there is little fractionation during this step. Thus C_4 plants have average $\delta^{13}C$ of -13‰, much less than C_3 plants. As in the case of RuBP photosynthesis, the fractionation appears to depend on the ambient concentration of CO_2.

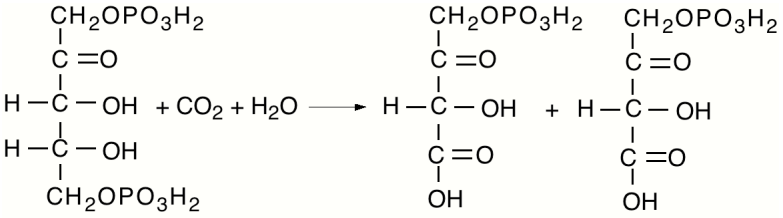

Figure 9.12. Ribulose bisphosphate (RuBP) carboxylation, the reaction by which C_3 plants fix carbon during photosynthesis.

A third group of plants, the CAM plants, has a unique metabolism called the *Crassulacean acid metabolism*. These plants generally use the C_4 pathway, but can use the C_3 pathway under certain conditions. These plants are generally succulents adapted to arid environments and include pineapple and many cacti; they have $\delta^{13}C$ intermediate between C_3 and C_4 plants.

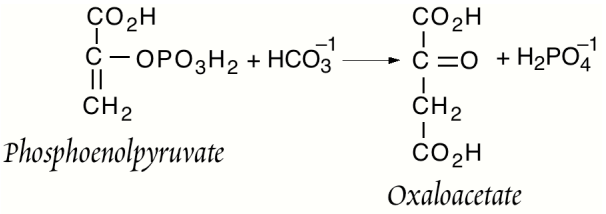

Figure 9.13. Phosphoenolpyruvate carboxylation, the reaction by which C_4 plants fix CO_2 during photosynthesis.

Terrestrial plants, which utilize CO_2 from the atmosphere, generally produce greater fractionations than marine and aquatic plants, which utilize dissolved CO_2 and HCO_3^-, together referred to as *dissolved inorganic carbon* or DIC. As we noted above, there is about a +8‰ equilibrium fractionation between dissolved CO_2 and HCO_3^-. Since HCO_3^- is about 2 orders of

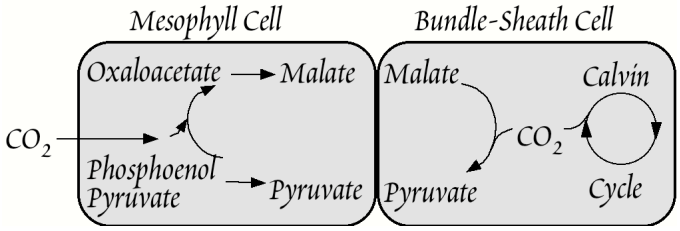

Figure 9.14. Chemical pathways in C_4 photosynthesis.

magnitude more abundant in seawater than dissolved CO_2, marine algae utilize this species, and hence tend to show a lower net fractionation between dissolved carbonate and organic carbon during photosynthesis. Diffusion is slower in water than in air, so diffusion is often the rate-limiting step. Most aquatic plants have some membrane-bound mechanism to pump DIC, which can be turned on when DIC is low. When DIC concentrations are high, fractionation in aquatic and marine plants is generally similar to that in terrestrial plants. When it is low and the plants are actively pumping DIC, the fractionation is less because most of the carbon pumped into cells is fixed. Thus carbon isotope fractionations between dissolved inorganic carbon and organic carbon can be as low as 5‰ in algae.

Not surprisingly, the carbon isotope fractionation in C fixation is also temperature dependent. Thus higher fractionations are observed in cold-water phytoplankton than in warm water species. However, this observation also reflects a kinetic effect: there is generally less dissolved CO_2 available in warm waters because of the decreasing solubility with temperature. As a result, a larger fraction of the CO_2 is utilized and there is consequently less fractionation. Surface waters of the ocean are generally enriched in ^{13}C (relative to ^{13}C) because of uptake of ^{12}C during photosynthesis (Figure 9.15). The degree of enrichment depends on the productivity: biologically productive areas show greater depletion. Deep water, on the other hand, is enriched in ^{12}C. Organic matter falls through the water column and is decomposed and "remineralized", i.e., converted to inorganic carbon, by the action of bacteria, enriching deep water in ^{12}C and total DIC. Thus biological activity acts to "pump" carbon, and particularly ^{12}C from surface to deep waters.

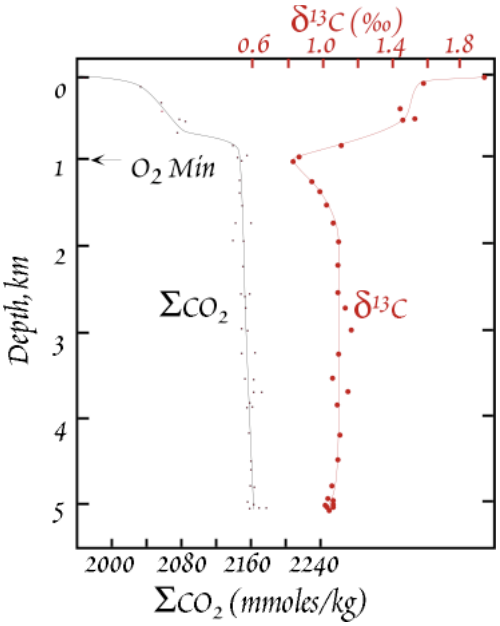

Figure 9.15. Depth profile of total dissolved inorganic carbon and $\delta^{13}C$ in the North Atlantic.

Nearly all organic matter originates through photosynthesis. Subsequent reactions convert the photosynthetically produced carbohydrates to the variety of other organic compounds utilized by organisms. Further fractionations occur in these reactions. These fractionations are thought to be kinetic in origin and may partly arise from organic C-H bonds being enriched in ^{12}C and organic C-O bonds are enriched in ^{13}C. ^{12}C is preferentially consumed in respiration (again, because bonds are weaker and it reacts faster), which enriches residual organic matter in ^{13}C. Thus the carbon isotopic composition of organisms becomes slightly more positive moving up the food chain.

The principal exception to the creation of organic matter through photosynthesis is *chemosynthesis*. In chemosynthesis, chemical reactions rather than light provides the energy to "fix" CO_2. Regardless of the energy source, however, fixation of CO_2 involves the Calvin-Benson cycle and RUBSICO. Not surprisingly, then, chemosynthesis typically results in carbon isotope fractionations similar to those of photosynthesis. Thus large carbon isotope fractionations are the signature of both photosynthesis and chemosynthesis.

9.5.2 Nitrogen Isotope Fractionation in Biological Processes

Nitrogen is another important element in biological processes, being an essential component of all amino acids, proteins, and other key compounds such as RNA and DNA. The understanding of isotopic fractionations of nitrogen is much less advanced than that of carbon. There are five important forms of inorganic nitrogen (N_2, NO_3^-, NO_2^-, NH_3 and NH_4^+). Equilibrium isotope fractionations occur between these five forms, and kinetic fractionations occur during biological assimilation of nitrogen. Ammonia is the form of nitrogen that is ultimately incorporated into organic matter by growing plants. Most terrestrial plants depend on symbiotic bacteria for *fixation* (i.e., reduction) of N_2 and other

forms of nitrogen to ammonia. Many plants, including many marine algae, can utilize oxidized nitrogen, NO_3^- and NO_2^-, and a few (blue-green algae and legumes, for example) are able to utilize N_2 directly. In these cases, nitrogen must first be reduced by the action of reductase enzymes. As with carbon, fractionation may occur in each of the several steps that occur in the nitrogen assimilation process. Denitrifying bacteria use nitrates as electron donors (i.e., as an oxidant) and reduce it without assimilating it. In this dissimilatory denitrification, there is a significant kinetic fractionation with the light isotope, ^{14}N, being preferentially reduced leaving residual nitrate enriched in ^{15}N by 6-7‰.

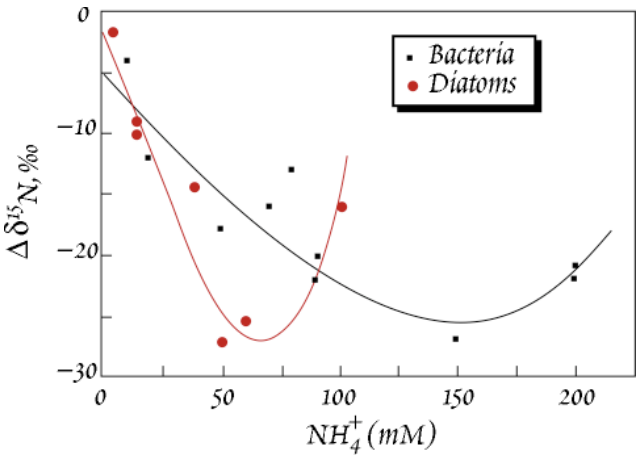

Figure 9.16. Dependence of nitrogen isotope fractionation by bacteria and diatoms on dissolved ammonium concentration.

While isotope fractionations during assimilation of ammonium are still poorly understood, it appears there is a strong dependence on the concentration of the ammonium ion. Such dependence has been observed, as for example in Figure 9.16. The complex dependence in Figure 9.16 is interpreted as follows. The increase in fractionation from highest to moderate concentrations of ammonium reflects the switching on of active ammonium transport by cells. At the lowest concentrations, essentially all available nitrogen is transported into the cell and assimilated, so there is little fractionation observed.

The isotopic compositions of marine particulate nitrogen and non-nitrogen-fixing plankton are typically –3‰ to +12‰ $\delta^{15}N$. Non-nitrogen fixing terrestrial plants unaffected by artificial fertilizers generally have a narrower range of +6‰ to +13 per mil, but are isotopically lighter on average. Marine blue-green algae range from -4 to +2, with most in the range of -4 to -2‰. Most nitrogen-fixing terrestrial plants fall in the range of –2 to +4‰, and hence are typically heavier than non-nitrogen fixing plants.

9.5.3 Oxygen and Hydrogen Isotope Fractionation by Plants

Oxygen is incorporated into biological material from CO_2, H_2O, and O_2. However, both CO_2 and O_2 are in oxygen isotopic equilibrium with water during photosynthesis, and water is the dominant source of O. Therefore, the isotopic composition of plant water determines the oxygen isotopic composition of plant material. The oxygen isotopic composition of plant material seems to be controlled by exchange reactions between water and carbonyl oxygens (oxygens doubly bound to carbon):

$$C={}^{16}O + H_2{}^{18}O \rightarrow C={}^{18}O + H_2{}^{16}O$$

Fractionations of +16 to +27‰ (i.e., the organically bound oxygen is heavier) have been measured for these reactions. Consistent with this, cellulose from most plants has $\delta^{18}O$ of +27±3‰. Other factors, however, play a role in the oxygen isotopic composition of plant material. First, the isotopic composition of water varies from $\delta^{18}O \approx -55$‰ in Arctic regions to $\delta^{18}O \approx 0$‰ in the oceans. Second, less than complete equilibrium may be achieved if photosynthesis is occurring at a rapid pace, result-

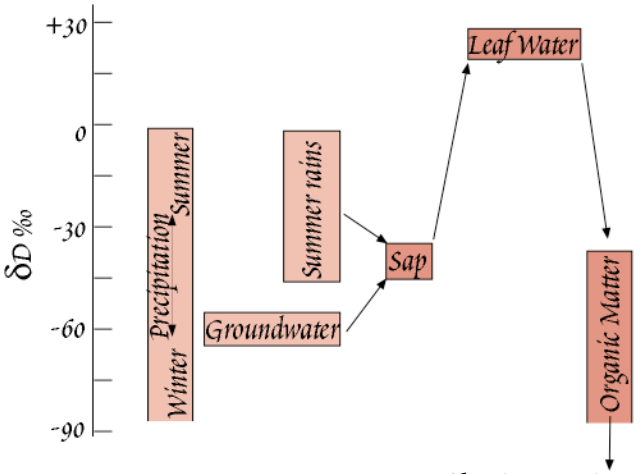

Figure 9.17. Isotopic Fractionations of hydrogen during primary production in terrestrial plants. After Fogel and Cifuentes (1993).

ing in less fractionation. Finally, some fractionation of water may occur during transpiration, with residual water in the plant becoming heavier.

Hydrogen isotope fractionation during photosynthesis occurs such that the light isotope is enriched in organic material. In marine algae, isotope fractionations of –100 to –150‰ have been observed, which is a little more than that observed in terrestrial plants (–86 to –120‰). Among terrestrial plants, there appears to be a difference between C_3 and C_4 plants. The former show fractionations of –117 to -121‰, while fractionations of –86 to –109‰ have been observed in C_4 plants. However, little is known in detail about the exact mechanisms of fractionation.

As for oxygen, variations in the isotopic composition of available water and fractionation during transpiration are important in controlling the hydrogen isotopic composition of plants. This is illustrated in Figure 9.17.

9.5.4 Biological Fractionation of Sulfur Isotopes

Though essential to life, sulfur is a minor component in living tissue (C:S atomic ratio is about 200). Plants take up sulfur as sulfate and subsequently reduce it to sulfide and incorporate it into cysteine, an amino acid. There is apparently no fractionation of sulfur isotopes in transport across cell membranes and incorporation, but there is a fractionation of +0.5 to –4.5‰ in the reduction process, referred to as *assimilatory sulfate reduction*. This is substantially less than the expected fractionation of about -20‰, suggesting most sulfur taken up by primary producers is reduced and incorporated into tissue.

Sulfur, however, plays two other important roles in biological processes. First, sulfur, in the form of sulfate, can act as an electron acceptor or oxidant, and is utilized as such by sulfur-reducing bacteria. This process, in which H_2S is liberated, is called *dissimilatory sulfate reduction* and plays an important role in biogeochemical cycles, both as a sink for sulfur and source for atmospheric oxygen. A large fractionation of +5 to –46‰ is associated with this process. This process produces by far the most significant fractionation of sulfur isotopes, and thus governs the isotopic composition of sulfur in the exogene. Sedimentary sulfate typically has $\delta^{34}S$ of about +17, which is similar to the isotopic composition of sulfate in the oceans (+20), while sedimentary sulfide has a $\delta^{34}S$ of –18. The living biomass has a $\delta^{34}S$ of ≈ 0.

The final important role of sulfur is a reductant. Sulfide is an electron acceptor used by some types of photosynthetic bacteria as well as other bacteria in the reduction of CO_2 to organic carbon. Unique among these perhaps are the chemosynthetic bacteria of submarine hydrothermal vents. They utilize H_2S emanating from the vents as an energy source and form the base of the food chain in these unique ecosystems. A fractionation of +2 to – 18‰ is associated with this process.

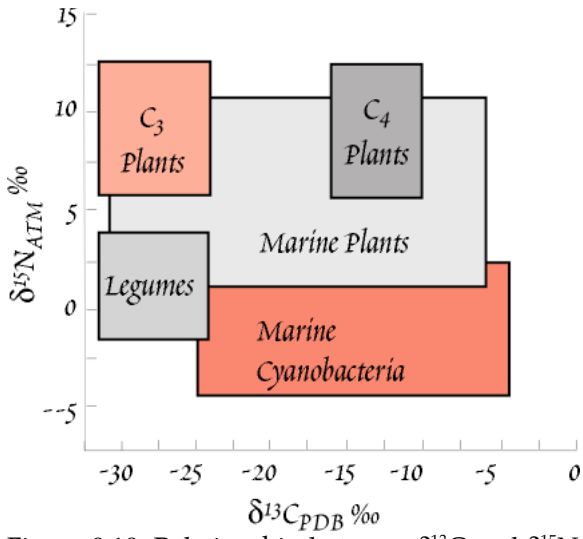

Figure 9.18. Relationship between $\delta^{13}C$ and $\delta^{15}N$ among the principal classes of autotrophs.

9.5.5 Isotopes and Diet: You Are What You Eat

As we have seen, the two main photosynthetic pathways, C_3 and C_4, lead to organic carbon with different carbon isotopic compositions. Terrestrial C_3 plants have $\delta^{13}C$ values that average of about -27‰, C_4 plants an average $\delta^{13}C$ of about -13‰. Marine plants (which are all C_3) utilized dissolved bicarbonate rather than atmospheric CO_2. Seawater bicarbonate is about 8.5‰ heavier than atmospheric CO_2, and marine plants average about 7.5‰ heavier than terrestrial C_3 plants. In addition, because the source of the carbon they fix is isotopically more variable, the isotopic composition of marine plants is also more variable. Finally, marine cyanobacteria (blue-green algae) tend to fractionate carbon isotopes less during photosynthesis than do true marine plants, so they tend to average 2 to 3‰ higher in $\delta^{13}C$.

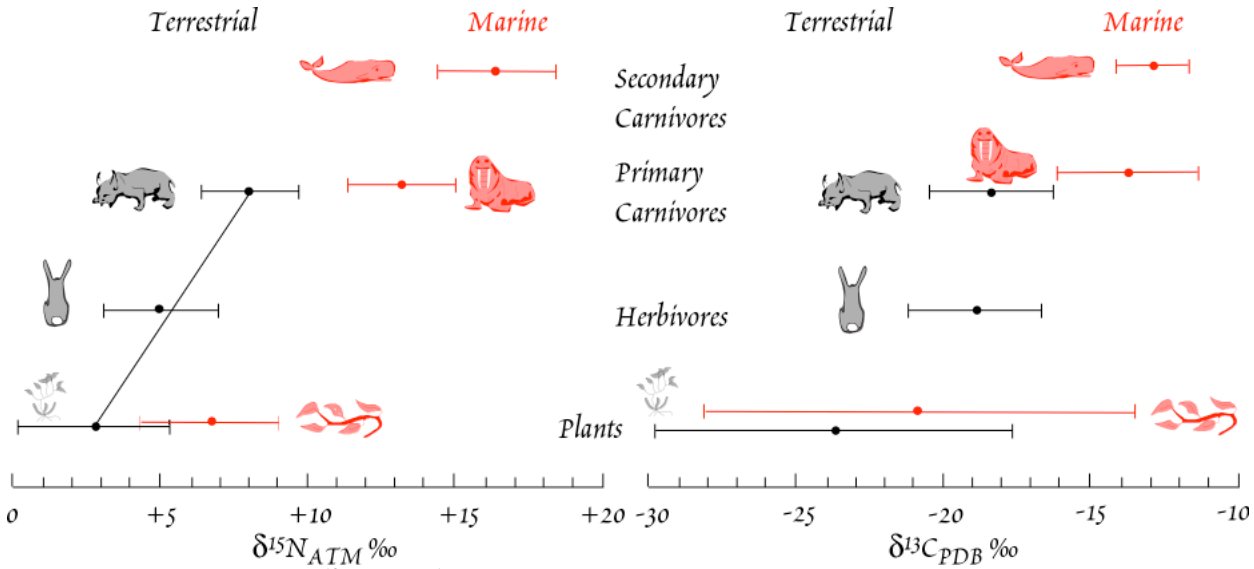

Figure 9.19. Values of $\delta^{13}C$ and $\delta^{15}N$ in various marine and terrestrial organisms. From Schoeninger and DeNiro (1984).

Plants may also be divided into two types based on their source of nitrogen: those that can utilized N_2 directly, and those that utilize only "fixed" nitrogen in ammonia and nitrate. The former include the legumes (e.g., beans, peas, etc.) and marine cyanobacteria. The legumes, which are exclusively C_3 plants, utilize both N_2 and fixed nitrogen, and have an average $\delta^{15}N$ of +1‰, whereas modern non-leguminous plants average about +3‰. Prehistoric nonleguminous plants were more positive, averaging perhaps +9‰, because the isotopic composition of present soil nitrogen has been affected by the use of chemical fertilizers. For both groups, there was probably a range in $\delta^{15}N$ of ±4 or 5‰, because the isotopic composition of soil nitrogen varies and there is some fractionation involved in uptake. Marine plants have $\delta^{15}N$ of +7±5‰, whereas marine cyanobacteria have $\delta^{15}N$ of –1±3‰. Thus based on their $\delta^{13}C$ and $\delta^{15}N$ values, autotrophs can be divided into several groups, which are summarized in Figure 9.18.

DeNiro and Epstein (1978) studied the relationship between the carbon isotopic composition of animals and their diet. They found that there is only slight further fractionation of carbon by animals and that the carbon isotopic composition of animal tissue closely reflects that of the animal's diet. Typically, carbon in animal tissue is about 1‰ heavier than their diet. The small fractionation between animal tissue and diet is a result of the slightly weaker bond formed by ^{12}C compared to ^{13}C. The weaker bonds are more readily broken during respiration, and, not surprisingly, the CO_2 respired by most animals investigated was slightly lighter than their diet. Thus only a small fractionation in carbon isotopes occurs as organic carbon passes up the food web. Terrestrial food chains usually do not have more than 3 trophic levels, implying a maximum further fractionation of +3‰; marine food chains can have up to 7 trophic levels, implying a maximum carbon isotope difference between primary producers and top predators of 7‰. These differences are smaller than the range observed in primary producers.

In another study, DeNiro and Epstein (1981) found that $\delta^{15}N$ of animal tissue reflects the $\delta^{15}N$ of the animal's diet, but is typically 3 to 4‰ higher than that of the diet. Thus in contrast to carbon, significant fractionation of nitrogen isotopes will occur as nitrogen passes up the food chain. These relationships are summarized in Figure 9.19. *The significance of these results is that it is possible to infer the diet of an animal from its carbon and nitrogen isotopic composition.*

Schoeninger and DeNiro (1984) found that the carbon and nitrogen isotopic composition of bone collagen in animals was similar to that of body tissue as a whole. Apatite in bone appears to undergo isotopic exchange with meteoric water once it is buried, but bone collagen and tooth enamel appear to be

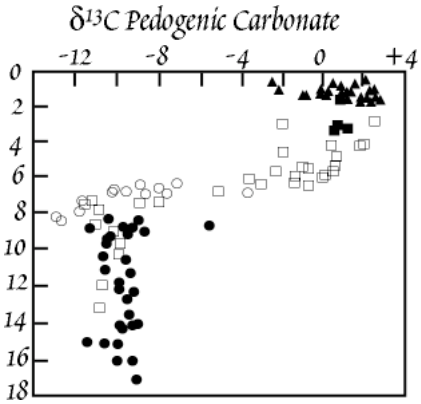

Figure 9.20. $\delta^{13}C$ in carbonates from paleosols of the Potwar Plateau in Pakistan. The change in $\delta^{13}C$ may reflect the evolution of C_4 plants. From Quade et al. (1989).

robust and retain their original isotopic compositions. This means that the nitrogen and carbon isotopic composition of fossil bone collagen and teeth can be used to reconstruct the diet of fossil animals.

Plant photosynthesis can also influence the isotopic composition of soil carbonate: when the plant dies, its organic carbon is incorporated into the soil and oxidized to CO_2 by bacteria and other soil organisms. In arid regions, some of this CO_2 precipitates as soil calcium carbonate. In an area of Pakistan presently dominated by C_4 grasses, Quade et al. (1989) found that a sharp shift in $\delta^{13}C$ in soil carbonate occurred about 7 million years ago (Figure 9.20). Quade et al. concluded that the shift marks the transition from C_3 dominant to C_4 dominant grasslands. They initially interpreted this as a response to the uplift of the Tibetan Plateau and the development of the monsoon. However, other evidence, including oxygen isotope data from Pakistani soil carbonates, suggests the monsoons developed about a million years earlier. Interestingly, other studies indicated that North American grasslands transitioned from C_3 to C_4 dominated about the same time. This synchronicity suggests a global cause, while the monsoons are a regional phenomenon. C_4 photosynthesis is more efficient at low concentrations of CO_2 that is the C_3 pathway. Thus the evolution of C_4 plants may have occurred in response to a decrease in atmospheric CO_2 suspected on other grounds (Cerling et al., 1993).

9.5.5.1 Isotopes in Archaeology

The differences in nitrogen and carbon isotopic composition of various foodstuffs and the preservation of these isotope ratios in bone collagen provides a means of determining what ancient peoples ate. In the first investigation of bone collagen from human remains, DeNiro and Epstein (1981) concluded that Indians of the Tehuacan Valley in Mexico probably depended heavily on maize (a C_4 plant) as early as 4000 BC, whereas archeological investigations had concluded maize did not become important in their diet until perhaps 1500 BC. In addition, there seemed to be steady increase in the dependence on legumes (probably beans) from 6000 BC to 1000 AD and a more marked increase in legumes in the diet after 1000 AD.

Mashed grain and vegetable charred onto potsherds during cooking provides an additional record of the diets of ancient peoples. DeNiro and Hasdorf (1985) found that vegetable matter subjected to conditions similar to burial in

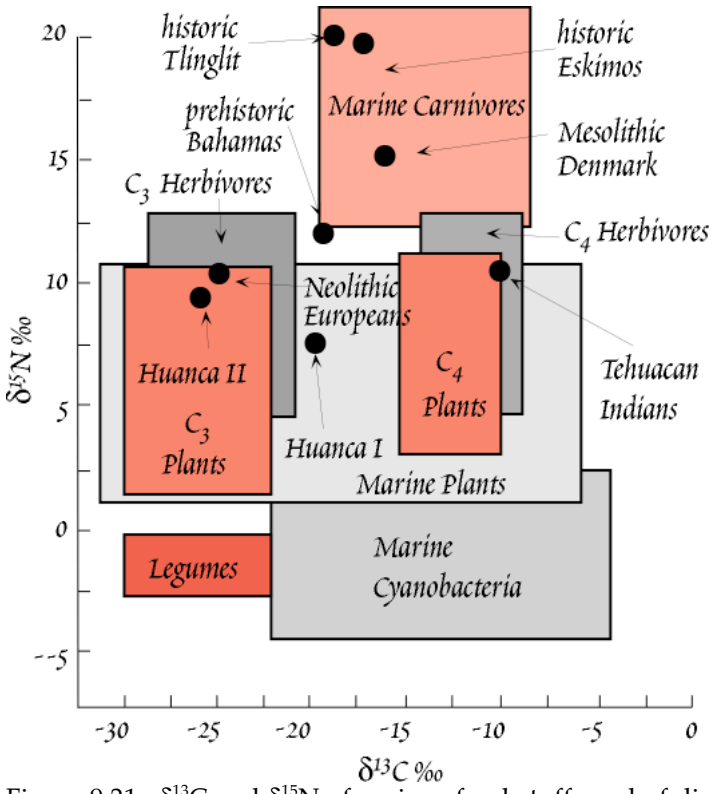

Figure 9.21. $\delta^{13}C$ and $\delta^{15}N$ of various food stuffs and of diets reconstructed from bone collagen and vegetable matter charred onto pots by DeNiro and colleagues. The Huanca people were from the Upper Mantaro Valley of Peru. Data from pot sherds of the Huanca I period (AD 1000-1200) suggest both C_3 and C_4 plants were cooked in pots, but only C_3 plants during the Huanca II period (AD 1200-1470).

soil underwent large shifts in $\delta^{15}N$ and $\delta^{13}C$ but that vegetable matter that was burned or charred did not. The carbonization (charring, burning) process itself produced only small (2 or 3‰) fractionations. Since these fractionations are smaller than the range of isotopic compositions in various plant groups, they are of little significance. Since potsherds are among the most common artifacts recovered in archeological sites, this provides a second valuable means of reconstructing the diets of ancient peoples.

Figure 9.21 summarizes the results obtained in a number of studies of bone collagen and potsherds (DeNiro, 1987). Studies of several modern populations, including Eskimos and the Tlinglit Indians of the Northwest U.S. were made as a control. Judging from the isotope data, the diet of Neolithic Europeans consisted entirely of C_3 plants and herbivores feeding on C_3 plants, in contrast to the Tehuacan Indians, who depended mainly on C_4 plants. Prehistoric peoples of the Bahamas and Denmark depended both on fish and on agriculture. In the case of Mesolithic Denmark, other evidence indicates the crops were C_3, and the isotope data bear this out. Although there is no corroborating evidence, the isotope data suggest the Bahamians also depended on C_3 rather than C_4 plants. The Bahamians had lower $\delta^{15}N$ because the marine component of their diet came mainly from coral reefs. Nitrogen fixation is particularly intense on coral reefs, which leads to ^{15}N depletion of the water, and consequently, of reef organisms.

9.5.6 Isotopic "Fossils" and the Earliest Life

As noted earlier, large carbon isotope fractionations are common to all autotrophs. Consequently, $\delta^{13}C$ values of -20‰ or less are generally interpreted as evidence of biologic origin of those compounds. Schidlowski (1988) first reported $\delta^{13}C$ as low as -26‰ in carbonate rocks from West Greenland that are ostensibly older than 3.5 Ga. In 1996, Mojzsis and others reported $\delta^{13}C$ between -20 to -50‰ graphite inclusions in grains of apatite in 3.85 Ga in banded-iron formations (BIFs) from the same area. In 1999, Rosing reported $\delta^{13}C$ of -19‰ from graphite in tubiditic and pelagic metasedimentary rocks from the Isua greenstone belt in the same area. These rocks are thought to be older than 3.7 Ga. In each case, these negative $\delta^{13}C$ values were interpreted as evidence of a biogenic origin of the carbon, and therefore that life existed on Earth at this time. This interpretation remains, however, controversial.

There are several reasons for the controversy, but all ultimately relate to the extremely complex geological history of the area. The geology of the region includes not only the early Archean rocks, but also rocks of middle and late Archean age as well. Most rocks are multiply and highly deformed and metamorphosed and the exact nature, relationships, and structure of the precursor rocks are difficult to decipher. Indeed, Rosing et al. (1996) argued that at least some of the carbonates sampled by Schidlowski (1988) are veins deposited by metamorphic fluid flow rather than metasediments. Others have argued that the graphite in these rocks formed by thermal decomposition of siderite ($FeCO_3$) and subsequent reduction of some of the carbon. Further effort will be needed to resolve this controversy.

9.6 Paleoclimatology

Perhaps one of the most successful and significant application of stable isotope geothermometry has been paleoclimatology. At least since the work of Louis Agassiz in 1840, geologists have contemplated the question of how the Earth's climate might have varied in the past. Until 1947, they had no means of quantifying paleotemperature changes. In that year, Harold Urey initiated the field of stable isotope geochemistry. In his classic 1947 paper, Urey calculated the temperature dependence of oxygen isotope fractionation between calcium carbonate and water and proposed that the isotopic composition of carbonates could be used as a paleothermometer. Urey's students and post-doctoral fellows empirically determined temperature dependence of the fractionation between calcite and water as:

$$T\,^{\circ}C = 16.9 - 4.2\Delta_{cal-H_2O} + 0.13\Delta^2_{cal-H_2O} \qquad 9.58$$

For example, a change in $\Delta_{cal\text{-}H_2O}$ from 30 to 31 permil implies a temperature change from 8° to 12°. Urey suggested that the Earth's climate history could be recovered from oxygen isotope analyses of ancient marine carbonates. Although the problem has turned out to be much more complex than Urey anticipated, this has proved to be an extremely fruitful area of research. Deep-sea carbonate oozes con-

tained an excellent climate record, and, as we shall see, several other paleoclimatic records are available as well.

9.6.1 The Marine Quaternary $\delta^{18}O$ Record and Milankovitch Cycles

The principles involved in paleoclimatology are fairly simple. As Urey formulated it, the isotopic composition of calcite secreted by organisms should provide a record of paleo-ocean temperatures because the fractionation of oxygen isotopes between carbonate and water is temperature dependent. In actual practice, the problem is somewhat more complex because the isotopic composition of the shell, or test, of an organism will depend not only on temperature, but also on the isotopic composition of water in which the organism grew, "vital effects" (i.e., different species may fractionate oxygen isotopes somewhat differently), and post-burial isotopic exchange with sediment pore water. As it turns out, the vital effects and post-burial exchange are usually not very important for late Tertiary/Quaternary carbonates, but the isotopic composition of water is.

The first isotopic work on deep-sea sediment cores with the goal of reconstructing the temperature history of Pleistocene glaciations was by Cesare Emiliani (1955), who was then a student of Urey at the University of Chicago. Emiliani analyzed $\delta^{18}O$ in foraminifera from piston cores from the world's oceans. Remarkably, many of Emiliani's findings are still valid today, though they have been revised to various degrees. Rather than just the 5 glacial periods that geomorphologists had recognized, Emiliani found 15 glacial–interglacial cycles over the last 600,000 years. He found that these were global events, with notable cooling even in low latitudes and concluded that the fundamental driving force for Quaternary climate cycles was variations in the Earth's orbit and consequent variations in the solar energy flux, *insolation*.

Emiliani had realized that the isotopic composition of the ocean would vary between glacial and interglacial times as isotopically light water was stored in glaciers, thus enriching the oceans in ^{18}O. He estimated that this factor accounted for about 20% of the observed variations. The remainder he attributed to the effect of temperature on isotope fractionation. Subsequently, Shackleton and Opdyke (1973) concluded that storage of isotopically light water in glacial ice was the main effect causing oxygen isotopic variations in biogenic carbonates, and that the temperature effect was only secondary.

The question of just how much of the variation is deep-sea carbonate sediments in due to ice build-up and how much is due to the effect of temperature on fractionation is an important one. The resolution depends, in part, on the isotopic composition of glacial ice and how much this might vary between glacial and interglacial times. It is fairly clear that the average $\delta^{18}O$ of glacial ice is probably less than –15‰, as Emiliani had assumed. Typical values for Greenland ice are –30 to -35‰ (relative to SMOW) and as low as -50‰ for Antarctic ice. If the exact isotopic composition of ice and the ice volume were known, it would be a straightforward exercise to calculate the effect of continen-

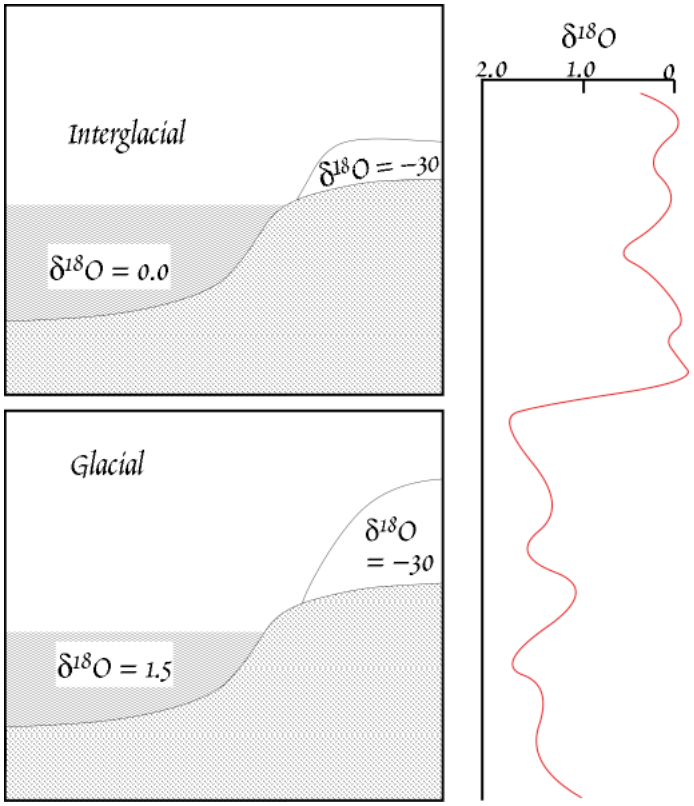

Figure 9.22. Cartoon illustrating how $\delta^{18}O$ of the ocean changes between glacial and interglacial periods.

tinental ice build-up on ocean isotopic composition. For example, the present volume of continental ice is 27.5×10^6 km^3, while the volume of the oceans is 1350×10^6 km^3. Assuming glacial ice has a mean $\delta^{18}O$ of –30‰ relative to SMOW, we can calculate the $\delta^{18}O$ of the total hydrosphere as –0.6‰ (neglecting freshwater reservoirs, which are small). At the height of the Wisconsin Glaciation (the most recent one), the volume of glacial ice is thought to have increased by 42×10^6 km^2, corresponding to a lowering of sea level by 125 m. If the $\delta^{18}O$ of ice was the same then as now (-30‰), we can readily calculate that the $\delta^{18}O$ of the ocean would have increased by 1.59‰. This is illustrated in Figure 9.22.

We can use equation 9.58 to see how much the effect of ice volume on seawater $\delta^{18}O$ affects estimated temperature changes. According to this equation, at 20° C, the fractionation between water and calcite should be 33‰. Assuming present water temperature of 20° C, Emiliani would have calculated a temperature change of 6° C for an observed increase in the $\delta^{18}O$ of carbonates between glacial times and present $\delta^{18}O$ of 2‰, after correction for 0.5‰ change in the isotopic composition of water. In other words, he would have concluded that surface ocean water in the same spot would have had a temperature of 14° C. If the change in the isotopic composition of water is actually 1.5‰, the calculated temperature difference is only about 2° C. Thus the question of the volume of glacial ice and its isotopic composition must be resolved before $\delta^{18}O$ in deep-sea carbonates can be used to calculate paleotemperatures.

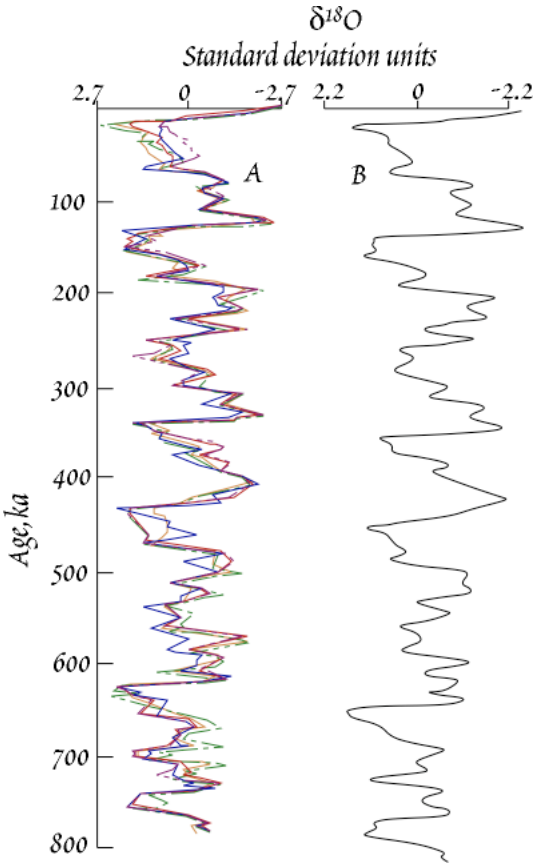

Figure 9.23. A. "Stacking of five cores" selected by Imbrie et al. (1984). Because the absolute value of $\delta^{18}O$ varies in from core to core, the variation is shown in standard deviation units. B. Smoothed average of the five cores in A. After Imbrie et al. (1984).

Comparison of sealevel curves derived from dating of terraces and coral reefs indicate that each 0.011‰ variation in $\delta^{18}O$ represents a 1 m change in sealevel. Based on this and other observations, it is now generally assumed that the $\delta^{18}O$ of the ocean changed by about 1.5‰ between glacial and interglacial periods, but the exact value is still debated.

By now hundreds, if not thousands, of deep-sea sediment cores have been analyzed for oxygen isotope ratios. Figure 9.23 shows the global $\delta^{18}O$ record constructed by averaging analyses from 5 key cores (Imbrie, et al., 1984). A careful examination of the global curve shows a periodicity of approximately 100,000 years. The same periodicity was apparent in Emiliani's initial work and led him to conclude that the glacial-interglacial cycles were due to variations in the Earth's orbital parameters. These are often referred to as the Milankovitch cycles, after Milutin Milankovitch, a Serbian astronomer who argued in the 1920's and 1930's[†] that they caused the ice ages (Milankovitch, 1938).

Let's explore Milankovitch's idea in a bit more detail. The *eccentricity* (i.e., the degree to which the orbit differs from circular) of the Earth's orbit about the Sun and the degree of tilt, or *obliquity*, of the Earth's rotational axis vary slightly. In addition, the direction in which the Earth's rotational axis tilts varies, a phenomenon called *precession*. These variations are illustrated in Figure 9.24. Though variation in these "Milankovitch parameters" has negligible effect on the *total* radiation the Earth receives,

[†]While Milankovitch was a strong and early proponent of the idea that variations in the Earth's orbit caused ice ages, he was not the first to suggest it. J. Croll of Britain first suggested it in 1864, and published several subsequent papers on the subject.

they do affect the *pattern* of incoming radiation. For example, tilt of the rotational axis determines seasonality and the latitudinal gradient of insolation. The gradient is extremely important because it drives atmospheric and oceanic circulation. If the tilt is small, seasonality will be reduced (cooler summers, warmer winters). Precession relative to the eccentricity of the Earth's orbit also affects seasonality. For example, presently the Earth is closest to the Sun in January. As a result, northern hemisphere winters (and southern hemisphere summers) are somewhat warmer than they would be otherwise. For a given latitude and season, precession will result in a ±5% difference in insolation. While the Earth's orbit is only slightly elliptical, and variations in eccentricity are small, these variations are magnified because insolation varies with the inverse square of the Earth-Sun distance.

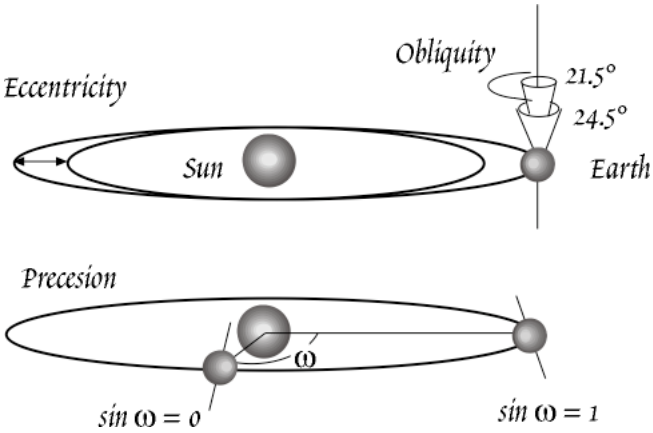

Figure 9.24. Illustration of the *Milankovitch parameters*. The eccentricity is the degree the Earth's orbit departs from circular. Obliquity is the tilt of the Earth's rotation axis with respect to the plane of the ecliptic and varies between 21.5° and 24.5°. Precision is the variation in the direction of tilt at the Earth's closest approach to the Sun (perihelion). The parameter ω is the angle between the Earth's position on June 21 (summer solstice), and perihelion.

Variation in tilt approximates a simple sinusoidal function with a period of 41,000 yrs. Variations in eccentricity can be approximately described with period of 100,000 years. In actuality, however, eccentricity variation is more complex, and is more accurately described with periods of 123,000 yrs, 85,000 yrs, and 58,000 yrs. Similarly, variation in precession has characteristic periods of 23,000 and 18,000 yrs.

Although Emiliani suggested that $\delta^{18}O$ variations were related to variations in these orbital parameters, the first quantitative approach to the problem was that of Hayes et al. (1976). They applied Fourier analysis to the $\delta^{18}O$ curve (Fourier analysis is a mathematical tool that transforms a complex variation such as that in Figure 9.23 to the sum of a series of simple sin functions). Hayes et al. then used spectral analysis to show that much of the spectral power of the $\delta^{18}O$ curve occurred at frequencies similar to those of the Milankovitch parameters. The most elegant and convincing treatment is that of Imbrie (1985). Imbrie's treatment involved several refinements and extension of the earlier work of Hayes et al. (1976). First, he used improved values for Milankovitch frequencies. Second, he noted these Milankovitch parameters vary with time (the Earth's orbit and tilt are affected by the gravitational field of the Moon and other planets, and other astronomical events, such as bolide impacts), and the climate system's response to them might also vary over time. Thus Imbrie treated the first and second 400,000 years of Figure 9.23 separately.

Imbrie observed that climate does not respond instantaneously to forcing. For example, maximum temperatures are not reached in Ithaca, New York until late July, 4 weeks after the maximum insolation, which occurs on June 21. Thus there is a *phase* lag between the forcing function (insolation) and climatic response (temperature). Imbrie (1985) constructed a model for response of global climate (as measured by the $\delta^{18}O$ curve) in which each of the 6 Milankovitch forcing functions was associated with a different gain and phase. The values of gain and phase for each parameter were found statistically by minimizing the residuals of the power spectrum of the $\delta^{18}O$ curve in Figure 9.23. The resulting "gain and phase model" is shown in comparison with the data for the past 400,000 years and the next 25,000 years in Figure 9.25. The model has a correlation coefficient, r, of 0.88 with the data. Thus about r^2, or 77%, of the variation in $\delta^{18}O$, and therefore presumably in ice volume, can be explained by Imbrie's Milankovitch model. The correlation for the period 400,000–782,000 yrs is somewhat poorer, around 0.80, but nevertheless impressive.

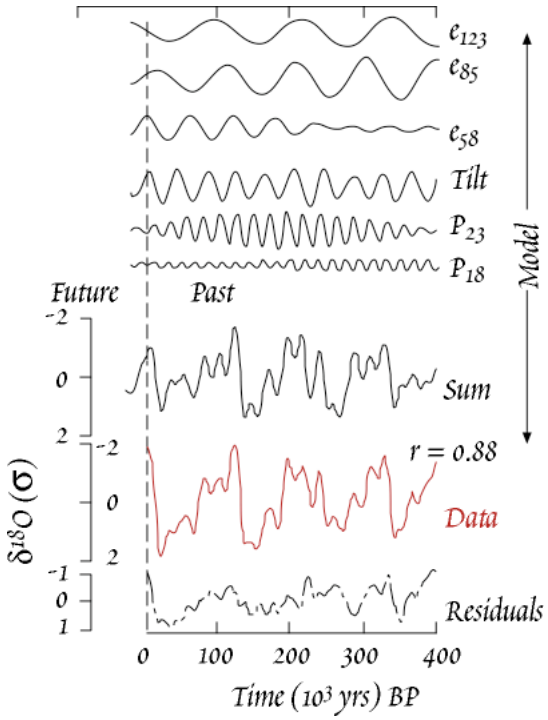

Figure 9.25. Gain and phase model of Imbrie relating variations in eccentricity, tilt, and precession to the oxygen isotope curve. Top shows the variation in these parameters over the past 400,000 and next 25,000 years. Bottom shows the sum of these functions with appropriated gains and phases applied and compares them with the observed data. After Imbrie (1985).

Since variations in the Earth's orbital parameters do not affect the average total annual insolation the Earth receives, but only its pattern in space and time, one might ask how this could cause glaciation. The key factor seems to be the insolation received during summer at high northern latitudes. This is, of course, the area where large continental ice sheets develop. The southern hemisphere, except for Antarctica, is largely ocean, and therefore not subject to glaciation. Glaciers apparently develop when summers are not warm enough to melt the winter's accumulation of snow in high northern latitudes.

Nevertheless, even at a given latitude the total variation in insolation is small, and not enough by itself to cause the climatic variations observed. Apparently, there are feedback mechanisms at work that serve to amplify the fundamental Milankovitch forcing function. One of these feedback mechanisms was identified by Agassiz, and that is ice albedo, or reflectance. Snow and ice reflect much of the incoming sunlight back into space. Thus as glaciers advance, they will cause further cooling. Any additional accumulation of ice in Antarctica, however, does not result in increased albedo, because the continent is fully ice covered even in interglacial times. Hence the dominant role of northern hemisphere insolation in driving climate cycles. Other possible feedback mechanisms include carbon dioxide and ocean circulation. The role of atmospheric CO_2 in controlling global climate is a particularly important issue because of burning of fossil fuels has resulted in a significant increase in atmospheric CO_2 concentration over the last 150 years. We will return to this issue in a subsequent chapter.

9.6.2 The Record in Glacial Ice

Climatologists recognized early on that continental ice preserves a stratigraphic record of climate change. Some of the first ice cores recovered for the purpose of examining the climatic record and analyzed for stable isotopes were taken from Greenland in the 1960's (e.g., Camp Century Ice Core). Subsequent cores have been taken from Greenland, Antarctica, and various alpine glaciers. The most remarkable and useful of these cores has been the 2000 m core recovered by the Russians from the Vostok station in Antarctica (Jouzel, et al., 1987, 1993, 1996), and is compared with the marine $\delta^{18}O$ record in Figure 9.25. The marine record shown is a smoothed version SPECMAP record, which is a composite record based on that of Imbrie et al. (1984), but with further modification of the chronology. The core provides a 240,000 year record of δD and $\delta^{18}O_{ice}$, as well as CO_2, and $\delta^{18}O_{O_2}$ in bubbles (the latter, which was subsequently published and not shown in Figure 9.26, provides a measure of $\delta^{18}O$ in the atmosphere and, indirectly, the ocean), which corresponds to a full glacial cycle.

Jouzel et al. (1987) converted δD to temperature variations after subtracting the effect of changing ice volume on δD of the oceans. The conversion is based on a 6‰/°C relationship between δD and temperature in modern Antarctic snow (they found a similar relationship using circulation models). The hydrogen isotopic fractionation of water is a more sensitive function of temperature than is oxygen fractionation. Their results, taken at face value, show dramatic 10° C temperature variations between glacial and interglacial times.

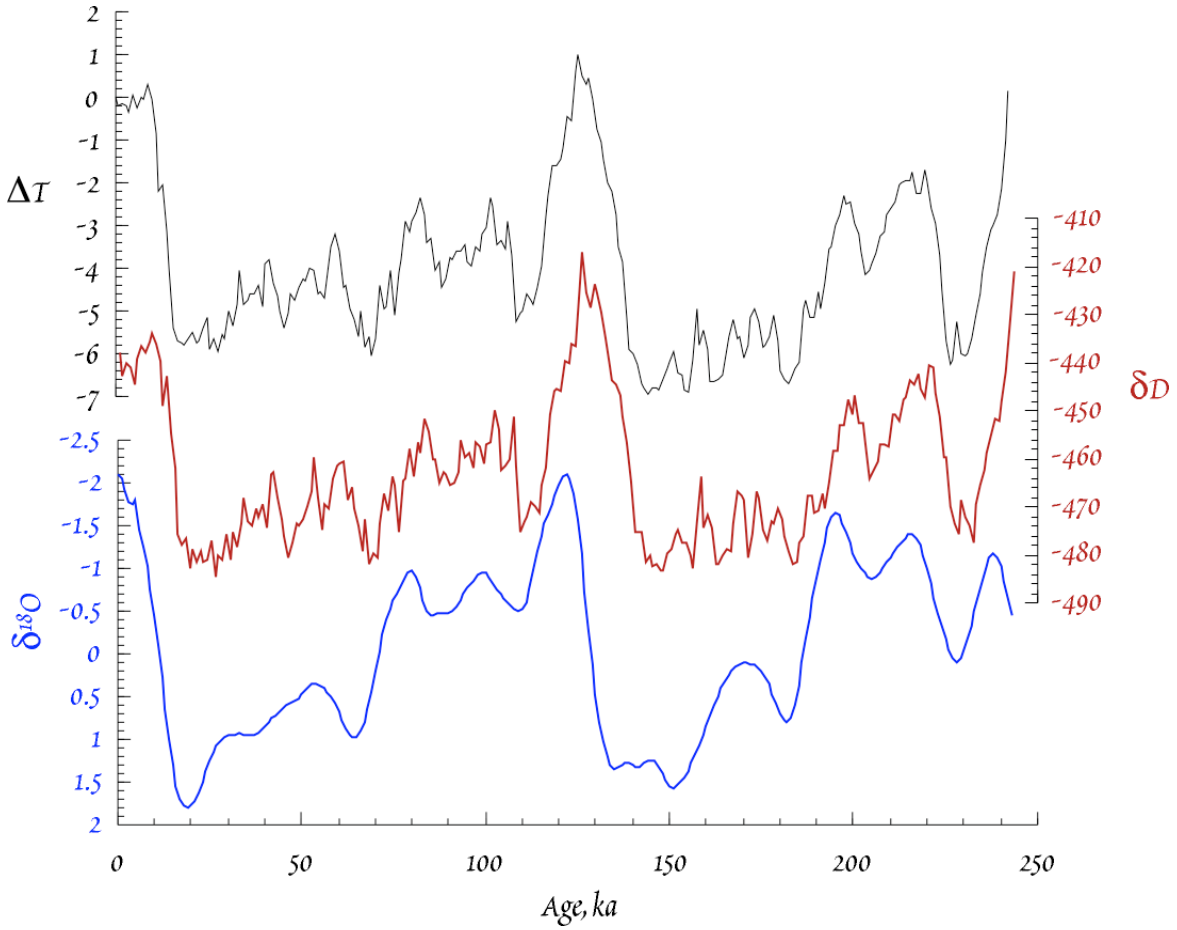

Figure 9.26. The lower curve shows smoothed $\delta^{18}O$ for marine carbonates (SPECMAP), the middle curve shows δD of ice in the Vostok ice core, and the upper curve the temperature calculated from δD at Vostok at the time of deposition of the ice relative to the present mean annual temperature. Vostok data is from Jouzel, et al., (1987, 1993, 1996).

Dating of the Vostok ice core was based only on an ice flow and accumulation model. Nevertheless, the overall pattern observed is in good agreement the marine $\delta^{18}O$ record, particular from 110,000 years to the present. The record of the last deglaciation is particularly similar to that of the marine $\delta^{18}O$ record, and even shows evidence of a slight return trend toward glacial conditions from 12 kyr to 11 kyr BP, which corresponds to the well-documented Younger Dryas event of the North Atlantic region. It is also very significant that spectral analysis of the Vostok isotope record shows strong peaks in variance at 41 kyr (the obliquity frequency), and at 25 kyr, which agree with the 23 kyr precessional frequency when the age errors are considered. Thus the Vostok ice core data appear to confirm the importance of Milankovitch climatic forcing. It is interesting and significant that even in this core, taken at 78° S, it is primarily insolation at 65° N that is the controlling influence. There are, however, significant differences between the Vostok record and the marine record. Some of these are probably due to inaccuracies in dating; others may reflect differences in northern and southern hemisphere response to orbital forcing.

9.6.3 Soils and Paleosols

As we found in Chapter 6, the concentration of CO_2 in soils is very much higher than in the atmosphere, reaching 1% by volume. As a result, soil water can become supersaturated with respect to carbonates. In soils where evaporation exceeds precipitation, soil carbonates form. The carbonates form

in equilibrium with soil water, and there is a strong correlation between $\delta^{18}O$ in soil carbonate and local meteoric water, though soil carbonates tend to be about 5‰ more enriched than expected from the calcite-water fractionation. There are 2 reasons why soil carbonates are heavier. First, soil water is enriched in ^{18}O relative to meteoric water due to preferential evaporation of isotopically light water molecules. Second, rain (or snow) falling in wetter, cooler seasons in more likely to run off than that falling during warm seasons. Taking these factors into consideration, the isotopic composition of soil carbonates may be used as a paleoclimatic indicator.

Figure 9.27 shows one example of $\delta^{18}O$ in paleosol carbonates used in this way. The same Pakistani paleosol samples analyzed by Quade et al. (1989) for $\delta^{13}C$ (Figure 9.19) were also analyzed for $\delta^{18}O$. The $\delta^{13}C$ values recorded a shift toward more positive values at 7 Ma that apparently reflect the appearance of C_4 grasslands. The $\delta^{18}O$ shows a shift to more positive values at around 8 Ma, or a million years before the $\delta^{13}C$ shift. Quade et al. interpreted this as due to an intensification of the Monsoon system at that time, an interpretation consistent with marine paleontological evidence.

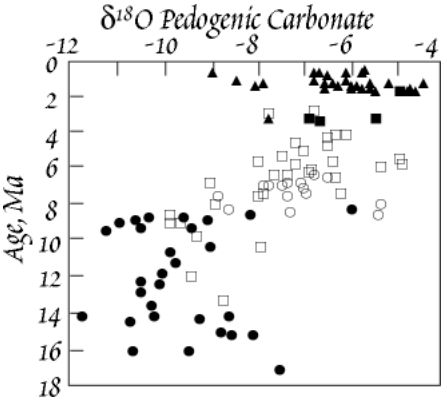

Figure 9.27. $\delta^{18}O$ in paleosol carbonate nodules from the Potwar Plateau in northern Pakistan. Different symbols correspond to different, overlapping sections that were sampled. After Quade et al. (1989).

Clays, such as kaolinites, are another important constituent of soil. Lawrence and Taylor (1972) showed that during soil formation, kaolinite and montmorillonite form in approximate equilibrium with meteoric water so that their $\delta^{18}O$ values are systematically shifted by +27 ‰ relative the local meteoric water, while δD are shifted by about 30‰. Thus kaolinites and montmorillonites define a line parallel to the meteoric water line (Figure 9.28), the so-called *kaolinite line*. From this observation, Sheppard et al. (1969) and Lawrence and Taylor (1972) reasoned that one should be able to deduce the isotopic composition of rain at the time ancient kaolinites formed from their δD values. Since the isotopic composition of precipitation is climate dependent, ancient kaolinites provide another continental paleoclimatic record.

There is some question as to the value of hydrogen isotopes in clays for paleoclimatic studies. Lawrence and Meaux (1993) concluded that most ancient kaolinites have exchanged hydrogen subsequent to their formation, and therefore are not a good paleoclimatic indicator. Others argue that clays to do not generally exchange hydrogen unless recrystallization occurs or the clay experiences temperatures in excess of 60-80° C for extended periods (A. Gilg, pers. comm., 1995).

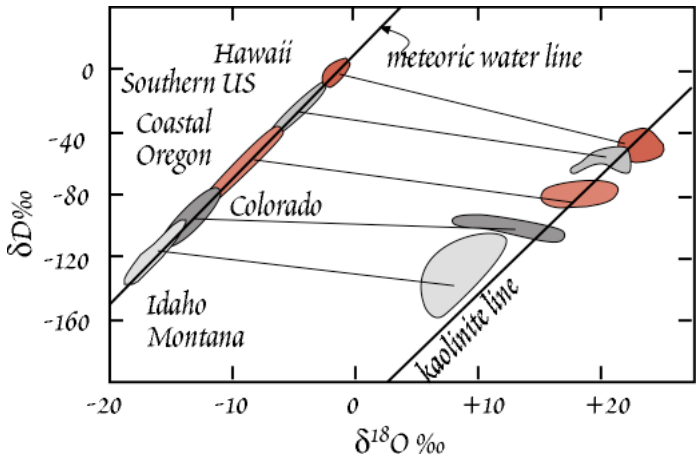

Figure 9.28. Relationship between δD and $\delta^{18}O$ in modern meteoric water and kaolinites. Kaolinites are enriched in ^{18}O by about 27‰ and ^{2}H by about 30‰. After Lawrence and Taylor (1972).

Lawrence and Meaux (1993) concluded, however, that oxygen in kaolinite does preserve the original $\delta^{18}O$, and that can, with some caution, be used as a paleoclimatic indicator. Figure 9.29 compares the $\delta^{18}O$ of ancient Cretaceous North American kaolinites with the isotopic composition of modern precipitation. If the Cretaceous climate were the same as the present one, the kaolinites should be systematically 27‰ heavier than modern precipitation. For the southeastern US, this is

approximately true, but the difference is generally less than 27‰ for other kaolinites, and the difference decreases northward. This indicates these kaolinites formed in a warmer environment than the present one. Overall, the picture provided by Cretaceous kaolinites confirm what has otherwise be deduced about Cretaceous climate: the Cretaceous climate was generally warmer, and the equator to pole temperature gradient was lower. A drawback with this approach, however, is the lack of good ages on paleosols, which have proven to be very difficult to date precisely. The ages of many paleosols used by Lawrence and Meaux (1993) were simply inferred from stratigraphy.

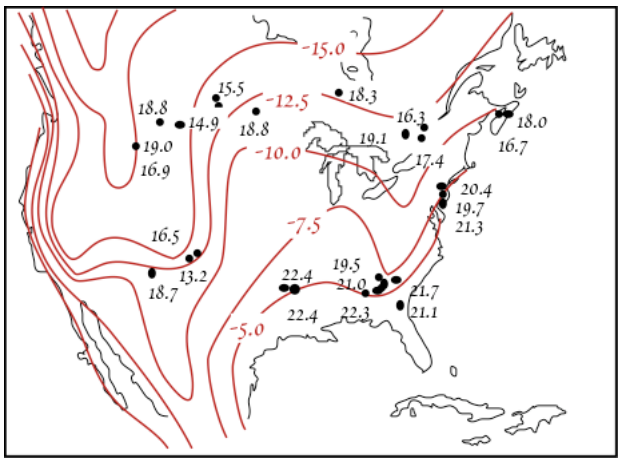

Figure 9.29. $\delta^{18}O$ in Cretaceous kaolinites from North American (black) compared with contours of $\delta^{18}O$ (in red) of present-day meteoric water. After Lawrence and Meaux (1993).

9.7 Hydrothermal Systems and Ore Deposits

When large igneous bodies are intruded into high levels of the crust, they heat the surrounding rock and the water in the cracks and pore in this rock, setting up convection systems. The water in these hydrothermal systems reacts with the hot rock and undergoes isotopic exchange; the net result is that both the water and the rock change their isotopic compositions.

One of the first of many important contributions of stable isotope geochemistry to understanding hydrothermal systems was the demonstration by Harmon Craig (another student of Harold Urey) that water in these systems was meteoric, not magmatic (Craig, 1963). The argument is based upon the data shown in Figure 9.30. For each geothermal system, the δD of the "chloride" type geothermal waters is the same as the local precipitation and groundwater, but the $\delta^{18}O$ is shifted to higher values. The shift in $\delta^{18}O$ results from high temperature ($\lesssim 300°C$) reaction of the local meteoric water with hot rock. However, because the rocks contain virtually no hydrogen, there is little change in the hydrogen isotopic composition of the water. If the water involved in these systems were magmatic, it would not have the same isotopic composition as local meteoric water (it is possible that these systems contain a few percent magmatic water).

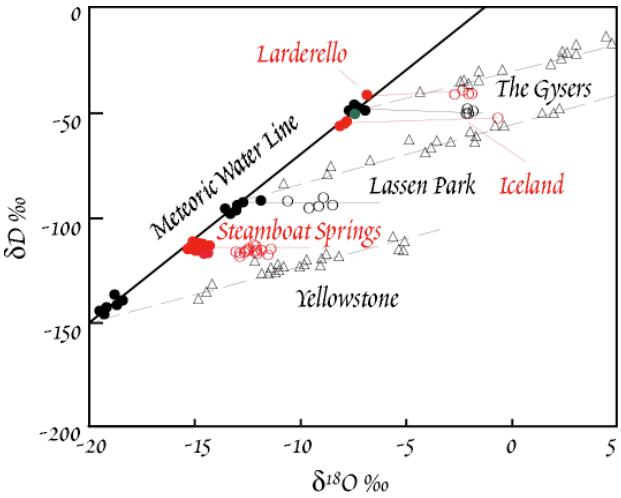

Figure 9.30. δD and $\delta^{18}O$ in meteoric hydrothermal systems. Closed circles show the composition of meteoric water in Yellowstone, Steamboat Springs, Mt. Lassen, Iceland, Larderello, and The Geysers, and open circles show the isotopic composition of chloride-type geothermal waters at those locations. Open triangles show the location of acidic, sulfide-rich geothermal waters at those locations. Solid lines connect the meteoric and chloride waters, dashed lines connect the meteoric and acidic waters. The "Meteoric Water Line" is the correlation between δD and $\delta^{18}O$ observed in precipitation in Figure 9.10.

Acidic, sulfur-rich waters from hydrothermal systems can have δD that is different from local meteoric water. This shift occurs when hydrogen isotopes are fractionated during boiling of geothermal waters. The steam produced is enriched in sulfide. The steam mixes with cooler meteoric water, condenses, and the sulfide is oxidized to sulfate, resulting in their acidic character. The mixing

lines observed reflect mixing of the steam with meteoric water as well as the fractionation during boiling.

Estimating temperatures at which ancient hydrothermal systems operated is a fairly straight–forward application of isotope geothermometry, which we have already discussed. If we can measure the oxygen (or carbon or sulfur) isotopic composition of any two phases that were in equilibrium, and if we know the fractionation factor as a function of temperature for those phases, we can estimate the temperature of equilibration. We will focus now on water-rock ratios, which may also be estimated using stable isotope ratios.

9.7.1 WATER-ROCK RATIOS

For a closed hydrothermal system, we can write two fundamental equations. The first simply describes isotopic equilibrium between water and rock:

$$\Delta = \delta_w^f - \delta_r^f \qquad 9.59$$

where we use the subscript w to indicate water, and r to indicate rock. The superscript f indicates the final value. So 9.59 just says that the difference between the final isotopic composition of water and rock is equal to the fractionation factor (we implicitly assume equilibrium). The second equation is the mass balance for a closed system:

$$c_w W \delta_w^i + c_r R \delta_r^i = c_w W \delta_w^f + c_r R \delta_r^f \qquad 9.60$$

where c indicates concentration (we assume concentrations do not change, which is valid for oxygen, but perhaps not valid for other elements), W indicates the mass of water involved, R the mass of rock involved, the superscript i indicates the initial value and f again denotes the final isotope ratio. This equation just says the amount of an isotope present before reaction must be the same as after reaction. We can combine these equations to produce the following expression for the water-rock ratio:

$$\frac{W}{R} = \frac{\delta_r^f - \delta_r^i}{\delta_w^f - \delta_r^i}\frac{c_r}{c_w} \qquad 9.61$$

The initial $\delta^{18}O$ can generally be inferred from unaltered samples and from the δD–$\delta^{18}O$ meteoric water line and the final isotopic composition of the rock can be measured. The fractionation factor can be estimated if we know the temperature and the phases in the rock. For oxygen, the ratio of concentration in the rock to water will be close to 0.5 in all cases.

Equation 9.61 is not very geologically realistic because it applies to a closed system. A completely open system, where water makes one pass through hot rock, would be more realistic. In this case, we might suppose that a small parcel of water, dW, passes through the system and induces an incremental change in the isotopic composition of the rock, $d\delta_r$. In this case, we can write:

$$Rc_r d\delta_r = \delta_w^i - [\Delta + \delta_r]c_w dW \qquad 9.62$$

This equation states that the mass of an isotope exchanged by the rock is equal to the mass of that isotope exchanged by the water (we have substituted $\Delta + \delta_r$ for δ_w^f). Rearranging and integrating, we have:

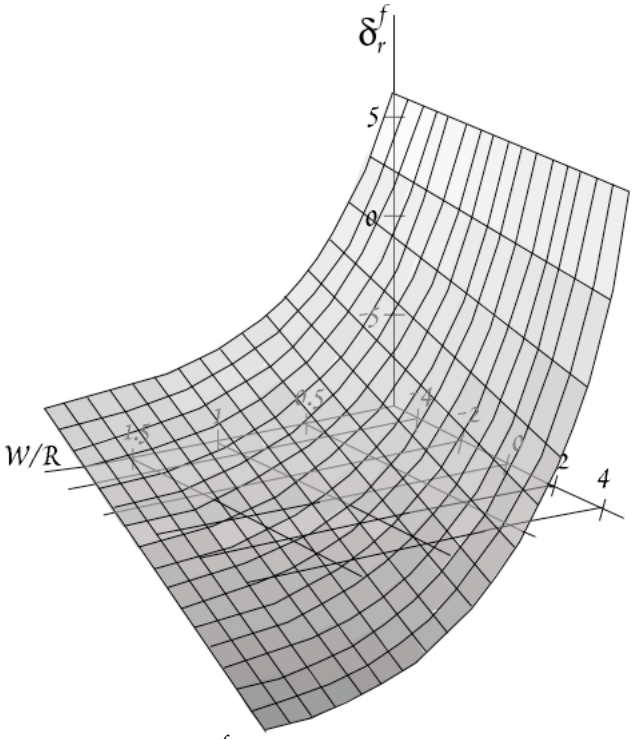

Figure 9.31. $\delta^{18}O_r^f$ as a function of W/R and Δ computed from equation 9.63.

$$\frac{W}{R} = \ln\left(\frac{\delta_r^f - \delta_r^i}{-\delta_r^f + \delta_w^i - \Delta} + 1\right)\frac{c_w}{c_r} \qquad 9.63$$

Thus it is possible to deduce the water rock ratio for an open system as well as a closed one.

Oxygen isotope studies can be a valuable tool in mineral exploration. Mineralization is often (though not exclusively) associated with the region of greatest water flux, such as areas of upward moving hot water above intrusions. Such areas are likely to have the lowest values of $\delta^{18}O$. To understand this, let's solve equ. 9.63 for δ_r^f, the final value of $\delta^{18}O$ in the rock:

$$\delta_r^f = \left(\delta_r^i - \delta_w^i + \Delta\right)e^{-\frac{Wc_w}{Rc_r}} + \delta_w^i + \Delta \qquad 9.64$$

Assuming a uniform initial isotopic composition of the rocks and the water, all the terms on the r.h.s. are constants except W/R and Δ, which is a function of temperature. Thus the final values of $\delta^{18}O$ are functions of the temperature of equilibration, and an exponential function of the W/R ratio. Figure 9.31 shows $\delta^{18}O_r^f$ plotted as a function of W/R and Δ, where $\delta^{18}O_r^i$ is assumed to be +6 and $\delta^{18}O_w^i$ is assumed to be –13. In a few cases, ores apparently have precipitated by fluids derived from the magma itself. In those cases, this kind of approach does not apply.

Figure 9.32 shows an example of the $\delta^{18}O$ imprint of an ancient hydrothermal system: the Bohemia Mining District in Lane Country, Oregon, where Tertiary volcanic rocks of the western Cascades have been intruded by a series of dioritic plutons. Approximately $1,000,000 worth of gold was removed from the region between 1870 and 1940. $\delta^{18}O$ contours form a bull's eye pattern, and the region of low $\delta^{18}O$ corresponds roughly with the area of propylitic (i.e., greenstone) alteration. Notice that this region is broader than the contact metamorphic aureole. The primary area of mineralization occurs within the $\delta^{18}O < 0$ contour. In this area, relatively large volumes of gold-bearing hydrothermal solution cooled, perhaps due to mixing with groundwater, and precipitated gold. This is an excellent example of the value of oxygen isotope studies to mineral exploration. Similar bull's eye patterns are found around many other hydrothermal ore deposits.

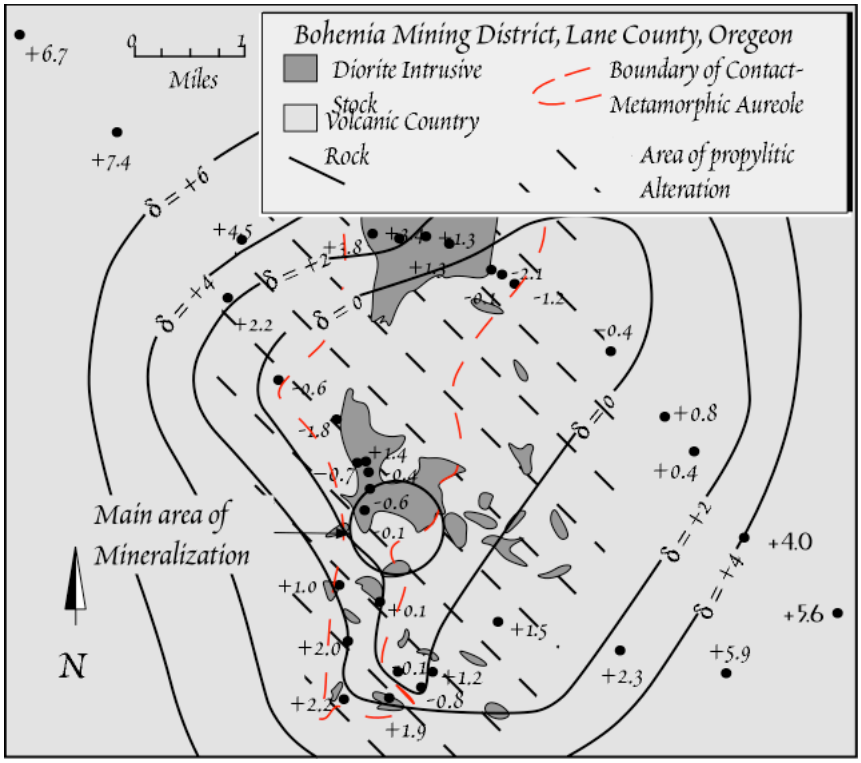

Figure 9.32. $\delta^{18}O$ variations in the Bohemia mining district, Oregon. Note the bull's eye pattern of the $\delta^{18}O$ contours. After Taylor (1974).

9.7.2 Sulfur Isotopes and Ore Deposits

A substantial fraction of base and noble metal ores are sulfides. These have formed in a great variety of environments and under a great variety of conditions. Sulfur isotope studies have been very valuable in sorting out the genesis of these deposits. Of the various stable isotope systems we will consider here, sulfur isotopes are undoubtedly the most complex. This complexity arises in part because there are four common valence states in which sulfur can occur in the Earth, +6 (e.g.,

$BaSO_4$), +4 (e.g., SO_2), 0 (e.g., S), –1 (e.g., FeS_2) and –2 (H_2S). Significant equilibrium fractionations occur between these valence states. Each of these valence states forms a variety of compounds, and fractionations can occur between these as well (e.g., Figure 9.7). Finally, sulfur is important in biological processes and fractionations in biologically mediated oxidations and reductions are often different from fractionations in the abiological equivalents.

There are two major reservoirs of sulfur on the Earth that have uniform sulfur isotopic compositions: the mantle, which has $\delta^{34}S$ of ~0 and in which sulfur is primarily present in reduced form, and seawater, which has $\delta^{34}S$ of +20* and in which sulfur is present as SO_4^{2-}. Sulfur in sedimentary, metamorphic, and igneous rocks of the continental crust may have $\delta^{34}S$ that is both greater and smaller than these values (Figure 9.33). All of these can be sources of sulfide in ores, and further fractionation may occur during transport and deposition of sulfides. Thus the sulfur isotope geochemistry of sulfide ores is remarkably complex.

At magmatic temperatures, reactions generally occur rapidly and most systems appear to be close to equilibrium. Below 200°C, however, sulfur isotopic equilibration is slow even on geologic time scales, hence equilibration is rare and kinetic effects often dominate. Isotopic equilibration between two sulfide species or between two sulfate species is achieved more readily than between sulfate and sulfide species. Sulfate-sulfide reaction rates have been shown to depend on pH (reaction is more rapid at low pH). In addition, equilibration is much more rapid when sulfur species of intermediate valence species are present. Presumably, this is because reaction rates between species of adjacent valance states (e.g., sulfate and sulfite) are rapid, but reaction rates between widely differing valence states (e.g., sulfate and sulfide) are much slower.

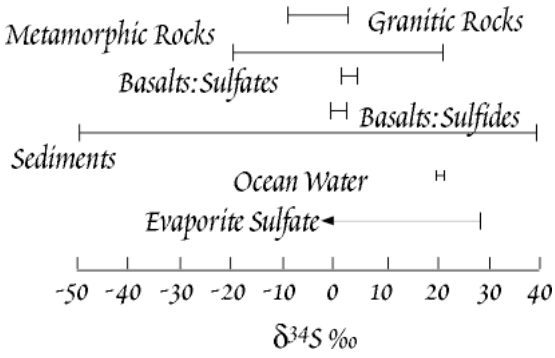

Figure 9.33. $\delta^{34}S_{CDT}$ in various geologic materials (after Hoefs, 1987).

Mississippi Valley type deposits provide an interesting example of how sulfur isotopes can be used to understand ore genesis. These are carbonate-hosted lead and zinc sulfides formed under relatively low temperature conditions. Figure 9.34 shows the sulfur isotope ratios of some examples. They can be subdivided into Zn-rich and Pb-rich classes. The Pb-rich and most of the Zn rich deposits were formed between 70 and 120° C, while some of the Zn-rich deposits, such as those of the Upper Mississippi Valley, were formed at temperatures up to 200° C, though most were formed in the range of 90° to 150° C.

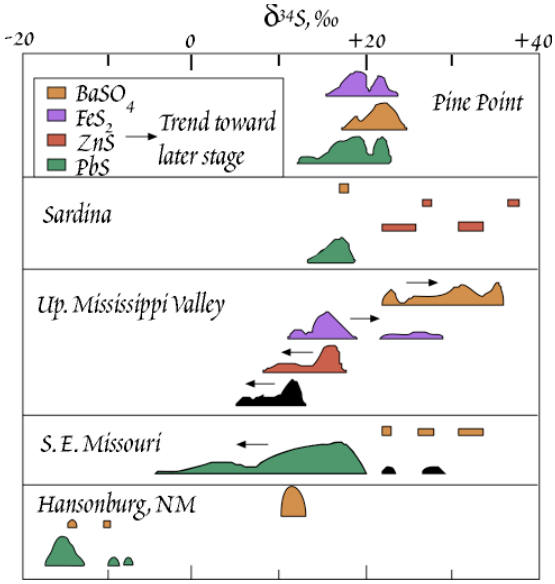

Figure 9.34. Sulfur isotope ratios in some Mississippi Valley-type Pb and Zn deposits. After Ohmoto and Rye (1979).

Figure 9.35 illustrates a generalized model for the genesis of Mississippi Valley type deposits. In most instances, metals and sulfur appear to have been derived distant from sedimentary units, perhaps particularly from evaporites, by hot, deep-circulating formation water. In North America, most of these seem to have formed during or shortly after the late Paleozoic Appalachian-Ouchita-Marathon Orogeny. The direct cause of precipitation of the ore probably may have differed

*This is the modern value for seawater. As we shall see in a subsequent chapter, though the sulfur isotopic composition of seawater is uniform at any time, this value has varied with time.

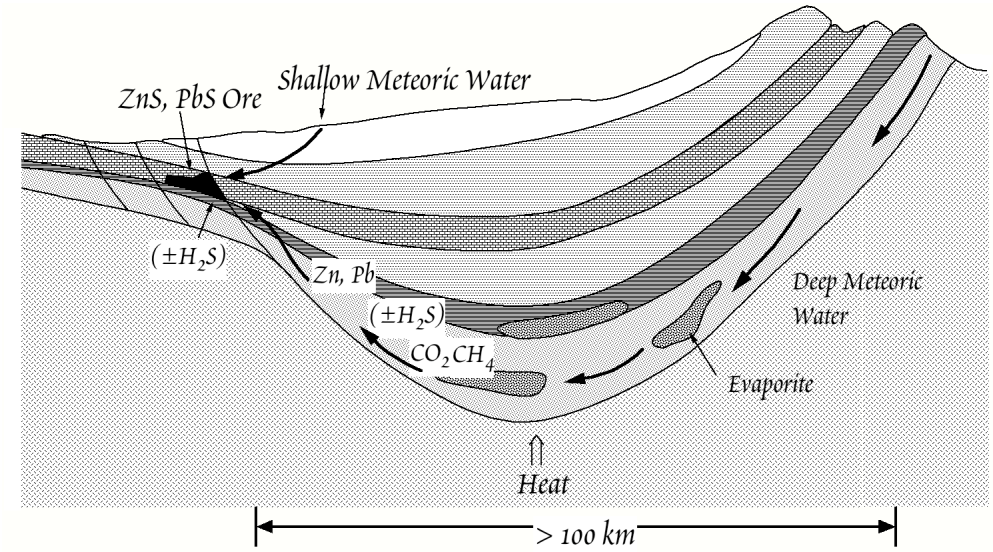

Figure 9.35. Cartoon illustrating the essential features of the genesis of Mississippi Valley sulfide ores. After Ohmoto (1986).

in the different localities. Oxygen and hydrogen isotope data suggest that mixing of the hot saline fluids with cooler low salinity ground water was probably the immediate cause of metal precipitation in some instances. In others, such as Pine-Point, local reduction of sulfate in the fluids to sulfide may have cause precipitation (Ohmoto, 1986). Local production of sulfide shortly before ore deposition may help to account for the lack of isotopic equilibrium in this deposit, since time is an element in the attainment of isotopic equilibrium. In other cases, mixing of separate S-bearing and metal-bearing fluids from different aquifers may have been the cause.

The sulfur isotope data suggest there are a number of possible sources of sulfur. In many cases, sulfur was apparently derived sulfate in evaporites, in others sulfur was derived from brines produced by evaporative concentration of seawater. In many cases, the sulfate was reduced by reaction with organic matter at elevated temperature (thermochemical reduction). In other cases, it may have been bacterially reduced. Other sulfur sources include sulfide from petroleum. In at least some deposits, sulfur appears to have been derived from more than one of these sources.

Sulfur isotope ratios in the S. E. Missouri district are quite variable and $\delta^{34}S$ is correlated with Pb isotope ratios in galenas. This suggests there was more than one source of the sulfur. Based on a combined Pb and S isotopic study, Goldhaber et al. (1995) concluded that the main stage ores of the S.E. Missori district were produced by mixing of fluids from several aquifers. They concluded that Pb was derived from the Lamont Sandstone (which directly overlies basement). Fluid in this aquifer was maintained at relatively high pε by the presence of hematite, and hence had low sulfide concentrations. This allowed leaching and transport of the Pb. Isotopically heavy S was produced by dissolution of evaporite sulfate and thermochemical reduction and migrated through the Sillivan Siltstone member of the upper Bonneterre Formation, which overlies the Lamont Sandstone. Both Pb and isotopically light sulfur migrated through the lower part of the Bonneterre Formation. PbS precipitated when the fluids were forced to mix by pinchout of the Sillivan Siltstone.

9.7.3 Mass Independent Sulfur Isotope Fractionation and the Rise of Atmospheric Oxygen

In the modern Earth, variations in sulfur isotope ratios are almost always mass dependent and $\delta^{33}S$ and ^{36}S are related to variations in $\delta^{34}S$ as

$$\delta^{33}S = 0.515 \times \delta^{34}S \qquad \text{and} \qquad \delta^{336}S = 1.90 \times \delta^{34}S$$

However, Farquhar et al. (2000) found that relationships do not hold for sulfur in many Archean sediments and ore deposits. Let's define the quantities $\Delta^{33}S$ and $\Delta^{36}S$ as:

$$\Delta^{33}S = \delta^{33}S - 0.515 \times \delta^{34}S \qquad 9.65$$

and

$$\Delta^{36}S = \delta^{36}S - 1.90 \times \delta^{34}S \qquad 9.66$$

Farquhar et al. found that many sulfides (primarily pyrite) in sediments and metasediments formed prior to 2500 Ma have positive $\Delta^{33}S$ and negative $\Delta^{36}S$ while hydrothermal sulfide ores and sedimentary sulfates (mainly barite) have negative $\Delta^{33}S$ and positive $\Delta^{36}S$ (Figure 9.36). During the Archean, $\Delta^{33}S$, i.e., deviations from mass dependent fractionation, of over 3‰ occurred. Farquhar et al. found smaller deviations, up to ½ ‰ in rocks from the period 2500-2000 Ma. They found no significant deviations from mass dependent fractionation in rocks younger than 2000 Ma.

This raises the obvious question of what process or processes operated during the Archean that could produce mass independent fractionation? Why does this process no longer operate? As mentioned earlier, mass independent isotope fractionation has been observed during laboratory photolysis of SO_2 and SO using ultraviolet light. This, together with the observation that ozone and molecular oxygen absorb ultraviolet radiation, provides a possible explanation. Modern volcanic eruptions loft vast quantities of SO_2 into the atmosphere and Archean eruptions likely did as well. If the Archean atmosphere lacked O_2 and O_3, ultraviolet radiation could penetrate deeply into it and photodissociate SO_2. According to experiments, these reactions produce sulfate with negative $\Delta^{33}S$ and elemental sulfur with positive $\Delta^{33}S$. The sulfate would dissolve in rain and ultimately find its way into the oceans. Some of this would precipitate as barite, $BaSO_4$. Some sulfate would be reduced in hydrothermal systems and precipitate as metal sulfides. Both these processes occur in modern oceans. The S would form particulate S_8 and also be swept out of the atmosphere by rain and ultimately incorporated into sediments, where it would react to form sedimentary sulfides. The latter also requires an absence of O_2 in the atmosphere – elemental S in the modern atmosphere would be quickly oxidized.

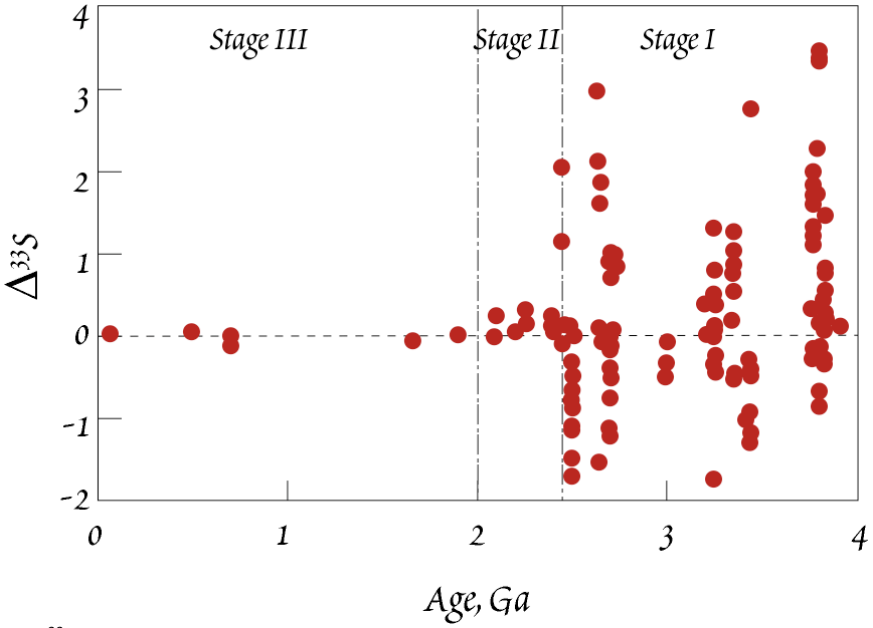

Figure 9.36. $\Delta^{33}S$ in sulfur through time. During Stage 1 (prior to 2.45 Ga), extensive mass independent fractionation occurred as evidenced by $\Delta^{33}S$ up to 3.5‰, indicating the lack of atmospheric oxygen. During Stage 2 (2.45 to 2.0 Ga), limited amounts of atmospheric oxygen (up to 1% of present levels) absorbed most UV radiation and limited mass independent fractionation to <0.5‰. High levels of atmospheric oxygen in Stage 3 (since 2.0 Ga) effectively eliminate UV radiation and mass independent fractionation. From Farquhar and Wing (2003).

Mass independent fractionation in Archean sulfur thus provides evidence that the early atmosphere lacked free oxygen. This is entirely consistent with other evidence, such as the oxidation state of paleosols and detrital minerals, that the atmosphere did not contain significant amounts of O_2 until the early Proterozoic, about 2 – 2.3 billion years ago. Farquhar and Wing (2003) and Kasting and Catling (2003) provide excellent reviews on this topic.

9.8 Stable Isotopes in the Mantle and Magmatic Systems

9.8.1 Stable Isotopic Composition of the Mantle

The mantle is the largest reservoir for oxygen, and may be for H, C, N, and S as well. Thus we need to know the isotopic composition of the mantle to know the isotopic composition of the Earth. Variations in stable isotope ratios in mantle and mantle-derived materials also provide important insights on mantle and igneous processes.

9.8.1.1 Oxygen

Assessing the oxygen isotopic composition of the mantle, and particularly the degree to which its oxygen isotope composition might vary, has proved to be more difficult than expected. One approach has been to use basalts as samples of mantle, as is done for radiogenic isotopes. Isotope fractionation occurring during partial melting are small, so the oxygen isotopic composition of basalt should the similar to that of its mantle source. However, assimilation of crustal rocks by magmas and oxygen isotope exchange during weathering complicate the situation. An alternative is to use direct mantle samples such as xenoliths occasionally found in basalts. However, these are considerably rarer than are basalts.

Figure 9.37 shows the oxygen isotope composition of olivines and clinopyroxenes in 76 peridotite xenoliths analyzed by Mattey et al. (1994) using the laser fluorination technique. The total range of values observed is only about twice that expected from analytical error alone, suggesting the mantle is fairly homogeneous in its isotopic composition. The difference between co-existing olivines and clinopyroxenes

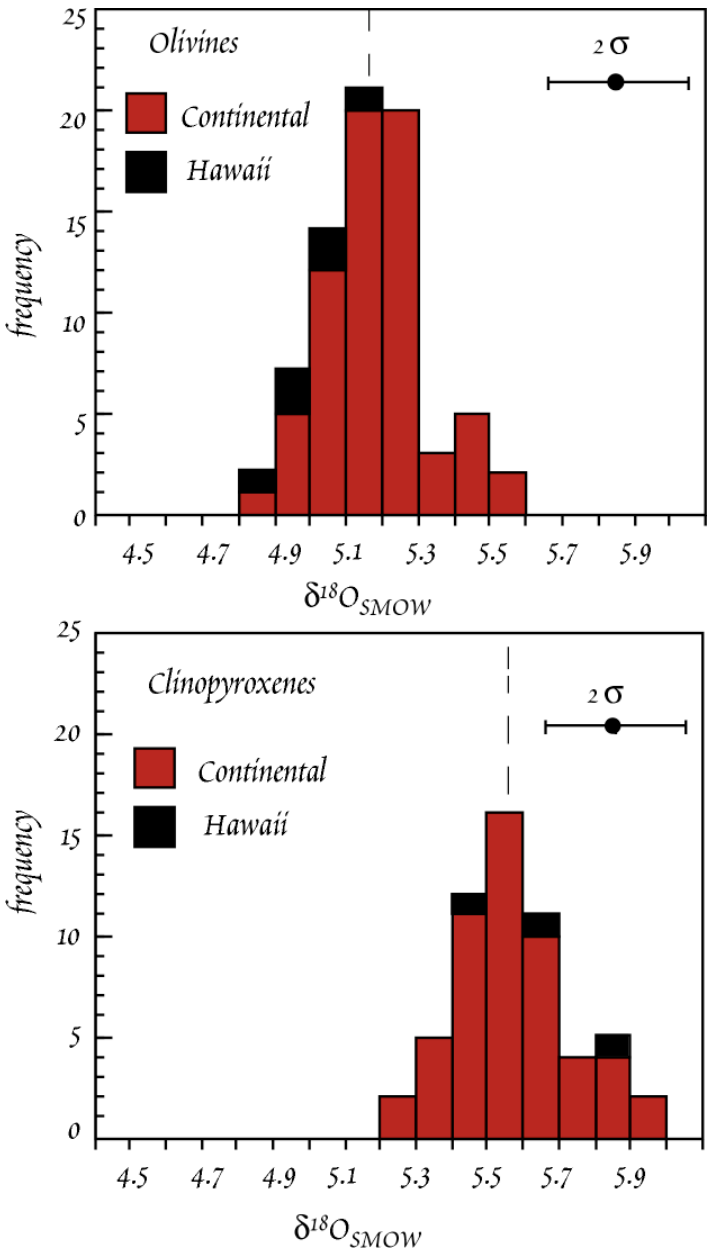

Figure 9.37. Oxygen isotope ratios in olivines and clinopyroxenes from mantle peridotite xenoliths. Data from Mattey et al. (1994).

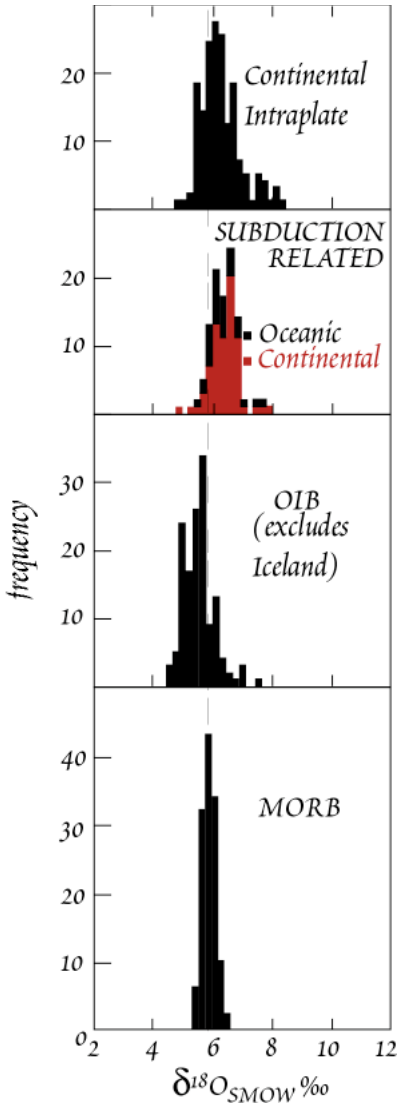

Figure 9.38. $\delta^{18}O$ in young, fresh basalts. Dashed line is at the mean of MORB (+5.7). After Harmon and Hoefs (1995).

averages about 0.5 per mil, which is consistent with the expected fractionation between these minerals at mantle temperatures. Mattey et al. (1994) estimated the bulk composition of these samples to be about +5.5 per mil.

Figure 9.38 shows the distribution of $\delta^{18}O$ in basalts from 4 different groups. To avoid weathering problems, Harmon and Hoefs (1995) included only submarine basaltic glasses and basalts having less than 0.75% water or have erupted historically in their compilation. There are several points worth noting in these data.

MORB have a mean $\delta^{18}O_{SMOW}$ of +5.7‰, with a relatively smaller variation about this mean. Thus the depleted upper mantle appears to be a relatively homogeneous reservoir for oxygen. The homogeneity observed in MORB is consistent with that observed in mantle-derived xenoliths. The small difference between the means of the two groups (0.2‰), may well reflect fractionation occurring during partial melting.

The other groups show significantly greater heterogeneity than either MORB or peridotite xenoliths. Oceanic island basalts, which presumably sample mantle plumes, have a mean identical to that of peridotite xenoliths, but are more variable. Subduction-related basalts (i.e., island arc basalts and their continental equivalents) are shifted to more positive $\delta^{18}O$ values, as are continental intraplate volcanics.

Whether the variability in these groups reflects mantle heterogeneity, the melting process, assimilation, or merely weathering remains unclear. Hawaii is the one locality where high quality data exists for both basalts and xenoliths and comparisons can be made. Both Hawaiian basalts and olivines in Hawaiian xenoliths (Figure 9.37) have lower $\delta^{18}O$ than their equivalents from elsewhere. This suggests the possibility, at least, that part of the variability in oceanic basalts reflects mantle heterogeneity. However, additional studies will be required to establish this with certainty.

9.8.1.2 Hydrogen

Estimating the isotopic composition of mantle hydrogen, carbon, nitrogen, and sulfur is even more problematic. These are all volatile elements and are present at low concentrations in mantle materials. They partitioning partially or entirely into the gas phase of magmas upon their eruption. This gas phase is lost, except in deep submarine eruptions. Furthermore, C, N, and S have several oxidation states, and isotopic fractionations occur between the various compounds these elements form (e.g., CO_2, CO, CH_4, H_2, H_2O, H_2S, SO_2). This presents two problems. First, significant fractionations can occur during degassing, even at magmatic temperatures. Second, because of loss of the gas phase, the concentrations of these elements are low. Among other problems, this means their isotope ratios are subject to disturbance by contamination. Thus the isotopic compositions of these elements in igneous rocks do not necessarily reflect those of the magma or its mantle source.

Hydrogen, which is primarily present as water, but also as H_2 H_2S, and CH_4, can be lost from magmas during degassing. However, basalts erupted beneath a kilometer or more of ocean retain most of their dissolved water. Thus mid-ocean ridge basalts and basalts erupted on seamounts are important sources of information of the abundance and isotopic composition of hydrogen in the mantle.

As Figure 9.39 indicates, MORB have a mean δD_{SMOW} of about –67.5‰ and a standard deviation of ±14‰. How much of this variability reflects fractionation during degassing and contamination is un-

clear. Kyser (1986) has argued that mantle hydrogen is isotopically homogeneous with δD_{SMOW} of -80‰. The generally heavier isotopic composition of MORB, he argues, reflects H_2O loss and other processes. Others, for example, Poreda et al. (1986), Chaussidon et al. (1991) have observed correlations between δD and Sr and Nd isotope ratios and have argued that these provide clear evidence of that mantle hydrogen is isotopically heterogeneous. Chausidon et al. (1991) have suggested a δD value for the depleted upper mantle of about -55‰.

The first attempt to assess the hydrogen isotopic composition of the mantle materials was that of Sheppard and Epstein (1970), who analyzed hydrous minerals in xenoliths and concluded δD was variable in the mantle. Since then, a number of additional studies of these materials have been carried out. As Figure 9.39 shows, phlogopites ($KMg_3AlSi_3O_{10}(OH)_2$) have δD that is generally similar to that of MORB, though heavier values also occur. Amphiboles have much more variable δD and have heavier hydrogen on average. Part of this difference probably reflects equilibrium fractionation. The fractionation between water and phlogopite is close to 0‰ in the temperature range 800°-1000°C, whereas the fractionation between water and amphibole is about –15‰. However, equilibrium fractionation alone cannot explain either the variability of amphiboles or the difference between the mean δD of phlogopites and amphiboles. Complex processes that might include Rayleigh distillation may be involved in the formation of mantle amphiboles. This would be consistent with the more variable water content of amphiboles compared to phlogopites. There are also clear regional variations in δD in xenoliths that argue for large-scale heterogeneity. For example, Deloule et al. (1991) found that δD in amphiboles from xenoliths in basalts in the Massif Central of France have systematically high δD (-59 to -28‰) while those from Hawaii can be very low (-125‰). At the opposite extreme, Deloule et al. (1991) also observed isotopic heterogeneity within single crystals, which they attribute to incomplete equilibration with magmas or fluids.

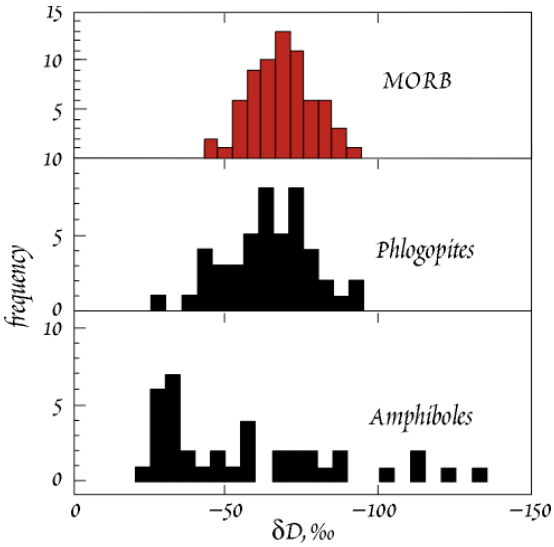

Figure 9.39. δD in MORB and in mantle phlogopites and amphiboles. The MORB and phlogopite data suggest the mantle has δD_{SMOW} of about –60 to –90.

9.8.1.3 Carbon

Most carbon in basalts is in the form of CO_2, which has limited solubility in basaltic liquids. As a result, basalts begin to exsolve CO_2 before they erupt. Thus virtually every basalt, including those erupted at mid-ocean ridges, has lost some carbon, and subareal basalts have lost virtually all carbon (as well as most other volatiles). Therefore only basalts erupted beneath several km of water provide useful samples of mantle carbon, so the basaltic data set is essentially restricted to MORB and samples recovered from seamounts and the submarine part of Kilauea's East Rift Zone. The question of the isotopic composition of mantle carbon is further complicated by fractionation and contamination. There is a roughly 4‰ fractionation between CO_2 dissolved in basaltic melts and the gas phase, with ^{13}C enriched in the gas phase. Carbonatites and diamonds provide alternative, and generally superior, samples of mantle carbon, but their occurrence is extremely restricted.

MORB have a mean $\delta^{13}C$ of –6.5‰ (Figure 9.40), but the most CO_2-rich MORB samples have $\delta^{13}C$ of about –4‰. Since they are the least degassed, they presumably best represent the isotopic composition of the depleted mantle (Javoy and Pineau, 1991). Carbonatites also have a mean $\delta^{13}C$ close to -4‰. Oceanic island basalts erupted under sufficient water depth to preserve some CO_2 in the vesicles appear to have similar isotopic compositions. Gases released in subduction zone volcanos and back-arc basin basalts (Figure 9.38), which erupt behind subduction zones and are often geochemically similar to island arc basalts, have carbon that can be distinctly lighter (lower $\delta^{13}C$), though most $\delta^{13}C$ values are in

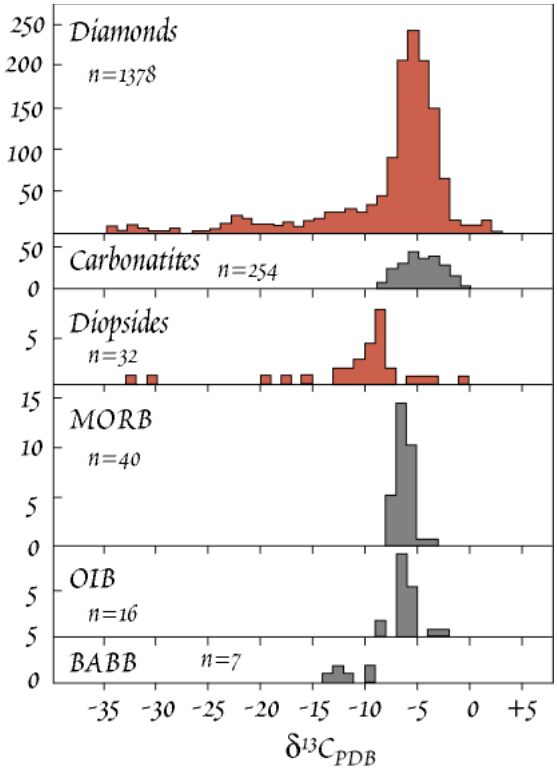

Figure 9.40. Carbon isotope ratios in mantle (red) and mantle-derived materials (gray). After Mattey (1987).

the range of –2 to –4‰, comparable to the most gas-rich MORB. Carbon in mantle diopsides (clinopyroxenes) appears to be isotopically lighter on average, and the significance of this is unclear.

Diamonds show a large range of carbon isotopic compositions (Figure 9.40). Most diamonds have $\delta^{13}C$ within the range of -2 to -8‰, hence similar to MORB. However, some diamonds have much lighter carbon. Based on the inclusions they contain, diamonds can be divided between peridotitic and eclogitic. Most peridotitic diamonds have $\delta^{13}C$ close to –5‰, while eclogitic diamonds are much more isotopically variable. Most, though not all, of the diamonds with very negative $\delta^{13}C$ are eclogitic. Many diamonds are isotopically zoned, indicating they grew in several stages.

Three hypotheses have been put forward to explain the isotopic heterogeneity in diamonds: primordial heterogeneity, fractionation effects, and recycling of organic carbon from the Earth's surface into the mantle. Primordial heterogeneity seems unlikely for a number of reasons. Among these is the absence of very negative $\delta^{13}C$ in other materials, such as MORB, and the absence of any evidence for primordial heterogeneity from the isotopic compositions of other elements. Boyd and Pillinger (1994) have argued that since diamonds are kinetically sluggish (witness their stability at the surface of the Earth, where they are thermodynamically out of equilibrium), isotopic equilibrium might not achieved during their growth. Large fractionations might therefore occur due to kinetic effects. However, these kinetic fractionations have not been demonstrated, and fractionations of this magnitude (20‰ or so) would be surprising at mantle temperatures.

On the other hand, several lines of evidence support the idea that isotopically light carbon in some diamonds had its origin as organic carbon at the Earth's surface. First, such diamonds are primarily of eclogitic paragenesis, and ecolgite is the high pressure equivalent of basalt. Subduction of oceanic crust continuously carries large amounts of basalt into the mantle. Oxygen isotope heterogeneity observed in some eclogite xenoliths suggests these eclogites do indeed represent subducted oceanic crust. Second, the nitrogen isotopic composition of isotopically light diamonds is anomalous relative to nitrogen in other mantle materials. Finally, Farquhar et al. (2002) found mass independent fractionation ($\Delta^{33}S$ up to 0.6‰) in sulfide inclusions in eclogitic diamonds. If, as is believed the mass independent fractionation arises from UV photolysis in the atmosphere, then the sulfur in these diamonds must once have been at the surface of the Earth.

9.8.1.4 NITROGEN

The solubility of N_2 in magmas is very limited, hence of volcanic rocks, once again only submarine basalts provide useful samples of mantle N. There are both contamination and analytical problems with determining nitrogen isotope ratios in basalts, which, combined with its low abundance (generally less than a ppm), mean that accurate measurements are difficult to make. Nitrogen substitutes readily for carbon in diamonds, which can contain up to 2000 ppm N, making diamonds important samples of mantle N. Nitrogen may be present as the ammonium ion in many kinds of rocks. NH_4^+ substitutes readily for K in many minerals; consequently N concentrations in sediments and metasediments may reach several hundred ppm. In all, a fair amount of data is now available for a variety of mantle and crustal materials and these data are summarized in Figure 9.41. Measurements of $\delta^{15}N_{ATM}$ in MORB

range from about –10 to +8‰, with a mean value of about -3 to -5‰. Peridotitic diamonds show a similar range, but are a little lighter on average. Eclogitic diamonds show considerably greater scatter in $\delta^{15}N_{ATM}$, with the most common values in the range of -12 to -6‰. Interestingly, oceanic island basalts, which presumably sample mantle plumes, have distinctly more positive $\delta^{15}N_{ATM}$, with a mean in the range of +3 to +4‰. The N isotopic composition of mantle plumes thus appears to match well with that of organic matter in post-Archean sediments, metamorphic rocks, and subduction-related volcanic rocks. This observation led Marty and Dauphas (2003) to propose that nitrogen in mantle plumes is largely recycled from the surface of the Earth. They argue that because nitrogen can be bound in minerals as ammonium, it is more readily subducted and recycling into the mantle than other gases.

Figure 9.41 also illustrates an interesting shift in $\delta^{15}N$ in organic matter in sediments in the late Archean. Marty and Dauphas (2003) suggest 2 possible causes. First, the absence of atmospheric oxy-

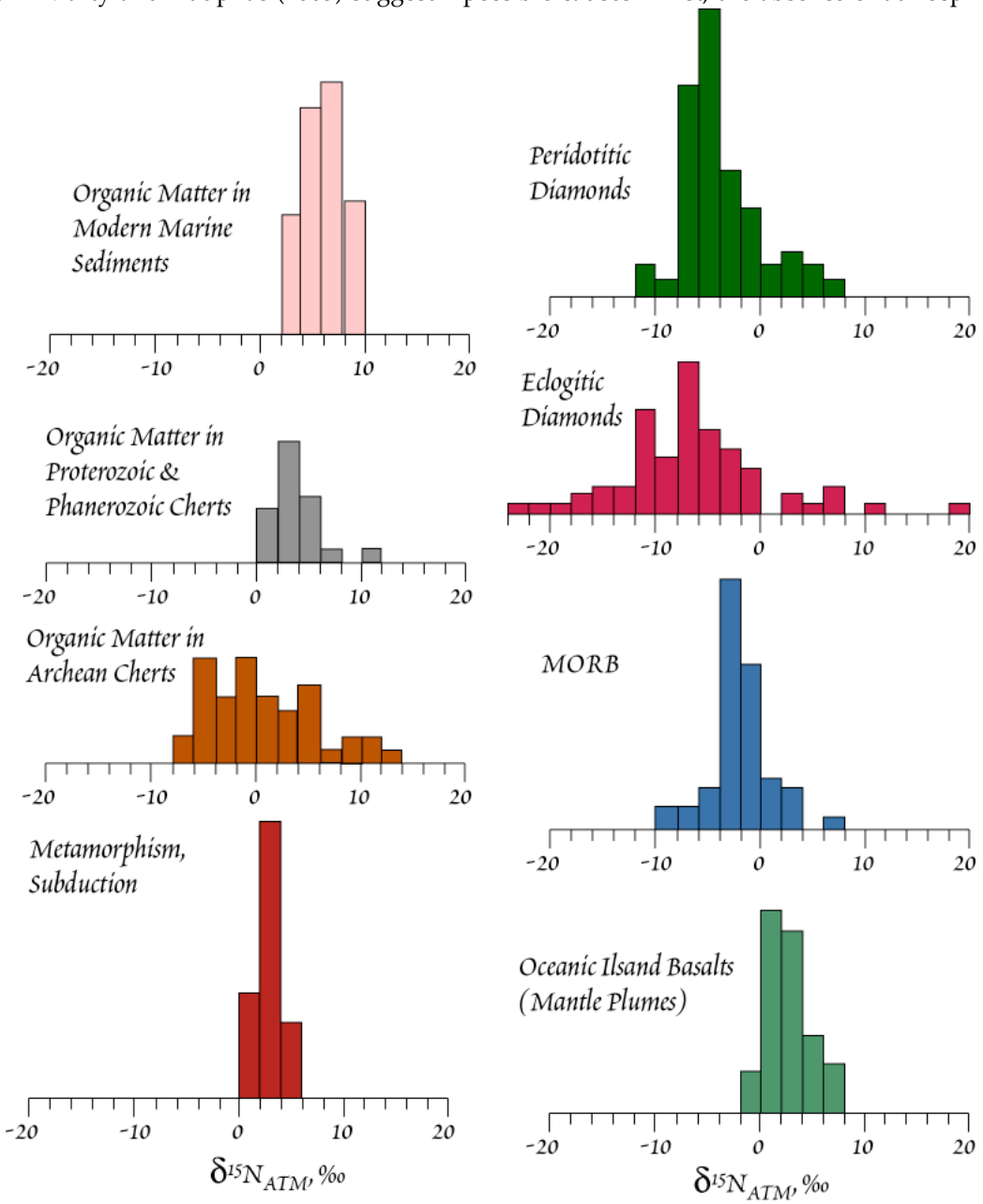

Figure 9.41. Isotopic composition of nitrogen in rocks and minerals of the crust and mantle. Modified from Marty and Dauphas (2003).

gen in the Archean meant that there was no nitrate, and hence no dissimilatory denitrification and consequently no fractionation associated with that process. Second, chemosynthetic life may have dominated the Archean. Modern chemosynthetic bacteria from hydrothermal vent ecosystems have a lower $\delta^{15}N$ than most plants, meaning the N isotopic composition of organic matter in Archean sediments would have been lighter than in post-Archean sediments.

9.8.1.5 Sulfur

There are also relatively few sulfur isotope measurements on basalts, in part because sulfur is lost during degassing, except for those basalts erupted deeper than 1 km below sealevel. In the mantle, sulfur is probably predominantly or exclusively in the form of sulfide, but in basalts, which tend to be somewhat more oxidized, some of it may be present as SO_2 or sulfate. Equilibrium fractionation should lead to SO_2 being a few per mil lighter than sulfate. If H_2S is lost during degassing the remaining sulfur would become heavier; if SO_2 or SO_4 is lost, the remaining sulfur would become lighter. Total sulfur in MORB has $\delta^{34}S_{CDT}$ in the range of +1.3 to –1‰, with most values in the range 0 to +1‰. Sakai et al. (1984) found that sulfate in MORB, which constitutes 10-20% of total sulfur, was 3.5 to 9‰ heavier than sulfide. Basalts from Kilauea's East Rift Zone have a very restricted range of $\delta^{34}S$ of +0.5 to +0.8 (Sakai, et al., 1984) .

Chaussidon et al. (1989) analyzed sulfides present as inclusions in minerals, both in basalts and in xenoliths, and found a wide range of $\delta^{34}S$ (–5 to +8‰). Low Ni sulfides in oceanic island basalts, kimberlites, and pyroxenites had more variable $\delta^{34}S$ that sulfides in peridotites and peridotite minerals. They argued there is a fractionation of +3‰ between sulfide liquid and sulfide dissolved in silicate melt. Carbonatites have $\delta^{34}S$ between +1 and –3‰ (Hoefs, 1986; Kyser, 1986). Overall, it appears the mantle has a mean $\delta^{34}S$ in the range of 0 to +1‰, which is very similar to meteorites, which average about +0.1‰.

Chaussidon, et al. (1987) found that sulfide inclusions in diamonds of peridotitic paragenesis ($\delta^{13}C$ ~ –4‰) had $\delta^{34}S$ of about +1‰ while eclogitic diamonds had higher, and much more variable $\delta^{34}S$ (+2 to +10‰). Eldridge et al. (1991) found that $\delta^{34}S$ in diamond inclusions was related to the Ni content of the sulfide. High Ni sulfide inclusions, which they argued were of peridotitic paragenesis, had $\delta^{34}S$ between +4‰ and –4‰. Low Ni sulfides, which are presumably of eclogitic paragenesis, had much more variable $\delta^{34}S$ (+14‰ to –10). These results are consistent with the idea that eclogitic diamonds are derived from subducted crustal material.

9.8.2 Stable Isotopes in Crystallizing Magmas

The variation in stable isotope composition produced by crystallization of a magma depends on the manner in which crystallization proceeds. The simplest, and most unlikely, case is *equilibrium* crystallization. In this situation, the crystallizing minerals remain in isotopic equilibrium with the melt until crystallization is complete. At any stage during crystallization, the isotopic composition of a mineral and the melt will be related by the fractionation factor, α. Upon complete crystallization, the rock will have precisely the same isotopic composition as the melt initially had. At any time during the crystallization, the isotope ratio in the remaining melt will be related to the original isotope ratio as:

$$\frac{R_\ell}{R_o} = \frac{1}{f + \alpha(1-f)};\ \alpha \equiv \frac{R_s}{R_\ell} \qquad 9.67$$

where R_l is the ratio in the liquid, R_s is the isotope ratio of the solid, R_0 is the isotope ratio of the original magma, f is the fraction of melt remaining. This equation is readily derived from mass balance, the definition of α, and the assumption that the O concentration in the magma is equal to that in the crystals; an assumption valid to within about 10%. It is more convenient to express 9.67, in terms of δ:

$$\Delta = \delta_{melt} - \delta_0 \cong \left[\frac{1}{f + \alpha(1-f)}\right] * 1000 \qquad 9.68$$

where δ_{melt} is the value of the magma after a fraction f-1 has crystallized and δ_o is the value of the original magma. For silicates, α is not likely to much less than 0.998 (i.e., $\Delta = \delta^{18}O_{xtals} - \delta^{18}O_{melt} >= -2$). For α

= 0.999, even after 99% crystallization, the isotope ratio in the remaining melt will change by only 1 per mil.

The treatment of *fractional crystallization* is analogous to Rayleigh distillation. Indeed, it is governed by the same equation:

$$\Delta = 1000\left(f^{\alpha-1} - 1\right) \quad (9.46)$$

The key to the operation of either of these processes is that the product of the reaction (vapor in the case of distillation, crystals in the case of crystallization) is only instantaneously in equilibrium with the original phase. Once it is produced, it is removed from further opportunity to attain equilibrium with original phase. This process is more efficient at producing isotopic variations in igneous rocks, but its effect remains limited because α is generally not greatly different from 1. Figure 9.42 shows calculated change in the isotopic composition of melt undergoing fractional crystallization for various values of Δ (≈ 1000(α–1)). In reality, Δ will change during crystallization because of (1) changes in temperature (2) changes in the minerals crystallizing, and (3) changes in the liquid composition. The changes will generally mean that the effective Δ will increase as crystallization proceeds. We would expect the greatest isotopic fractionation in melts crystallizing non-silicates such as magnetite and melts crystallizing at low temperature, such as rhyolites, and the least fractionation for melts crystallizing at highest temperature, such as basalts.

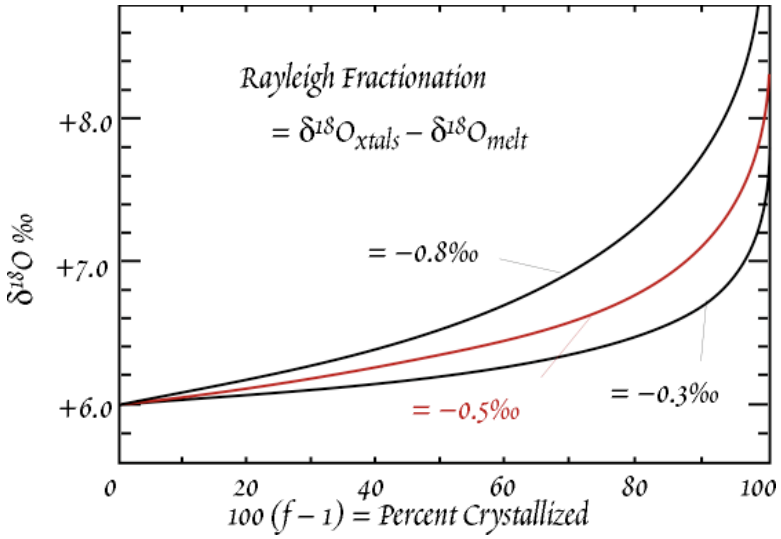

Figure 9.42. Plot of $\delta^{18}O$ versus fraction of magma solidified during Rayleigh fractionation, assuming the original $\delta^{18}O$ of the magma was +6. After Taylor and Sheppard (1986).

Figure 9.43 shows observed $\delta^{18}O$ as a function of temperature in two suites: one from a propagating rift on the Galapagos Spreading Center, the other from the island of Ascension. There is a net change in $\delta^{18}O$ between the most and least differentiated rocks in the Galapagos of about 1.3‰; the change in the Ascension suite is only about 0.5‰. These, and other suites, indicate the effective Δ is generally small, on the order of 0.1 to 0.3‰. Consistent with this is the similarity of $\delta^{18}O$ in peridotites and MORB, which suggests a typical fractionation during melting of 0.2‰ or less.

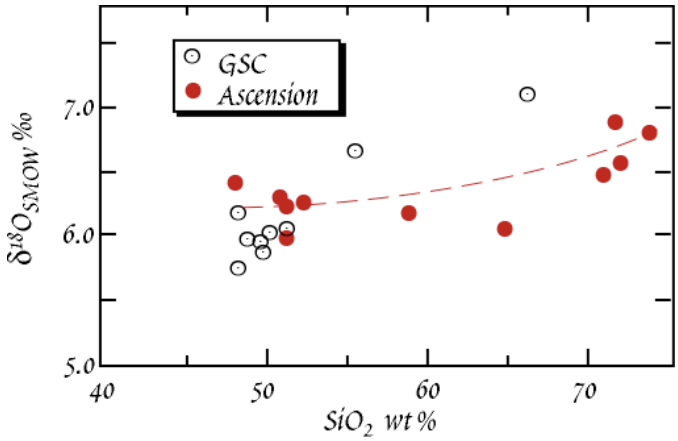

Figure 9.43. $\delta^{18}O$ as a function of SiO_2 in a tholeiitic suite from the Galapagos Spreading Center (GSC) (Muehlenbachs and Byerly, 1982) and an alkaline suite from Ascension Island (Sheppard and Harris, 1985). Dashed line shows model calculation for the Ascension suite.

We can generalize the temperature dependence of oxygen isotope fractionations by saying that at low temperature (i.e., Earth surface temperatures up to the temperature of hydrothermal systems, 300-400° C), oxygen isotope ratios are changed by chemical processes. The amount of change can be used as an indication of the nature of the process involved, and, under equilibrium conditions, of the temperature at which the process oc-

curred. *At high temperatures (temperatures of the interior of the Earth or magmatic temperatures), oxygen isotope ratios are minimally affected by chemical processes and can be used as tracers much as radiogenic isotope ratios are.*

These generalizations lead to an axiom: *igneous rocks whose oxygen isotopic compositions show significant variations from the primordial value (+6) must either have been affected by low temperature processes, or must contain a component that was at one time at the surface of the Earth* (Taylor and Sheppard, 1986).

9.8.3 Combined Fractional Crystallization and Assimilation

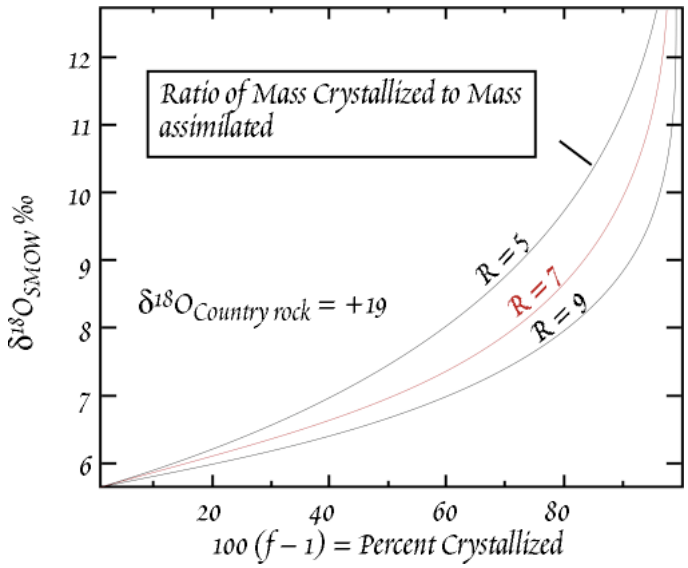

Figure 9.44. Variation in $\delta^{18}O$ of a magma undergoing AFC vs. amount crystallized. Initial $\delta^{18}O$ of the magma is +5.7. After Taylor (1980).

Because oxygen isotope ratios of mantle-derived magmas are reasonably uniform (±1‰ of 5.6‰) and generally different from rocks that have equilibrated with water at the surface of the Earth, oxygen isotopes are a useful tool in identifying and studying the assimilation of country rock by intruding magma. We might think of this process as simple mixing between two components: magma and country rock. In reality, it is always at least a three-component problem, involving country rock, magma, and minerals crystallizing from the magma. Magmas are essentially never superheated; hence the heat required to melt and assimilate surrounding rock can only come from the latent heat of crystallization of the magma. Approximately 1 kJ/g would be required to heat rock from 150° C to 1150°C and another 300 J/g would be required to melt it. If the latent heat of crystallization is 400 J/g, crystallization of 3.25 g of magma would be required to assimilate 1 g of country rock. Since some heat will be lost by simple conduction to the surface, we can conclude that the amount of crystallization will inevitably be greater than the amount of assimilation (the limiting case where mass crystallized equals mass assimilated could occur only at great depth in the crust where the rock is at its melting point to begin with). The change in isotopic composition of a melt undergoing the combined process of assimilation and fractional crystallization (AFC) is given by:

$$\delta_m - \delta_0 = \left(\left[\delta_a - \delta_0\right] - \Delta \times R\right)\left\{1 - f^{1/(R-1)}\right\} \qquad 9.69$$

where R is the mass ratio of material crystallized to material assimilated, Δ is the difference in isotope ratio between the magma and the crystals ($\delta_{maggma} - \delta_{crystals}$), f is the fraction of liquid remaining, δ^m is the $\delta^{18}O$ of the magma, δ_o is the initial $\delta^{18}O$ of the magma, and δ_a is the $\delta^{18}O$ of the material being assimilated. The assumption is made that the concentration of oxygen is the same in the crystals, magma and assimilant, which is a reasonable assumption. This equation breaks down at R = 1, but, as discussed above, R is generally significantly greater than 1. Figure 9.44 shows the variation of $\delta^{18}O$ of a magma with an initial $\delta^{18}O = 5.7$ as crystallization and assimilation proceed.

Combining stable and radiogenic isotope ratios provides an even more powerful tool to examine assimilation. We shall consider this in Chapter 12.

9.9 Isotopes of Boron and Lithium

Although there are a few earlier works in the literature, there was little interest in the isotopic composition of boron and lithium until about 20 years ago. This is perhaps because both elements have low abundances in the Earth compared to the other elements we have discussed thus far. It is perhaps also because of the analytical problems: neither B nor Li form gaseous species that can be analyzed in the gas-source mass spectrometers used for analysis of other stable isotopes, and the fractionation pro-

duced in thermal ionization mass spectrometers, which are used for elements such as Sr, Nd, and Pb, would exceed the natural ones. Since the development of new analytical techniques that overcame this latter problem in the 1980's, the field of boron isotope geochemistry has developed rapidly, and a range of about 9% in the $^{11}B/^{10}B$ ratio in terrestrial materials has been observed. Boron isotope geochemistry has been used to address a wide variety of geochemical problems. Most notable among these are: hydrothermal processes, the nature and origin of ore-forming fluids, the origin of evaporites and brines, pH of ancient oceans, the origin of subduction-related magmas, and geochemical evolution of the mantle.

Though both lithium and boron can occur as stoichiometric components of minerals, these minerals have limited occurrence, and these elements generally substitute for other elements in silicates. Boron is relatively abundant in seawater, with a concentration of 4.5 ppm. Lithium is somewhat less abundant, with a concentration of 0.17 ppm. In silicate rocks, the concentration of boron ranges from a few tenths of a ppm or less in fresh basalts and peridotites to several tens of ppm in clays. Lithium concentrations in these materials typically range from a few ppm to a few tens of ppm. The $^{11}B/^{10}B$ is reported as per mil variations, $\delta^{11}B$, from the NIST SRM* 951 standard. The $^{7}Li/^{6}Li$ ratio is reported as per mil variation, $\delta^{7}Li$, from the NIST SRM 8545 Li_2CO_3 (L-SVEC) standard (Table 9.1). Prior to 1996, Li isotope ratios were often reported as $\delta^{6}Li$, i.e., deviations from the $^{6}Li/^{7}Li$ ratio. However, the standard used was the same, so that for variations less than about 10, $\delta^{7}Li \approx \delta^{6}Li$; at higher deviations, a more exact conversion is necessary, e.g., -38.5‰ $\delta^{6}Li$ = 40‰ $\delta^{7}Li$. The analytical precision for most of the Li isotope now in the literature is about 1‰, but recent advances, particularly the use of multiple-collector inductively coupled plasma mass spectrometers, promises to reduce uncertainty to as little as 0.2‰.

9.9.1 BORON ISOTOPES

In nature, boron has a valence of +3 is almost always bound to oxygen or hydroxyl groups in either trigonal (e.g., BO_3) or tetrahedral (e.g., $B(OH)_4^-$) coordination (the only exception is boron bound to fluorine, e.g., BF_3). Since the bond strengths and vibrational frequencies of trigonal and tetrahedral forms differ, we can expect that isotopic fractionation will occur between these two forms. This is confirmed by experiments which show a roughly 20‰ fractionation between $B(OH)_3$ and $B(OH)_4^-$, with ^{11}B preferentially found in the $B(OH)_3$ form.

In natural aqueous solutions boron occurs as both boric acid, $B(OH)_3$, and the borate ion, $B(OH)_4^-$, the dominant species being determined by pH. At pH of around 9 and above, $B(OH)_4^-$, dominates, at lower pH $B(OH)_3$ dominates. In seawater which has a pH in the range of 7.6 to 8.1, about 80-90% of boron will be in the $B(OH)_3$ form. Most fresh waters are a little more acidic so $B(OH)_3$ will be more dominant; only in highly alkaline solutions, such as saline lakes, will $B(OH)_4^-$ be dominant. The most common boron mineral in the crust is tourmaline ($Na(Mg,Fe,Li,Al)_3Si_6O_{18}(BO_3)_3(OH,F)_4$), in which boron is present in BO_3 groups. In clays, boron appears to occur primarily as $B(OH)_4^-$, most likely substituting for silica in tetrahedral layers. The coordination of boron in common igneous minerals is uncertain, possibly substituting for Si in tetrahedral sites. As we noted in Chapter 7, boron is an incompatible element in igneous rocks and is very fluid mobile. It is also readily adsorbed onto the surfaces of clays. There is an isotopic fractionation between dissolved and adsorbed B of –20 to -30‰ (i.e, adsorbed B is ^{11}B poor), depending on pH and temperature (Palmer et al., 1987).

Figure 9.45 illustrates the variation in B isotopic composition in a variety of geologic materials. Spivack and Edmond (1987) found the $\delta^{11}B$ of seawater to be +39.5‰, and was uniform within analytical error (±0.25‰). Fresh mid-ocean ridge basalts typically have $\delta^{11}B$ of about -4‰. Oceanic island basalts (OIB) have slightly lighter $\delta^{11}B$ (e.g., Chaussidon and Jambon, 1994). The average B isotopic composition of the continental crust probably lies between -13‰ and -8‰ (Chaussidon and Abarède, 1992).

Perhaps the most remarkable aspect of B isotope geochemistry is the very large fractionation of B isotopes between the oceans and the silicate Earth. It was recognized very early that this difference re-

* NIST stands for the U.S. National Institute of Standards and Technology and was formerly known as the National Bureau of Standards (NBS). SRM stands for standard reference material.

flected the fractionation that occurred during adsorption of boron on clays (e.g., Schwarcz, et al., 1969). However, as we noted above, this fractionation is only about 30‰ or less, whereas the difference between the continental crust and seawater is close to 50‰. Furthermore, the net effect of hydrothermal exchange between the oceanic crust and seawater is to decrease the $\delta^{11}B$ of seawater (Spivack and Edmond, 1977). The discrepancy reflects the fact that the ocean is not a simple equilibrium system, but rather a kinetically controlled open one. Since all processes operating in the ocean appear to preferentially remove ^{10}B from the ocean, seawater is driven to an extremely ^{11}B-rich composition. In addition, it is possible that additional fractionations of boron isotopes may occur during diagenesis. Ishikawa and Nakamura (1993) noted that ancient limestones and cherts have more negative $\delta^{11}B$ than their modern equivalents, calcareous and siliceous oozes, and suggested that further fractionation occurred during diagenesis.

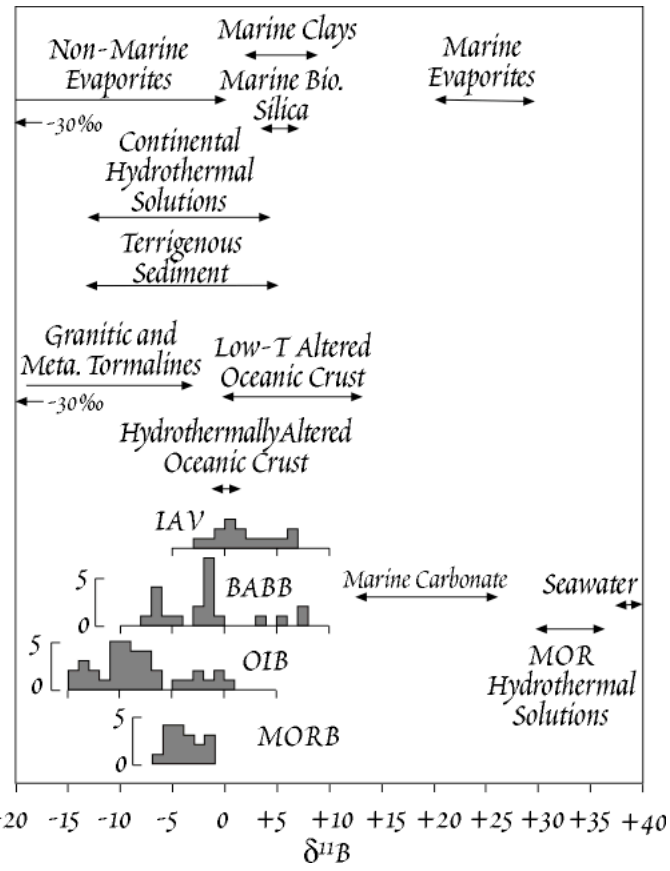

Figure 9.45. Boron isotopic composition in crystalline rocks (MORB: mid-ocean ridge basalts; OIB: oceanic island basalts; BABB: back-arc basin basalts, IAV: island arc volcanics), sediments, groundwater, freshwater, salt lakes, seawater, and mid-ocean ridge hydrothermal solutions.

Spivack and Edmond (1987) investigated the exchange of boron between seawater and oceanic crust. Boron is readily incorporated into the alteration products of basalt, so that even slightly altered basalts show a dramatic increase in B concentration and an increase in $\delta^{11}B$, with altered oceanic crust having $\delta^{11}B$ in the range of 0 to +25‰. Smith et al. (1995) estimated that average altered oceanic crust contains 5 ppm B and $\delta^{11}B$ of +3.4‰. During high temperature interaction between seawater and oceanic crust, Spivack and Edmond (1987) concluded that boron was quantitatively extracted from the oceanic crust by hydrothermal fluids. The isotopic composition of these fluids is slightly lower than that of seawater. They inferred that the B in these fluids is a simple mixture of seawater- and basalt-derived B and that little or no isotopic fractionation was involved. Analysis of hydrothermal altered basalts recovered by the Ocean Drilling Project generally confirm these inferences, as they are boron-poor and have $\delta^{11}B$ close to 0 (Ishikawa and Nakamura, 1992).

The more positive $\delta^{11}B$ values of island arc volcanics (IAV) relative to MORB must in part reflect the incorporation of subducted marine sediment and altered oceanic crust into the sources of island arc magmas (e.g., Palmer, 1991). This idea is consistent with a host of other data, which we will discuss in Chapter 12. There is, however, some debate as to the extent the more positive $\delta^{11}B$ values in IAV might also reflect assimilation of sediment or altered oceanic crust during magma ascent (e.g., Chaussidon and Jambon, 1994).

The differences in $\delta^{11}B$ between oceanic island basalts (OIB) and MORB is perhaps more problematic. Though no experimental or theoretical studies have been carried out, it seems unlikely that significant fractionation of boron isotopes will occur during melting of the mantle, both because the temperatures are high, and because the atomic environment of B in silicate melts is probably similar to that in silicate

solids. Thus, as we found was the case for O isotopes, B isotope fractionation probably occurs only at the surface of the Earth, and the difference between OIB and MORB must somehow reflect surface processes. Chaussidon and Marty (1995) argued that the boron isotopic composition of the mantle is that of OIB (-10‰) and that the higher $\delta^{11}B$ of MORB reflects contamination of MORB magmas by altered oceanic crust. This seems unlikely for several reasons. First, although there are still relatively few data available, MORB appear to be relatively homogeneous in their boron isotopic composition. This means assimilation would have to be systematic and pervasive and that all MORB magmas would have to assimilate roughly the same amount of material. Both of these seem highly improbable. Second, there is little or no other evidence for assimilation of oceanic crust by MORB magmas. Third, oceanic island basalts have an opportunity to assimilate not only altered oceanic crust, but also overlying sediment. Yet, according to the Chaussidon and Marty (1995) hypothesis, they are not systematically contaminated. Although they are not *systematically* contaminated, there is evidence of occasional assimilation of oceanic crust and/or sediment by oceanic island basalt magmas from both B and Os isotope geochemistry. This may explain some of the lower $\delta^{11}B$ values in OIB seen in Figure 9.45 (Chaussidon and Jambon, 1994).

The alternative explanation for the lower $\delta^{11}B$ in OIB is that they contain a component of material recycled into the mantle, through subduction, from the surface of the Earth. The idea that mantle plumes, and the OIB magmas they produce, contain material recycled from the surface of the Earth has been suggested on other grounds (Hofmann and White, 1982), and we shall discuss it further in Chapter 11. You (1994) points out that significant fractionation of B isotopes will occur during sediment dewatering at moderate temperatures during the initial stages of subduction. The fluid produced will be enriched in ^{11}B, leaving the sediment depleted in ^{11}B. Thus the effect of subduction zone processes will be to lower the $\delta^{11}B$ of oceanic crust and sediment carried into the deep mantle. Deciding between this view and that of Chaussidon and Marty (1995) will require further research.

One of the more interesting applications of boron isotopes has been determining the paleo-*pH* of the oceans. Boron is readily incorporated into carbonates, with modern marine carbonates having B concentrations in the range of 15-60 ppm. In modern foraminfera, $\delta^{11}B$ is roughly 20‰ lighter than the seawater in which they grow. This fractionation seems to result from the kinetics of B coprecipitation in $CaCO_3$, in which incorporation of B in carbonate is preceded by surface adsorption of $B(OH)_4^-$ (Vengosh et al., 1991; Heming and Hanson, 1992).

We noted above that boron is present in seawater both as $B(OH)_3$, and . Since the reaction between the two may be written as:

$$B(OH)_3 + H_2O \rightleftarrows B(OH)_4^- + H^+ \qquad 9.70$$

The equilibrium constant for this reaction is:

$$-pK^{app} = \ln \frac{B(OH)_4^-}{B(OH)_3} - pH \qquad 9.71$$

The relative abundance of these two species is thus pH dependent. Furthermore, we can easily show that the isotopic composition of these two species must vary if the isotopic composition of seawater is constant. From mass balance we have:

$$\delta^{11}B_{SW} = \delta^{11}B_3 f + \delta^{11}B_4(1-f) \qquad 9.72$$

where f is the fraction of $B(OH)_3$ (and $1 - f$ is therefore the fraction of $B(OH)_4^-$), $\delta^{11}B_3$ is the isotopic composition of $B(OH)_3$, and $\delta^{11}B_4$ is the isotopic composition of $B(OH)_4^-$. If the isotopic composition of the two species are related by a constant fractionation factor, $\Delta_{3\text{-}4}$, we can write 9.72 as:

$$^{11}B_{SW} = \delta^{11}B_3 f + \delta^{11}B_4 - \delta^{11}B_4 f = \delta^{11}B_4 - \Delta_{3\text{-}4} f \qquad 9.73$$

Solving for $\delta^{11}B_4$, we have:

$$\delta^{11}B_4 = {}^{11}B_{SW} + \Delta_{3\text{-}4} f \qquad 9.74$$

Thus assuming a constant fractionation factor and isotopic composition of seawater, the $\delta^{11}B$ of the two B species will depend only on f, which, as we can see in equation 9.71, will depend on pH.

If the mechanism for incorporation of B in carbonate presented above is correct, the fractionation of $^{11}B/^{10}B$ between calcite and seawater will be pH dependent. There is still some debate as to as to the exact mechanism of boron incorporation in carbonate, in particular whether only borate ion or both boric acid and borate ion can be incorporated. Regardless of the exact mechanism, the isotopic composition of boron in carbonate precipitated from seawater has been shown to be a strong function of pH (Sanyal et al., 2000), allowing in principle the reconstruction of paleo-seawater pH from carbonates. There are a some additional factors that must be considered: (1) different carbonate-secreting species may fractionate B isotopes slightly differently, perhaps because they alter the pH of their micro-environment, or perhaps because $B(OH)_3$ is also utilized to varying degrees, (2) the fractionation factor is temperature dependent, and (3) the B isotopic composition of seawater may vary with time. Nevertheless, if care is exercised to account for "vital" effects and variation in the isotopic composition and temperature of seawater, the B isotopic composition of marine biogenic carbonate preserved in sediment should reflect the pH of the water from which they were precipitated.

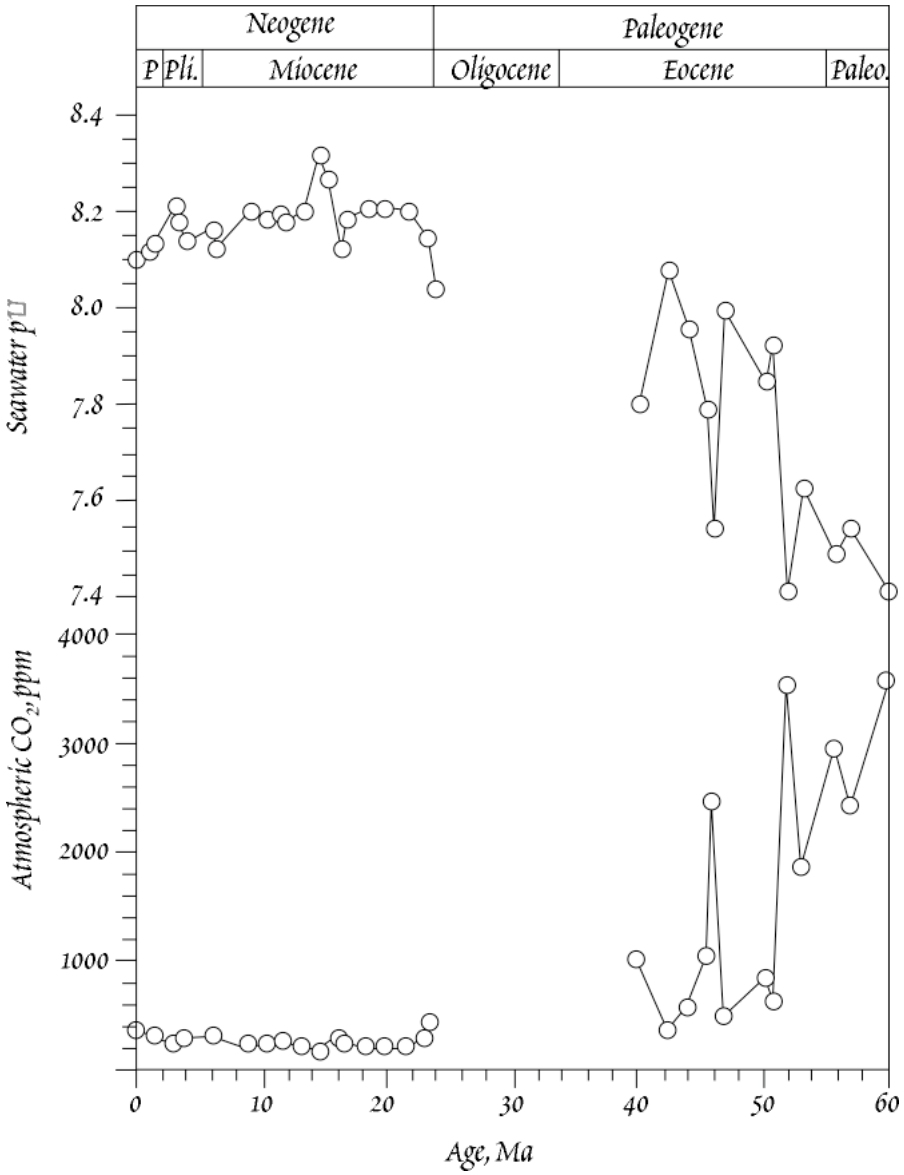

Figure 9.46. Top graph shows the variation *pH* of surface seawater during Tertiary time as inferred from $\delta^{11}B$ in shells of planktonic foraminifera in ODP cores. Bottom graph shows the concentration of atmospheric CO_2 calculated from seawater pH. Adapted from Pearson and Palmer (2000).

The pH of seawater, in turn, is largely controlled by the carbonate equilibrium, and depends therefore on the partial pressure of CO_2 in the atmosphere (Example 6.2 explores how pH of a solution will depend on p_{CO_2}). Thus if the pH of ancient seawater can be determined, it should be possible to estimate p_{CO_2} of the ancient atmosphere. Given the concern about the relation of future climate to future p_{CO_2}, it is obviously interesting to know how these factors related in the past.

Pearson and Palmer (2000) measured $\delta^{11}B$ in foraminiferal carbonate extracted from Ocean Drilling Program (ODP) cores and from this calculated pH based on equations 9.71 and 9.74. To minimize the effect of temperature on the fractionation factor, they restricted their study to cores from regions that were tropical at the time of deposition. To minimize vital effects, they used only 1 species of planktonic foraminifera for the Neogene period, *G. trilobus* (also known as *G. sacculifer*), which is thought to incorporate B with no vital effect. For the Paleogene, they used 6 species where the vital effect was arguably minimal. They argue that changes in the B isotopic composition of seawater should be slow to occur since the residence time of B in seawater is roughly 20 million years. Nevertheless, they account for a small variation, roughly 1.7‰, in seawater $\delta^{11}B$ over Tertiary time. The results suggest dramatically lower seawater pH and dramatically higher p_{CO_2} in the Paleogene. The apparent variation in p_{CO_2} is qualitatively consistent with what is known about Tertiary climate change – namely that a long-term cooling trend began in the early to middle Eocene. In contrast to the Paleogene, Figure 9.46 shows that the Neogene is characterized by atmospheric p_{CO_2} near or slightly below modern pre-industrial levels.

On a more limited time scale, Hönish and Hemming (2005) investigated $\delta^{11}B$ over the last two glacial cycles (0-140 and 300-420 ka). In this study, the controlled for temperature by analyzing the Mg/Ca ratio of the carbonate shells, which is know to be strongly temperature dependent. Their calculated pH values ranged from 8.11 to 8.32, which in turn correspond to a p_{CO_2}range of ~180 to ~325 ppm. These calculated p_{CO_2} values are in good agreement with CO_2 concentrations measured in bubbles in the Vostok ice core.

Nevertheless, paleo-seawater pH reconstruction based on boron isotopes remains somewhat controversial. Pagani et al. (2005) and Zeebe (2005) point out that the fractionation factor between $B(OH)_3$ and $B(OH)_4^-$ has not been experimentally determined and remains somewhat uncertain. Attempts to calculate it theoretically are hampered by uncertainties in experimental determination of vibrational frequencies, and attempts to calculate it *ab initio* from molecular orbital theory also result in uncertainties that are too large to be useful. In addition to this, there are additional uncertainties in the mechanism of incorporation of boron into carbonate and the associated fractionation factor, and uncertainties in how $\delta^{11}B$ in seawater has varied with time.

9.9.2 Li Isotopes

Terrestrial lithium isotopic variation is dominated by the strong fractionation that occurs between minerals, particularly silicates, and water. Indeed, this was first demonstrated experimentally by Urey in the 1930's. This fractionation in turn reflects the chemical behavior of Li. Li forms bonds with a high degree of covalent character. The ionic radius of Li^{1+} is small (78 pm) and Li readily substitutes for Mg^{2+}, Fe^{2+}, and Al^{3+} in crystal lattices, mainly in octahedral sites. In aqueous solution, it is tetrahedrally coordinated by 4 water molecules (the solvation shell) to which it is strongly bound, judging from the high solvation energy. These differences in atomic environment, differences in binding energies, the partly covalent nature of bonds, and the low mass of Li all lead to strong fractionation of Li isotopes.

Modern study of Li isotope ratios began with the work of Chan and Edmond (1988). They found that the isotopic composition of seawater was uniform within analytical error with a δ^7Li value of +33‰. Subsequent work suggests that δ^7Li in seawater might vary by as much as 4‰, but the degree to which this variation reflects analytical error and inter-laboratory biases remains unclear, as the residence time of Li in the ocean (1.5-3 Ma) is much longer than the mixing time.

As is the case for boron, seawater represents one extreme of the spectrum of isotopic compositions in the Earth. During mineral-water reactions, the heavier isotope, ^7Li, is preferential partitioned into the solution. Thus weathering on the continents results in river water being isotopically heavy, +23.5‰ on average, compared to average continental crust, which has δ^7Li of ~0, and the suspended load of rivers which have $\delta^7Li \approx +2$ (Teng et al., 2004). Thus seawater is some 10 per mil heavier than average river

water, so additional fractionation must occur marine environment. This likely includes adsorption on particles (although Li is less prone to absorption than most other metals), authigenic clay formation, and low temperature alteration of oceanic crust. Chan et al. (1992) estimated the fractionation factor for clay-solution exchange at -19‰ and the fractionation factor for low-temperature alteration of basalt. Reported δ^7Li values in marine non-carbonate sediments range from -1 to +15‰, but Chan and Frey (2003) suggested, based on new data and reanalysis of older samples that the range is only +1 to +6‰. Marine carbonate sediments, which tend to be Li-poor, typically have higher δ^7Li than non-carbonate sediment.

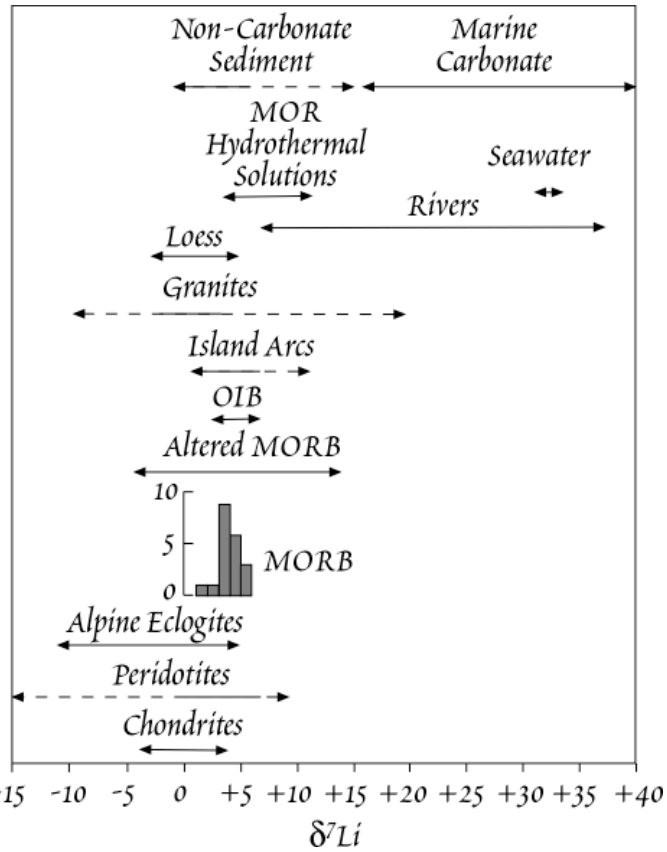

Figure 9.47. Li isotopic composition of terrestrial materials.

Fresh MORB has a very limited range of δ^7Li of +1 to +6‰, with most values falling between +3 and +5, a range not much larger than that expected from analytical error alone. Oceanic island basalts (OIB) range to only slightly higher values, +7‰, than MORB, but only Hawaii has been studied in any detail. There appears to be little the relationship between δ^7Li and other geochemical parameters, such as MgO concentration, suggesting Li experiences little isotopic fractionation during fractional crystallization, and perhaps also partial melting. Mantle peridotites show a considerable range, from -15‰ to +10‰, but unmetasomatized peridotites have a range of only 0‰ to +7‰, just slightly larger than that of MORB. Alpine eclogites can have distinctly light isotopic compositions. These rocks are thought to be fragments of basaltic oceanic crust deeply subducted and metamorphosed then subsequently rapidly exhumed during the Alpine orogeny. Their light isotopic compositions presumably reflect preferential partitioning of ^{7}Li into the fluid produced as the rocks were dehydrated during metamorphism.

δ^7Li in oceanic crust altered by seawater at low temperatures takes up Li from solution and has high δ^7Li compared to fresh basalt. In hydrothermal reactions, however, Li is extracted from basalt into the solution and hydrothermal fluids can Li concentrations up to 50 times greater than seawater. ^{7}Li is extracted more efficiently than ^{6}Li during this process, so hydrothermally altered basalt can have δ^7Li as low as -2‰. Serpentinites (hydrothermally altered peridotite) can have even lower δ^7Li. However, because they extract Li from oceanic crust so completely, hydrothermal solutions have Li isotopic compositions intermediate between MORB despite this fractionation.

Island arc lavas have a range of δ^7Li of +1 to +11, but all but a few values in the range +2 to +6, which is not very different from the range in MORB. This is somewhat surprising since other isotopic evidence (e.g., ^{10}Be – Chapter 7) clearly demonstrates island arc magmas contain components derived from subducted oceanic crust and sediment. Furthermore, while δ^7Li have been shown in some cases to correlate with chemical and isotopic indicators of a subduction component, this is not always the case.

It seems nevertheless likely that the subduction process has profoundly influenced the isotopic composition of the mantle over time. As a consequence of fractionation occurring during weathering, seawater is strongly enriched in ^{7}Li. This enrichment is imprinted upon the oceanic crust as it reacts with

seawater. When the oceanic crust is returned to the mantle during subduction, the mantle becomes progressively enriched in ^{7}Li. The continental crust, on the other hand, becomes progressively depleted in ^{7}Li over time. Elliot et al. (2004) calculate that this process has increased $\delta^{7}Li$ in the mantle by 0.5 to 1‰ and decreased $\delta^{7}Li$ of the continental crust by 3‰ over geologic time.

REFERENCES AND SUGGESTIONS FOR FURTHER READING

Bigeleisen, J. and M. G. Mayer. 1947. Calculation of equilibrium constants for isotopic exchange reactions, *J. Chem. Phys.*, 15: 261-267.

Bowen, R. 1988. *Isotopes in the Earth Sciences*, Barking (Essex): Elsevier Applied Science Publishers.

Boyd, S. R. and C. T. Pillinger. 1994. A prelimiary study of $^{15}N/^{14}N$ in octahedral growth form diamonds. *Chem. Geol.* 116: 43-59.

Broecker, W. and V. Oversby. 1971. *Chemical Equilibria in the Earth*, New York: McGraw-Hill (Chapter 7).

Cerling, T. E., Y. Wang and J. Quade. 1993. Expansion of C_4 ecosystems as an indicator of global ecological change in the late Miocene, *Nature*, 361, 344-345.

Chan, L. H., J. M. Edmond, G. Thompson and K. Gillis. 1992. Lithium isotopic composition of submarine basalts: implications for the lithium cycle of the oceans. *Earth Planet. Sci. Lett.* 108: 151-160.

Chan, L.-H. and J. M. Edmond. 1988. Variation of lithium isotope composition in the marine environment: a preliminary report. *Geochim. Cosmochim. Acta*. 52: 1711-1717.

Chan, L.-H. and F. A. Frey, Lithium isotope goechemistry of the Hawaiian plume: results from the Hawaii Scientific Drilling Project and Koolau Volcano, *Geochem. Geophys. Geosyst.*, 4: DOI: 10.1029/2002GC000365, 2003.

Chaussidon, M. and A. Jambon. 1994. Boron content and isotopic composition of oceanic basalts: geochemical and cosmochemical implications. *Earth Planet. Sci. Lett*. 121: 277-291.

Chaussidon, M. and B. Marty. 1995. Primitive boron isotope composition of the mantle. *Science*. 269: 383-266.

Chaussidon, M. and F. Albarede. 1992. Secular boron isotope variations in the continental crust: an ion microprobe study. *Earth Planet. Sci. Lett.* 108: 229-241.

Chaussidon, M., F. Albarède and S. M. F. Sheppard. 1987. Sulphur isotope heterogeneity in the mantle from ion microprobe measurements of sulphide inclusions in diamonds. *Nature*. 330: 242-244.

Chaussidon, M., F. Albarede and S. M. F. Sheppard. 1989. Sulphur isotope variations in the mantle from ion microprobe analyses of micro-sulphide inclusions. *Earth Planet. Sci. Lett.* 92: 144-156.

Chaussidon, M., S. M. F. Sheppard and A. Michard. 1991. Hydrogen, sulfur and neodymium isotope variations in the mantle beneath the EPR at 12°50´´N. in *Stable Isotope Geochemistry: A Tribute to Samuel Epstein*, ed. H. P. Taylor, J. R. O'Niel and I. R. Kaplan. 325-338. San Antonio: Geochemical Society.

Chiba, H., T. Chacko, R. N. Clayton and J. R. Goldsmith. 1989. Oxygen isotope fractionations involving diopside, forsterite, magnetite, and calcite: application to geothermometry. *Geochim. Cosmochim. Acta*. 53: 2985-2995.

Craig, H. 1963. The isotopic composition of water and carbon in geothermal areas, in *Nuclear Geology on Geothermal Areas*, ed. by E. Tongiorgi, p. 17-53, Pisa: CNR Lab. Geol. Nucl.

Criss, R. E. and H. P. Taylor. 1986. Meteoric-hydrothermal systems, in *Stable Isotopes in High Temperature Geological Processes, Reviews in Mineralogy 16*, ed. by J. W. Valley, H. P. Taylor and J. R. O'Neil, p. 373-424, Washington: Mineral. Soc. Am., Washington.

Dansgaard, W. 1964. Stable isotopes in precipitation. *Tellus, 16*, 436-463.

Deloule, E., F. Albarede and S. M. F. Sheppard. 1991. Hydrogen isotope heterogeneity in the mantle from ion probe analysis of amphiboles from ultramafic rocks. 105: 543-553.

Elliott, T., A. Jeffcoate and C. Bouman, The terrestrial Li isotope cycle: light-weight constraints on mantle convection, *Earth Planet. Sci. Lett.*, 220: 231-245, 2004.

DeNiro, M. J. 1987. Stable Isotopy and Archaeology, *Am. Scientist*, 75: 182-191.

DeNiro, M. J. and C. A. Hasdorf. 1985. Alteration of $^{15}N/^{14}N$ and $^{13}C/^{12}C$ ratios of plant matter during the initial stages of diagenesis: studies utilizing archeological specimens from Peru, *Geochim. Cosmochim. Acta*, 49, 97-115.

DeNiro, M. J. and S. Epstein. 1978. Influence of diet on the distribution of carbon isotopes in animals, *Geochim. Cosmochim. Acta*, 42: 495-506.

DeNiro, M. J. and S. Epstein. 1981. Influence of diet on the distribution of nitrogen isotopes in animals, *Geochim. Cosmochim. Acta*, 45> 341-351.

Eldridge, C. S., W. Compston, I. S. Williams, J. W. Harris and J. W. Bristow. 1991. Isotope evidence for the involvement of recycled sediment in diamond formation. *Nature*. 353: 649-653.

Elliott, T., A. Jeffcoate and C. Bouman, The terrestrial Li isotope cycle: light-weight constraints on mantle convection, *Earth Planet. Sci. Lett.*, 220:231-245, 2004.

Emiliani, C. 1955. Pleistocene temperatures, *J. Geol.*, 63, 538-578.

Farquhar, J., H. Bao and M. Thiemens, Atmospheric influence of Earth's earliest sulfur cycle, *Science*, 289: 756-758, 2000.

Farquhar, J., B. A. Wing, K. D. McKeegan, J. W. Harris, P. Cartigny and M. Thiemens, Mass-independent fractionation sulfur of inclusions in diamond and sulfur recycling on early Earth, *Science*, 298: 2369-2372, 2002.

Farquhar, J. and B. A. Wing, Multiple sulfur isotopes and the evolution of atmospheric oxygen, *Earth Planet. Sci. Lett., 213: 1-13, 2003.*

Faure, G. 1986. Principles of Isotope Geology, 2nd ed., New York: J. Wiley & Sons.

Ferronsky, V. I., and V. A. Polyakov. 1982. *Environmental Isotopes in the Hydrosphere*, Chichester: John Wiley and Sons.

Fogel, M. L., and M. L. Cifuentes. 1993. Isotope Fractionation during Primary Production, in *Organic Geochemistry: Principles and Applications* edited by M. H. Engel and S. A. Macko, p. 73-98. New York: Plenum.

Goldhaber, M., S. E. Church, B. R. Doe, C. Taylor, J. C. Brannon, and C. A. Gent. 1995. Sources and transport paths for MVT ore deposit lead and sulfur in the midcontinent of the U.S.A. in *International Field Conference on Carbonate-Hosted Lead-Zinc Deposits - Extended Abstracts*. D. L. Leach and M. B. Goldhaber (ed.) p.111-114. Littleton (CO): Society of Economic Geologists.

Harmon, R. S., and J. Hoefs. 1995. Oxygen isotope heterogeneity of the mantle deduced from a global analysis of basalts from different geotectonic settings, *Contrib. Mineral. Petrol.*, in press.

Hayes, J. D., J. Imbrie and N. J. Shackleton. 1976. Variations in the Earth's orbit: pacemaker of the ice ages, *Science*, 194, 1121-1132.

Heming, N. G. and G. N. Hanson. 1992. Boron isotopic composition and concentration in modern marine carbonates. *Geochim. Cosmochim. Acta*. 56: 537-543.

Hoefs, J. 1988. *Stable Isotope Geochemistry*, 3 rd ed., Berlin: Springer-Verlag.

Hofmann, A. W. and W. M. White. 1982. Mantle plumes from ancient oceanic crust. *Earth Planet. Sci. Lett.* 57: 421-436.

Imbrie, J. 1985. A theoretical framework for the Pleistocene ice ages, *J. Geol. Soc. Lond.*, 142, 417-432.

Imbrie, J., J. D. Hayes, D. G. Martinson, A. McIntyre, A. Mix, et al., 1985. The orbital theory of Pleistocene climate: support from a revised chronology of the marine $\delta^{18}O$ record, in *Milankovitch and Climate, Part 1*, edited by A. L. Berger, J. Imbrie, J. Hayes, G. Kukla and B. Saltzman, p. 269-305. Dordrecht: D. Reidel.

Ishikawa, T. and E. Nakamura. 1992. Boron isotope geochemistry of the oceanic crust from DSDP/ODP Hole 504B. *Geochim. Cosmochim. Acta*. 56: 1633-1639.

Ishikawa, T. and E. Nakamura. 1993. Boron isotope systematics of marine sediments. *Earth Planet Sci. Lett.* 117: 567-580.

Javoy, M. 1977. Stable isotopes and geothermometry, *J. Geol. Soc. Lond., 133*, 609-639.

Javoy, M. and F. Pineau. 1991. The volatile record of a "popping" rock from the Mid-Atlantic Ridge at 14° N: chemical and isotopic composition of the gas trapped in the vesicles, *Earth Planet. Sci. Lett.*, 107, 598-611.

Johnson, C. M., B. L. Beard and F. Albarede, *Geochemistry of Non-Traditional Stable Isotopes*: *Reviews in Mineralogy Volume*, Washington, Mineralogical Society of America, 454, 2004.

Johnson, D. G., K. W. Jucks, W. A. Traub and K. V. Chance, 2001. Isotopic composition of stratospheric ozone, *J. Geohys. Res.*, 105:9025-9031.

Jouzel, J., N. I. Barkov, J. M. Barnola, M. Bender, J. Chappelaz, C. Genthon, V. M. Kotlyakov, V. Lipenkov, C. Lorius, R. Petit, *et al.*, 1993. Extending the Vostok ice-core record of paleoclimate to the penultimate glacial period, Nature, 364:407-412.

Jouzel, C., C. Lorius, J. R. Perfit, C. Genthon, N.I. Barkov, V. M. Kotlyakov, and V. N. Petrov. 1987. Vostok ice core: a continuous isotope temperature record over the last climatic cycle (160,000 years), *Nature,* 329: 403-403.

Jouzel, J., C. Waelbroeck, B. Malaizé, M. Bender, J. R. Petit, N. I. Barkov, J. M. Barnola, T. King, V. M. Kotlyakov, V. Lipenkov, et al., Climatic interpretation of the recently extended Vostok ice records, *Clim. Dyn.*, 12:513-521, 1996.

Kasting, J. F. and D. Catling, Evolution of a Habitable Planet, *Ann. Rev. Astron. Astrophys.*, 41:429-463, 2003.

Kawabe, I. 1979. Calculation of oxygen isotopic fractionation in quartz-water system with special reference to the low temperature fractionation, *Geochim. Cosmochim. Acta*, 42: 613-621.

Kyser, K. T. 1986. Stable isotope variations in the mantle, in *Stable Isotopes in High Temperature Geologic Processes*, edited by J. W. Valley, H. P. Taylor and J. R. O'Neil, p. 141-164, Washington: Mineral. Soc. Am.

Lawrence, J. R. and H. P. Taylor. 1972. Hydrogen and oxygen isotope systematics in weathering profiles, *Geochim. Cosmochim. Acta*, 36, 1377-1393.

Lawrence, J. R. and J. R. Meaux. 1993., The stable isotopic composition of ancient kaolinites of North America, in *Climate Change in Continental Isotopic Records, Geophysical Monograph 78*, edited by P. K. Swart, K. C. Lohmann, J. McKenzie and S. Savin, p. 249-261.Washington: AGU.

Marty, B. and N. Dauphas, The nitrogen record of crust-mantle interaction and mantle convection from Archean to present, *Earth Planet. Sci. Lett.*, 206: 397-410, 2003.

Mattey, D. P. 1987. Carbon isotopes in the mantle. *Terra Cognita*. 7: 31-38.

Mattey, D., D. Lowry and C. Macpherson. 1994. Oxygen isotope composition of mantle peridotite. *Earth Planet. Sci. Lett.* 128: 231-241.

Mauersberger, K. , 1987. Ozone isotope measurements in the stratosphere, *Geophys. Res. Lett.*, 14:80-83.

Milankovitch, M. 1938. Astronomische mittel zur erforschung der erdgeschlichtlichen klimate, *Handbuch der Geophysik*, 9: 593-698.

Mojzsis, S. J., G. Arrhenius, K. D. McKeegan, T. M. Harrison, A. P. Nutman and C. R. L. Friend, Evidence for life on Earth before 3800 million years ago, *Nature*, 384: 55-59, 1996.

Muehlenbachs, K. and G. Byerly. 1982. ^{18}O enrichment of silicic magmas caused by crystal fractionation at the Galapagos Spreading Center, *Contrib. Mineral. Petrol.*, 79, 76-79.

O'Leary, M. H. 1981. Carbon isotope fractionation in plants, *Phytochemistry*, 20, 553-567.

O'Neil, J. R. 1986. Theoretical and experimental aspects of isotopic fractionation, **in** *Stable Isotopes in High Temperature Geologic Processes, Reviews in Mineralogy Volume 16*, J. W. Valley, H. P. Taylor and J. R. O'Neil, eds., Mineralogical Society of America, Washington, pp. 1-40, 1986.

Ohmoto, H. and R. O. Rye, Isotopes of Sulfur and Carbon, in *Geochemistry of Hydrothermal Ore Deposits,* edited by H. Barnes, p. John Wiley and Sons, New York, 1979.

Ohmoto, H., Stable isotope geochemistry of ore deposits, in *Stable Isotopes in High Temperature Geological Processes, Reviews in Mineralogy 16*, edited by J. W. Valley, H. P. Taylor and J. R. O'Neil, p. 491-560. Washington: Mineral. Soc. Am.

Pagani, M., D. Lemarchand, A. J. Spivack and J. Gaillardet, A critical evaluation of the boron isotope-ph proxy: The accuracy of ancient ocean pH estimates, *Geochim. Cosmochim. Acta,* 69: 953-961, 2005.

Palmer, M. R. 1991. Boron-isotope systematics of Halmahera arc (Indonesia) lavas: evidence for involvement of the subducted slab. *Geology*. 19: 215-217.

Palmer, M., M. Spivack and J. M. Edmond. 1987. Temperature and pH controls over isotopic fractionation during adsorption of boron on marine clay. *Geochim. Cosmochim. Acta*. 51: 2319-2323.

Park, R. and S. Epstein. 1960. Carbon isotope fractionation during photosynthesis, *Geochim. Cosmochim. Acta*, 21, 110-126.

Quade, J., T. E. Cerling and J. R. Bowman. 1989. Development of Asian monsoon revealed by marked ecological shift during the latest Miocene in northern Pakistan, *Nature*, 342, 163-166.

Richet, P., Y. Bottinga and M. Javoy. 1977. A review of hydrogen, carbon, nitrogen, oxygen, sulphur, and chlorine stable isotope fractionation among gaseous molecules, *Ann. Rev. Earth Planet. Sci. Lett.*, 5, 65-110.

Rosing, M., ^{1}3C-depleted carbon microparticles in >3700 Ma sea-floor sedimentary rocks from West Greenland, *Science*, 283: 674-676, 1999.

Sakai, H., D. J. Des Marais, A. Ueda and J. G. Moore. 1984. Concentrations and isotope ratios of carbon, nitrogen, and sulfur in ocean-floor basalts, *Geochim. Cosmochim. Acta*, 48, 2433-2442, 1984.

Sanyal, A., N. G. Hemming, G. N. Hanson and W. S. Broecker. 1995. Evidence for a higher pH in the glacial ocean from boron isotopes in foraminifera. *Nature*. 373: 234-236.

Savin, S. M. and S. Epstein, The oxygen and hydrogen isotope geochemistry of clay minerals, *Geochim. Cosmochim. Acta*, 34, 25-42, 1970.

Schidlowski, M., A 3800-million year isotopic record of life from carbon in sedimentary rocks, Nature, 333: 1988.

Schoeninger, M. J. and M. J. DeNiro. 1984. Nitrogen and carbon isotopic composition of bone collagen from marine and terrestrial animals, *Geochim. Cosmochim. Acta*, 48, 625-639.

Schwarcz, H. P., E. K. Agyei and C. C. McMullen. 1969. Boron isotopic fractionation during clay adsorption from sea-water. *Earth Planet. Sci. Lett.* 6: 1-5.

Shackleton, N. J. and N. D. Opdyke. 1973. Oxygen isotope and paleomagnetic stratigraphy of an equatorial Pacific core V28-238: oxygen isotope temperatures and ice volumes on a 10^5 and 10^6 year time scale, *Quat. Res.*, 3, 39-55.

Sheppard, S. M. F. and C. Harris. 1985. Hydrogen and oxygen isotope geochemistry of Ascension Island lavas and granites: variation with fractional crystallization and interaction with seawater, *Contrib. Mineral. Petrol.*, 91, 74-81.

Sheppard, S. M. F. and S. Epstein. 1970. D/H and $^{18}O/^{16}O$ ratios of minerals of possible mantle or lower crustal origin. *Earth Planet. Sci. Lett.* 9: 232-239.

Sheppard, S. M. F., R. L. Nielsen and H. P. Taylor. 1969. Oxygen and hydrogen isotope ratios of clay minerals from porphyry copper deposits. *Econ. Geol.* 64: 755-777.

Smith, H. J., A. J. Spivack, H. Staudigel and S. R. Hart, The boron isotopic composition of altered oceanic crust, *Chem. Geol.*, 126: 119-135, 1995.

Spivack, A. and J. M. Edmond. 1987. Boron isotope exchange between seawater and the oceanic crust. *Geochim. Cosmochim. Acta.* 51: 1033-1044.

Spivack, A. J., C.-F. You and H. J. Smith. 1993. Foraminiferal boron isotope ratios as a proxy for surface ocean pH over the past 21 Myr. *Nature*. 363: 149-151.

Taylor, H. P. 1974. The application of oxygen and hydrogen studies to problems of hydrothermal alteration and ore deposition, *Econ. Geol.*, 69, 843-883.

Taylor, H. P. 1980. The effects of assimilation of country rocks by magmas on $^{18}O/^{16}O$ and $^{87}Sr/^{86}Sr$ systematics in igneous rocks., *Earth Planet. Sci. Lett.*, 47, 243-254.

Taylor, H. P. and S. M. F. Sheppard, 1986. Igenous rocks: I. Processes of isotopic fractionation and isotope systematics, in *Stable Isotopes in High Temperature Geological Processes,* edited by J. W. Valley, H. P. Taylor and J. R. O'Neil, Washington: Mineral. Soc. Am., p. 227-271.

Teng, F.-Z., W. F. McDonough, R. L. Rudnick, C. Dalpe, P. B. Tomascak, B. W. Chappell and S. Gao, Lithium isotopic composition and concentration of the upper continental crust, Geochim. Comsochim. Acta, 68:4167-4178, 2004.

Tomascak, P. B., Developments in the understanding and application of lithium isotopes in the Earth and planetary sciences, in C. M. Johnson, et al. (ed.), *Geochemistry of Non-Traditional Stable Isotopes*, *Reviews in Mineralogy Volume* 55, 153-195, 2004.

Urey, H. 1947. The thermodynamic properties of isotopic substances, *J. Chem. Soc. (London)*,1947: 562-581.

Valley, J. W., H. P. Taylor and J. R. O'Neil (editors). 1986. *Stable Isotopes in High Temperature Applications, Reviews in Mineralogy Volume 16*. Washington: Mineral. Soc. Am.

Vengosh, A., Y. Kolodny, A. Starinsky, A. Chivas and M. McCulloch. 1991. Coprecipitation and isotopic fractionation of boron in modern biogenic carbonates. *Geochim. Cosmochim. Acta*. 55: 2901-2910.

Wang, Y., C. E. Cerling and B. J. McFadden. 1994. Fossil horse teeth and carbon isotopes: new evidence for Cenozoic dietary, habitat, and ecosystem changes in North America, *Paleogeogr., Paleoclim., Paleoecol.* in press.

You, C.-F. 1994. Comment on "Boron content and isotopic composition of oceanic basalts: geochemical and cosmochemical implications" by M. Chaussidon and A. Jambon. *Earth Planet. Sci. Lett.* 128: 727-730.

Zeebe, R., Stable boron isotope fractionation between dissolved $B(OH)_3$ and $B(OH)_4^-$, *Geochim. Cosmochim. Acta*, 69:2753-2766, 2005.

PROBLEMS

1. Using the procedure and data in Example 9.1, calculate the fractionation factor $\Delta_{CO\text{-}O_2}$ for the $^{17}O/^{16}O$ ratio at 300°C. What is the expected ratio of fractionation of $^{17}O/^{16}O$ to that of $^{18}O/^{16}O$ at this temperature?

2. What would you predict would be the ratio of the diffusion coefficients of H_2O and D_2O in air?

3. A granite contains coexisting feldspar (3% An content) and biotite with $\delta^{18}O_{SMOW}$ of 9.2‰ and 6.5‰ respectively. Using the information in Table 9.2, find the temperature of equilibration.

4. Spalerite and galena from a certain Mississippi Valley deposit were found to have $\delta^{34}S_{CDT}$ of +13.2‰ and +9.8‰ respectively.

a. Using the information in Table 9.4, find the temperature at which these minerals equilibrated.

b. Assuming they precipitated from an H_2S-bearing solution, what was the sulfur isotopic composition of the H_2S?

5. Glaciers presently constitute about 2.1% of the water at the surface of the Earth and have a $\delta^{18}O_{SMOW}$ of ≈ –30. The oceans contain essentially all remaining water. If the mass of glaciers were to increase by 50%, how would the isotopic composition of the ocean change (assuming the isotopic composition of ice remains constant)?

6. Consider the condensation of water vapor in the atmosphere. Assume that the fraction of vapor remaining can be expressed as a function of temperature (in kelvins):

$$f = \frac{T - 223}{50}$$

Also assume that the fractionation factor can be written as:

$$\ln\alpha = 0.0018 + \frac{12.8}{RT}$$

Assume that the water vapor has an initial $\delta^{18}O_{SMOW}$ of -9‰. Make a plot showing how the $\delta^{18}O$ of the remaining vapor would change as a function of f, fraction remaining.

7. Calculate the $\delta^{18}O$ of raindrops forming in a cloud after 80% of the original vapor has already condensed assuming (1.) the water initial evaporated from the ocean with $\delta^{18}O = 0$, (2.) the liquid-vapor fractionation factor, $\alpha = 1.0092$.

8. A saline lake that has no outlet receives 95% of its water from river inflow and the remaining 5% from rainfall. The river water has $\delta^{18}O$ of –10‰ and the rain has $\delta^{18}O$ of -5‰. The volume of the lake is steady-state (i.e., inputs equal outputs) and has a $\delta^{18}O$ of -3. What is the fractionation factor, α, for evaporation?

9. Consider a sediment composed of 70 mole percent detrital quartz ($\delta^{18}O = +10‰$) and 30 mole percent calcite ($\delta^{18}O = +30‰$). If the quartz/calcite fractionation factor, α, is 1.002 at 500° C, determine the O isotopic composition of each mineral after metamorphic equilibrium at 500° C. Assume that the rock is a closed system during metamorphism, i.e., the $\delta^{18}O$ of the whole rock does not change during the process.

10. Assume that α is a function of the fraction of liquid crystallized such that $\alpha = 1 + 0.008(1-f)$. Make a plot showing how the $\delta^{18}O$ of the remaining liquid would change as a function of $1-f$, fraction crystallized, assuming a value for Δ of 0.5‰.

11. A basaltic magma with a $\delta^{18}O$ of +6.0 assimilates country rock that $\delta^{18}O$ of +20 as it undergoes fractional crystallization. Assuming a value of α of 1.002, make a plot of $\delta^{18}O$ vs. f for R = 5 and R = 10 going from $f = 1$ to $f = 0.05$.